LESIONS IN THE CONNECTED BRAIN

A network perspective on brain tumors and lesional epilepsy

Edwin van Dellen

Cover design: Judith van Dellen

Lay-out: Lotte Jonkman

Printed by: Proefschriftmaken.nl || Uitgeverij BOXpress

Published by: Uitgeverij BOXPress, `s Hertogenbosch

ISBN: 978-90-8891-620-5

Printing of this thesis was kindly supported by:

Vrije Universiteit Amsterdam, Het Nationaal Epilepsie Fonds, Stophersentumoren.nl, Elekta BV. Neuralynx Systems, UCB Pharma, GlaxoSmithKline BV, and Eisai BV.

VRIJE UNIVERSITEIT

A network perspective on brain tumors and lesional epilepsy

ACADEMISCH PROEFSCHRIFT
ter verkrijging van de graad Doctor aan
de Vrije Universiteit Amsterdam,
op gezag van de rector magnificus
prof.dr. F.A. van der Duyn Schouten,
in het openbaar te verdedigen
ten overstaan van de promotiecommissie
van de Faculteit der Geneeskunde
op dinsdag 4 juni 2013 om 15.45 uur
in het auditorium van de universiteit,
De Boelelaan 1105

door

Edwin van Dellen
geboren te Leiderdorp

promotoren:	prof.dr. C.J. Stam
	prof.dr. J.J. Heimans
copromotoren:	dr. J.C. Reijneveld
	dr. L. Douw

CONTENTS

CHAPTER 1

General introduction

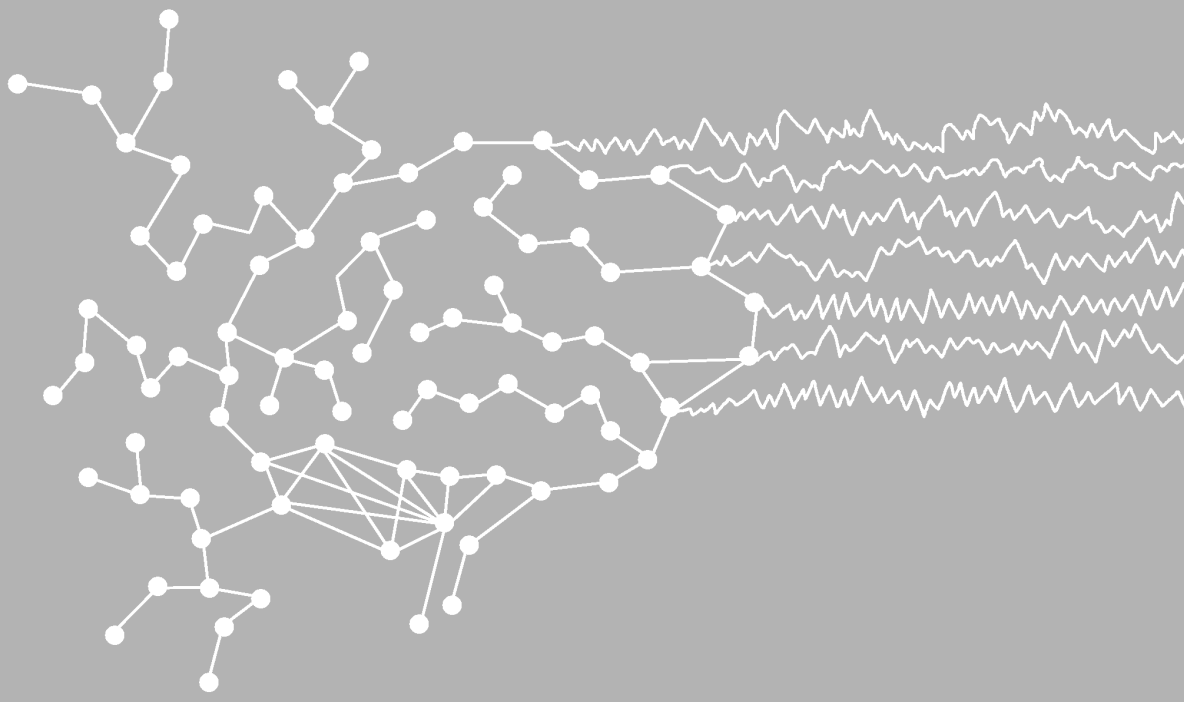

INTRODUCTION

In 2008, the documentary entitled ‘How Kevin Bacon cured cancer’ shed a light on a field of science called network theory, and suggested that the application of this theory in medicine may eventually help us to cure cancer. The title refers to a game where one has to link actor Kevin Bacon to any other actor in Hollywood. Two actors are said to be connected when they appeared in the same film or play. In this way, every actor can be described in terms of the number of connections that separates him or her from Kevin Bacon. The game is based on the concept of ‘six degrees of separation’, which states that only six handshakes are needed to connect you to any other person in the world. Network theory is the field of science that studies phenomena such as the six degrees of separation. It aims to quantify and characterize networks, ranging from the power grid that provides households with electricity to epidemical spreading of disease, from social networks to the stock exchanges, and from road maps to the human brain. An explosion of scientific papers on the application of network theory over the last decade in this wide range of applications underlines the potential of this framework to increase our understanding of the fundamental laws of nature.

Unfortunately, the use of network theory in medicine has not (yet) brought a cure for cancer. However, it has led to a new approach to the treatment brain tumors, a dramatic example of the high mortality of cancer. Primary brain tumors account for approximately 2 percent of all cancer types [128]. Gliomas are the most frequently occurring primary brain tumors, with an incidence of 7-8 per 100.000 people per year [137, 197]. Patients have a median life expectancy of 14 months to 14 years, depending on histopathology and genetic profile of the tumor [222, 239]. Gliomas cause severe neurological deficits such as epilepsy, loss of motor functioning, headaches, and nausea [18]. Some of these symptoms can be explained by local destruction of brain tissue in a well known functional area, or due to pressure on specific areas by an expanding mass. Epilepsy, however, is still a poorly understood symptom in these patients, while brain tumor patients have a lifetime risk of having epileptic seizures of 20-80% [235]. Deficits in complex cognitive processing such as attention and memory form another group of frequently occurring symptoms that are similarly difficult to elucidate [225]. The need for a better understanding of these symptoms and their relation to the brain tumor is underlined by negative effects of both epilepsy and cognitive deficits on the quality of life of glioma patients [1, 125]. Looking at the brain as a complex network may help us to elucidate how these symptoms arise, and increasing evidence suggests that it may even be used for more tailored treatment of gliomas, by using network information during surgical planning [226]. In this thesis, the framework of network theory is used to gain insight into the impact of brain tumors and of lesional epilepsy on the human brain. For this purpose, electrophysiological recordings of brain activity were analyzed, and functional interactions between brain areas were reconstructed.

AIMS

The general aim of this dissertation is to assess functional brain networks in patients with brain lesions, how these networks are related to epilepsy and cognitive functioning, and how they change after neurosurgical treatment. For this purpose, empirical as well as computational modeling studies were performed. The following research questions are discussed:

I) How do brain tumors or other, (non-neoplastic) lesions disturb functional brain networks?

   a. Does the impact of a lesion on functional brain networks depend on its histopathological fingerprint or growth pattern?

   b. Can we construct a model to describe the impact of lesions on functional connectivity in the brain?

II) How does network topology relate to epilepsy and how does it relate to cognitive deficits?

III) How are functional networks and, as a consequence, epilepsy and cognitive performance, affected by neurosurgery?

OUTLINE

Section 1

In **chapter 2**, network theory is explained more extensively, as well as methods to reconstruct structural and functional brain networks from neurophysiological- and neuroimaging data. Neural networks are described in health and disease, with a special focus on brain tumors, lesional epilepsy, and neurosurgical treatment of these diseases.

Section 2

Section 2 is a description of studies that have been performed on the effects of brain lesions on functional connectivity and neural networks in relation to epilepsy and cognitive deficits. In **chapter 3** local neural networks were studied in the temporal lobe of temporal lobe epilepsy patients. In this study, electrocorticography (ECoG) recordings were analyzed that had been obtained during surgery: this is a technique to measure neural activity directly on the cortex. In **chapter 4**, magnetoencephalography (MEG) recordings were used to compare functional networks in patients suffering from lesional epilepsy on the basis of various histopathological lesions to healthy controls. The relations between network characteristics and epilepsy and cognition in these patients were also studied. In **chapter 5**, results are shown of a longitudinal study in which MEG functional connectivity and network characteristics were analyzed in relation to epilepsy burden in glioma patients after neurosurgical treatment.

Section 3

In this section, the effects of interventions in patients with brain lesions on functional networks are described. The effects of resection on specific anatomical networks that are known to be involved in cognitive processing are described in **chapter 6**. The effects of resection on functional connectivity and network topology related to epilepsy outcome are described in **chapter 7**. In **chapter 8**, electroencephalography (EEG) recordings obtained during the Wada-test were studied. During this test, one hemisphere is temporarily sedated in order to determine the role of that hemisphere for memory and language tasks. The EEG recordings during this test have been used as a model to study how functional brain networks are altered when one hemisphere is functionally disconnected.

Section 4

Section 4 focuses on a modeling study that may help to explain the empirical findings described in sections 2 and 3. In **chapter 9**, an anatomically realistic computational model of human brain activity was used to study the effects of brain lesions on functional connectivity in the remaining brain areas.

Section 5

The final part of this thesis is a summary of the main findings which is provided in **chapter 10**. This is followed by a general discussion of the findings in **chapter 11**. In this general discussion an attempt is made to answer the research questions which were defined in the ‘aims’ section of this introduction.

CHAPTER 2

Neural network analysis, brain tumors and neurosurgical planning

E van Dellen, L Douw, I Bosma, JJ Heimans, CJ Stam, JC Reijneveld

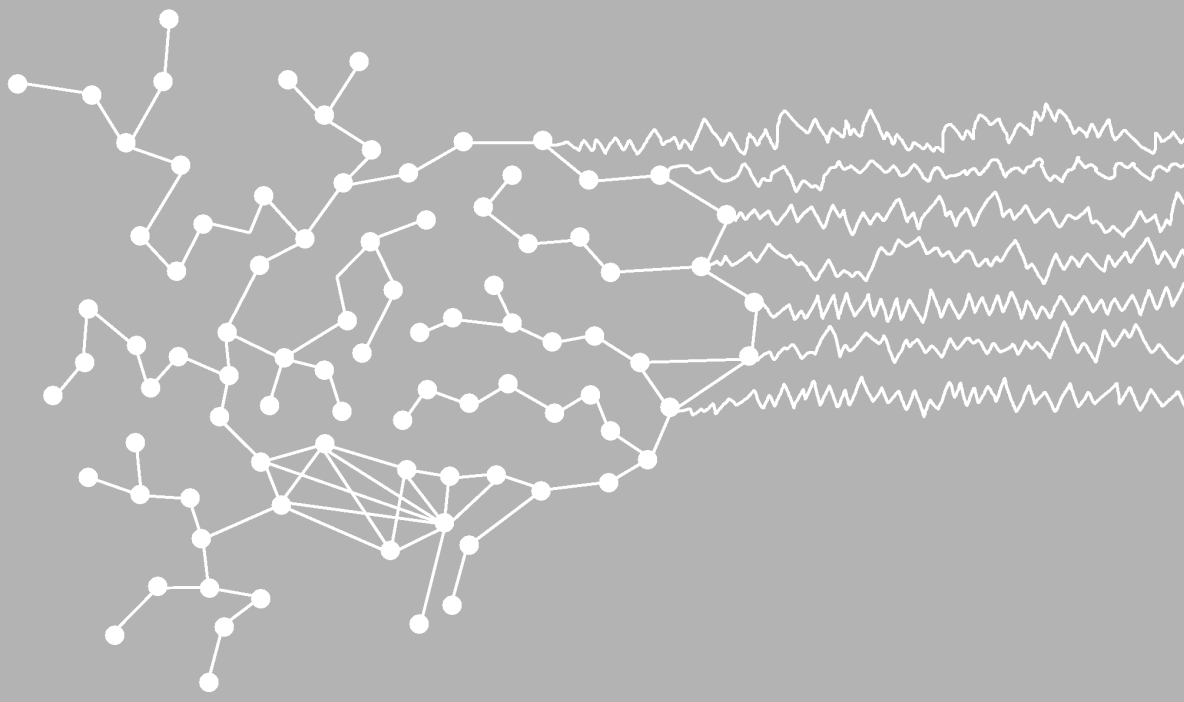

Adapted from:
Neural network analysis and its application in neurosurgical planning (2011).
In: Brain Mapping: From Neural Basis of Cognition to Surgical Applications,
H Duffau (Editor): 373

INTRODUCTION

The human brain is the most complex object known to man. Unraveling its wiring and functioning is one of the greatest challenges in modern science. It is now widely acknowledged that the brain should be seen as a complex network. Understanding the structure and dynamics of this network may form a crucial step towards the understanding of cognition. Moreover, it may help to explain the interaction between brain pathology and symptoms.

The research field focusing on neural networks has grown rapidly over the past ten years, now combining knowledge of computational models and animal studies with advanced human neuroimaging techniques [41, 187]. Network studies focus on both structural connections and functional interactions between brain regions. Structural networks can be reconstructed by mapping cortical areas with MRI, or white matter tracts using diffusion tensor imaging (DTI). Functional interactions can be studied directly using electrophysiological registrations such as electroencephalography (EEG) and magnetoencephalography (MEG), or indirectly from blood oxygen level based fMRI.

In this chapter we will give an overview of the basic concepts of network theory especially in relation to neuroscience. Additionally we will describe clinical neurological and neurosurgical applications. In this respect, we will give our view on perspectives of network theory in the surgical treatment of patients with brain lesions and focal epilepsy.

MODERN NETWORK THEORY

Modern network theory has its roots in both mathematics and sociology. Network theory crosses boundaries between different sciences, ranging from mathematics to language and social studies, which has led to great research advantages in recent years. Below we will discuss the basis of network theory as this is relevant for state of the art neuroscience. For a more detailed overview we recommend reviews by *Bullmore and Sporns* [41], *Stam et al.* [215], and *Reijneveld et al.* [187].

A brief history

The mathematician Leonard Euler was the first to use graph theory in 1736 when solving the problem of the bridges of Konigsberg. The question was whether it was possible to cross a river and its two islands by passing each of the seven connecting bridges only once. Euler presented the problem as an abstract network and showed that this was impossible. Since then, graph theory has become an important branch of mathematics, as it is a tool to analyse networks theoretically. It considers a given system as a collection of nodes and connections between these nodes. The nodes are referred to as vertices and the connections as edges. An important step forward in the field was the discovery of random networks, in which the vertices are connected with a fixed and equal likelihood p. Although random networks meant a boost for the science of graph theory, they were not sufficient to model real networks such as social communities or railway maps, as they are highly structured. The psychologist Stanley Milgram tried to bridge this

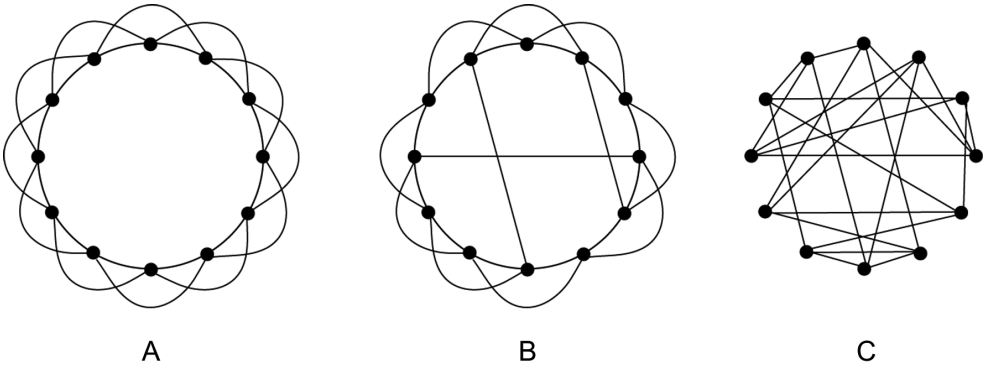

Figure 1. Three types of networks. Three network types based on the model of Watts and Strogatz, 1998. In an ordered network the points are connected to their nearest neighbours (left) but there are no long-distance connections. In a random network (right), there is no local clustering. In a small-world network (middle), some local connections are rewired to long distance connections, resulting in high clustering combined with a short path length.

gap, inspired by a short story called 'Chains' by the Hungarian writer Frigyes Karinthy in 1929. Karinthy challenged anyone to find a person that was not connected to any other person in the world through at most five others. Milgram took up the challenge by sending letters to randomly chosen subjects in the USA. The subjects were informed to send the letter to any other person that was closer to a target person living in Boston. In 1967 Milgram postulated that every letter was only sent on average 5.5 times before reaching its destination, which is now associated with the phrase 'six degrees of separation'. This was the first empirical proof of the 'small-world' phenomenon. Small-world properties can be found in many types of networks, including neural networks. In the next sections, we will discuss some basic concepts of graph theory and small-world networks.

Small-world networks

Watts and Strogatz were the first to define the concept of a small-world network [253]. They considered a simple model of a one-dimensional network on a ring in which the vertices were connected in a lattice configuration, i.e. each vertex is connected only to its direct neighbours and their neighbours (see figure 1). Two features characterize this network. The *clustering coefficient (C)*, which describes the probability that the neighbours of a node will also be connected to each other, is high. However, it takes a lot of steps to connect vertices at opposite sides of the network, which is described by the long *path length (L)* of the network. This feature is also termed low *efficiency*, which is defined as the inverse of path length. When the edges are rewired with likelihood p, the network becomes random for p=1. The path length is now short, but the system has a very low clustering coefficient. However, by only rewiring only a few edges, the network becomes small-world: high local clustering C is combined with a short path length L.

The small-world phenomenon is thought to increase the efficiency of information processing in a network to some sort of optimal state, as it combines high local clustering and high overall integration. C and L not only depend on topology but also on the size and the number of edges in the network. To correct for these factors, the measures are often divided by the C and L of a random equivalent network. The 'small-worldness' or small-world index is then defined by the ratio of these two values.

Network degree

In the Watts & Strogatz model, each vertex is considered to have only small fluctuations in the number of edges connected to it. However, some networks such as the internet do not follow this rule, because the number of connections varies widely between nodes. The *degree (k)* of a vertex is the number of edges that are connected to it. The distribution of the edges over the vertices, or *degree distribution*, is an important feature of network topology. The degree distribution P(k) is defined as the probability that a randomly chosen vertex will have degree k. The key vertices of a network, that have a large number of connecting edges, are known as *hubs*. In a random network, hubs are sparsely found. A network is called *scale-free* when the degree distribution follows a power law, meaning that it has a small number of highly connected vertices and a high number of poorly connected vertices. Scale-free networks greatly depend on a few hub nodes, which take care of most of the information processing in the network. The high importance of these hub nodes also make scale-free networks vulnerable to targeted attacks, because deletion of one or more of these nodes disrupts the whole network.

The *degree correlation* is used to determine to what extent vertices with a similar degree are connected. A high correlation is present in *assortative* networks, which can be seen as the equivalent of 'the rich getting richer'. When vertex degrees are anticorrelated, the network is called *disassortative*, which predicts a more important role for hubs in the network. Social networks such as a network of company directors tend to be assortative, whereas technological and biological networks, including the brain, tend to be disassortative [164].

Hierarchy and modularity

Networks can contain a number of communities or *modules*. A module is a subgraph with vertices that are more connected to other vertices within the module than to vertices outside the module. Each module contains highly interconnected edges, and relatively few connections with other modules. Various algorithms can be used to detect modules, of which *hierarchical* clustering seems most commonly used in neuroscience [41]. Hierarchical modularity allows the description of networks at different levels or resolutions. Most global modules can be divided in a number of submodules, which can consist of even smaller submodules, etcetera. In modular networks, nodes can be described based on their function in the network. Hubs are characterized as *provincial*, when having a high degree within the module, or as *connector*, when they have a large number of connections with other modules [97]. Modular structure may be part of an optimal configuration for networks, as modules have high local clustering, while intermodular connections ensure short path lengths [153].

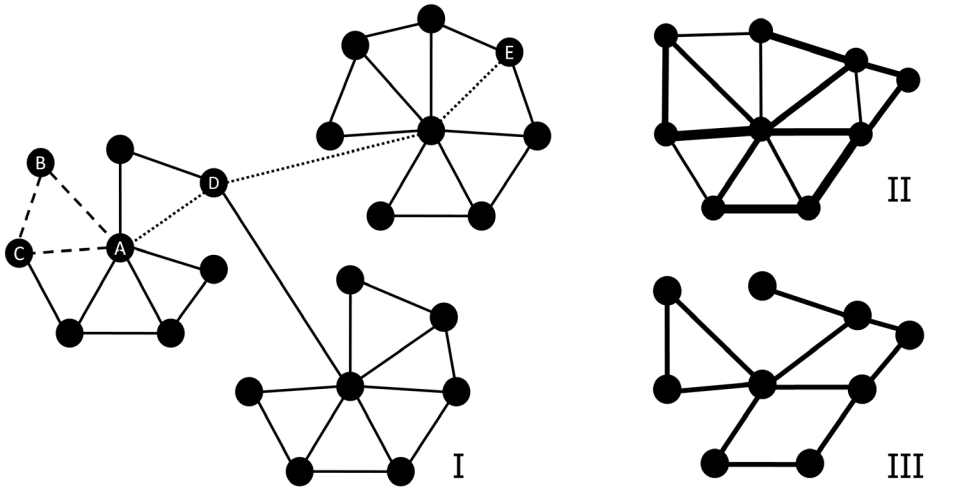

Figure 2. Network measures. Several measures can be used to characterize network topology. (I) The dashed line marks a local cluster, as nodes A, B and C are all interconnected. The dotted line marks the shortest path between node A and E (L = 3). Three modules can be recognized in the figure. Node A is a provincial hub node for the left cluster, while node D functions as a connector hub. (II) A weighted network is constructed, for example by using functional connectivity levels between brain regions to characterize connection strengths. (III) An unweighted network can be constructed from the connectivity matrix by application of a threshold. A connection exists when the threshold value is passed.

Weighted & unweighted graphs

In a binary or *unweighted* graph, edges either exist or do not exist. This is a convenient way to model a network as analysis of such networks is relatively easy. However, most neural network reconstructions are based on correlations in structural or functional recordings such as MRI or EEG. An unweighted graph can be constructed by application of a threshold to these data; a connection exists when correlations pass this threshold. However, the choice for a certain threshold is arbitrary. Setting it too high will exclude relevant connections and may introduce unconnected vertices, while a low threshold will introduce non-existing or unimportant edges into the network. Moreover, valuable information on the strength of connections is discarded.

In contrast, *weighted* networks include information about connection strengths in the graph. This approach is more accurate in many real networks, for instance when describing how well people know each other in a social network. Most network measures have also been described for weighted networks, such as weighted path length L, weighted local clustering C, and degree correlation [193]. Note that in a weighted network, the shortest path is not necessarily the path with the least number of edges. The path length in weighted networks is best calculated by first calculating the efficiency. In the case that a path does not exist, the path length becomes infinite and the efficiency is zero. The average shortest path length of the network is then defined as the harmonic mean of the inverse of the efficiencies [164].

Despite these efforts to improve the accuracy of network modeling, it remains difficult to compare networks of different sizes and degrees. The size or total number of vertices can differ between networks and change network characteristics. At present, there is no consensus

in the field how to address these questions, and approaches differ between scientific groups.

Dynamic processes on complex networks

An interesting branch of research in modern network theory, that is highly relevant for neuroscience, is the relationship between structure and function. The relationship between network topology and synchronization dynamics on these networks is crucial in this respect, as a wide range of studies have pointed out that brain areas interact through synchronizing activity. In brief, network synchronizability characterizes the stability of synchronized state of the network. We suggest that network dynamics will be of increasing interest when studying communication patterns in brain networks. For a more detailed description of dynamic processing on complex networks we recommend reviews by Stam and Reijneveld [215], and Bocaletti et al. [29].

NETWORKS IN THE BRAIN

Neural network modeling and experimental studies

Watts and Strogatz were not only the first to model small-world networks, but also made the connection between graph theory and neuroscience. They showed that the clustering coefficient and average shortest path length of the C. Elegans nervous system follow the small-world principle [253]. The same was shown for cortico-cortical connection data of the cat and macaque [102]. A model study based on neuro-anatomical data found the brainstem reticular formation network best described as small-world. However, the degree distributions did not follow a power law in the models, making a scale-free architecture less probable.

Besides these studies on structural connections, some functional requirements have been formulated for neural networks. The brain must be able to perform specific tasks, which require areas of highly interconnected neurons. These processes need to be coordinated in a system that combines and plans these tasks [205]. Sporns and others defined neuronal *complexity* as a measure for the extent to which functional connectivity patterns combine local segregation with global integration. Moreover, as part of a biological system, the network has to be highly cost effective in terms of ‘wiring’ and energy use. Computational models have been used to study network facilitation of neural processing. They showed that when networks optimize for complexity, this leads to increased small-world characteristics and decreased ‘wiring costs’ [205].

The macaque cortex has also been used to study the correlation between anatomical and functional connectivity patterns. Functional networks proved to overlap with underlying structural networks in a computational model of macaque cortex [108]. Epileptic activity was used as a model for functional interactions. The spread of (epileptic) activity was shown to follow a small-world pattern in lesioned cortex in vivo, suggesting a correlation between anatomical and functional connectivity. Based on the epileptic activity in a large-scale cat cortex model, association fibers and their connection strengths seem useful predictors of global activation patterns [129].

Although structural networks determine functional connectivity patterns to an important extent [108], this interaction may also work the other way around. Functional connectivity seems to

play a role in the development of neural networks at a cellular level. Scale-free topology was found in developing functional networks of the rat and mice hippocampus [32]. GABAergic interneurons

with widespread axonal aborizations function as hub neurons, and play an important role in the shaping of the network topology and dynamics.

Human brain networks

Brain networks can be studied at various levels, ranging from structural cellular networks to functional interactions between brain areas. In this section we will focus on networks based on *in vivo* neuroimaging and neurophysiological data. Global findings seem generally in this field, but it is important to realize that differences in imaging techniques and the construction of networks may limit comparability [134]. Various measures exist for connectivity, and the method of choice when defining brain regions of interest can lead to different results [252].

Structural networks

Structural networks of the human brain have been constructed from MRI recordings. Connections between brain areas were defined as a cross-correlation in cortical thickness across individual brains [99]. This network was found to be small-world, and a modular structure was shown with resemblance to functional systems including the sensorimotor cortex and visual cortex [53]. Structural networks of grey matter areas have also been constructed using diffusion tensor imaging (DTI). Again, small-world topology was found. Also, several hub regions were identified, including the precuneus, the insula, and the superior frontal and parietal cortex, and parts of the human default mode network [98]. Interestingly, overall connectivity was higher in women, and their cortical networks were more efficiently connected than male functional networks [91]. Furthermore, local connectivity decreased with age, and older brains showed a shift of efficient connections (i.e. shorter path length) from parietal and occipital to frontal and temporal regions [91]. Changes in modular structure based on age have also been described [152]. These findings raise the question how structural neural network topology relates to functioning.

Functional networks

In this section, we will focuss on topological characteristics of the functional brain networks, how these functional structures arise during maturation, and how this correlates to brain functioning. Functional interactions between brain areas can be studied based on the concept of *functional connectivity*. Functional connectivity denotes the statistical interdependencies between elements of the system, for instance the synchronization of two simultaneously recorded EEG signals [3]. It is thought that synchronization is a key process in communication between different brain areas and cognitive functioning [244]. The ability of the network to facilitate synchronizing activity is therefore of great interest. Characteristics such as small-world index, average degree, degree distribution and degree correlation effect network synchonizability [7, 263]. For weighted graphs, random networks seem most likely to synchronize, followed by small-world networks and regular networks respectively [51].

Functional brain networks can be constructed by studying functional connectivity (i.e. correlation) between neurophysiological time series from several brain areas. A connectivity matrix is then constructed, which can be analyzed using graph theory. The connectivity matrix of electrophysiological recordings reflects a measure of synchronization or phase coupling of time series with a potentially high *temporal* resolution. Functional networks based on fMRI potentially have the highest *spatial* resolution, and are relatively easily compared with

structural MRI anatomical networks. However, as with structural MRI, these images do not directly contain information about the functional coupling of brain regions. It is possible to construct a matrix of functional connectivity based on blood-oxygen level dependent (BOLD) contrast fMRI [41]. A series of recordings is made of the subject, and the correlation of BOLD responses between different regions of interest (ROIs) is calculated.

Small-world topology in the human brain was first shown with functional connectivity analysis of MEG recordings of 5 subjects [208]. The first fMRI network study on 90 ROIs of the human brain also showed small-world topology [195]. A more recent study dramatically increased network size by performing voxel-based analysis of connectivity [241]. Neural networks appear to be not only small-world, but also scale-free, which was also found earlier in the macaque cortex [83, 241]. This would implicate a major role for functional hub nodes in the human brain network. Another study showed that two types of hubs could be distinguished within the fMRI network: hubs with long-distance connections to other regions, and more 'cliquishly' connected regions [2].

These findings implicate a modular structure of the functional human brain. As might be expected, modularity studies show that functionally or anatomically related brain regions are more densely interconnected [87, 153]. A hierarchical structure was found with five modules at the global level in both studies. Hub nodes were especially found in the association areas.

Brain network topology seems to have a genetically determined component. Graph analysis of EEG recordings of 574 twins and their siblings showed that clustering, path length and small-world topology are heritable characteristics [202]. Moreover, network topology changes during brain maturation [31, 224]. Boersma and colleagues followed 227 children and compared EEG recordings at the age of 7 to EEGs recorded two years earlier at 5 years of age. At age 7, the children had increased path lengths and clustering, and a decrease of weight correlation in comparison to the recording of two years earlier.

Supekar and others compared fMRI networks of children with young adults [224]. In children (ages 7-9 yrs), subcortical areas were more strongly connected with primary sensory, association and paralimbic areas. Cortico-cortical connectivity between paralimbic, limbic, and association areas was stronger in young adults (ages 19-22 yrs). Although all subjects showed small-world brain topology, hierarchy was higher in young adults, indicating a higher number of locally clustered hubs. Moreover, DTI-based wiring analysis showed that short-distance connectivity weakens during development, while long-range functional connectivity becomes stronger. This indicates a possible correlation between functional connectivity and maturation of the white matter tracts. These maturation studies indicate that the brain network evolves to a more efficient topology during maturation.

Intelligence and cognitive functioning are related to efficient functional network organization [242]. Micheloyannis and colleagues constructed unweighted graphs from EEG recordings [155]. Subjects with a few years of formal education (LE) were compared to subjects with university degrees (UE) during a working memory test. The LE group showed more prominent small-world topology during the test than the UE group, which was interpreted as a higher need for efficient network processing in this group. Van den Heuvel and colleagues analyzed fMRI BOLD images of 19 subjects and constructed voxel-based networks [242]. Subjects' IQs correlated with shorter path lengths. The correlation was found to be most prominent in the medial prefrontal gyrus, the precuneus, and bilateral inferior parietal regions. Moreover, efficient wiring seems to be related not only to functional, but also to structural network topology. Li and colleagues showed that structural network topology is related to intelligence in 79 subjects [140]. Subjects with high intelligence have more efficient networks, based on

DTI, than subjects with average intelligence. IQ test scores are correlated with the global efficiency of their structural networks.

In summary, the human brain network is characterized by small-world and possibly scale-free topology, found in both structural and functional brain networks. Network topology has a heritable component but becomes more efficient during maturation. Efficient brain network organization is crucial for cognitive functioning, and a more efficient network topology seems to be related to higher intelligence.

NETWORK ALTERATIONS IN BRAIN DISEASE

As described above, efficient functional network topology is thought to reflect optimal brain functioning. Application of graph theory to brain recordings may also provide better insight into underlying mechanisms as well as diagnostic markers for brain disease. Differences have been described for a range of neurological and psychiatric diseases, including brain tumors, Alzheimer's disease, epilepsy, and schizophrenia (for an overview see [187]).

In this section, we will focus on changes in functional connectivity and network architecture of patients with lesional epilepsy, some of whom having a brain tumor, as these pathological conditions are particularly relevant for neurosurgical practice. Brain tumors and epilepsy have high co-morbidity; the incidence of epilepsy is 30% or more in brain tumor patients, depending on tumor type [235]. Conversely, the incidence of brain tumors in epilepsy patients is 4% [235]. Temporal lobe epilepsy, which accounts for half of the medically refractory epilepsies, is characterized by sclerosis of the medial temporal lobe. A better understanding of network alterations due to lesions may help to explain the frequent occurrence of epileptic seizures in these patients. We will first describe the state of the art in graph theoretical analysis of brain tumor and epilepsy patients. We will then focus on future prospects of using functional connectivity analysis as diagnostic marker and as tool for pre-surgical planning.

Brain tumors

Since graph analysis in brain tumor patients is a very novel approach, studies are still relatively sparse. Our first study in these patients was published in 2006, comparing MEG recordings of patients with various types of brain tumors with healthy controls [9, 10]. A general decrease of broad band functional connectivity (0.5-60 Hz) was found in the patient group. Separate frequency band analysis showed increased connectivity in the delta to alpha frequency ranges in the patient group, while lower connectivity was found in the beta and gamma band. Remarkably, alterations were not restricted to the lesional area, but were also found within the contralateral hemisphere [10]. Unweighted network analysis showed more random networks in patients, as clustering was decreased in the patient group in the theta and gamma band, as well as path length in the theta, beta and gamma band [9].

Guggisberg and colleagues also analyzed MEG recordings for functional connectivity patterns of 15 brain lesion patients of mixed pathology, and compared them to a healthy control group [96]. Patients with lesion-induced neurological deficits had decreased connectivity levels in the lesioned areas compared to the contralateral homologue areas. Interestingly, areas

with decreased connectivity could be resected without any deficits after surgery, as long as patients had no neurological deficits prior to the resection.

In two subsequent MEG studies, we analysed a more homogenous group of 17 low-grade glioma (LGG) patients and compared them to 17 healthy controls matched for age, gender and educational level [33, 34]. Again, patients had increased connectivity levels in the lower frequency bands but also in the lower gamma band, now for long-distance connections. However, the increase in long-distance connectivity was also found in the lower gamma band, while a decrease was found in the lower alpha band. A highly interesting finding in this study was that the functional connectivity changes were related to poorer cognitive functioning in the patient group [33]. Increased connectivity levels were again found in the theta band of the patient group. Unweighted network analysis showed increased theta band and decreased beta band clustering in patients, as well as lower small-world index in the beta band and lower degree correlations in the gamma band [34]. Lower degree correlation, higher clustering and longer path lengths in the delta and lower alpha band correlated with poorer cognitive performance in the patient group.

Brain tumor patients thus seem to have widespread altered functional connectivity patterns that may correlate with their cognitive deficits. Moreover, the alterations may predict surgical outcome regarding neurological deficits. This raises the question how functional connectivity patterns relate to surgical intervention. We have studied functional connectivity in MEG recordings of 15 brain tumor patients before and after surgery [71]. Long-distance interhemispheric functional connectivity in the theta band was found to decrease after tumor resection, which was not influenced by several treatment- and tumor-related factors. We speculated that the decreased connectivity after surgery may reflect recovery to a normal state, based on abovementioned increased theta band connectivity. Indeed, patients with a larger decrease of theta connectivity were more often seizure-free after tumor resection. Changes in functional networks may thus well be related to vulnerability to tumor-related epilepsy, especially in the theta band, as we will describe in section 4.4.

Summarizing these findings, we conclude that altered topology is found in the functional networks of brain tumor patients, along with widespread changes in functional connectivity. These changes seem to be related to cognitive deficits in these patients. Several clinical factors may be of influence on connectivity changes, such as tumor pathology, epilepsy and treatment, which is described in chapter 4 of this dissertation. Network analysis seems a promising tool to better predict surgical outcome, which should be subject of further research.

Epilepsy

Synchronization is crucial for information processing in the brain. However, it is also an important characteristic of epileptic seizures [138, 233]. Synchronization patterns not only differ between the ictal and interictal state, but also change during a seizure. Connectivity changes over a broad range of frequencies were found in EEG recordings prior to and during seizures in focal and absence epilepsy patients [180, 182, 199]. Graph analysis showed a regularization of network topology during seizures in the broad frequency band (0.5-70 Hz), but most explicit in low frequencies (below 13 Hz). A more detailed study at seizure onset by Kramer and others suggests that network changes have patient-specific topographical characteristics [131]. They studied intracranial EEG recordings of four pharmacoresistant epilepsy patients. Again, the average path length became longer during ictal activity, and small-worldness increased, as did *betweenness centralization* (which is a measure similar to *degree correlation* described in section 2.3). In general, the degree decreased, while clustering changes were reordered differently depending on topographical localization.

Modeling studies

These findings raise the question what triggers the transition towards a pathologically synchronized state, as this might explain how seizures arise. Several model studies of seizure dynamics have suggested that epilepsy patients have altered network topology not only during seizures, but also in the interictal state. Netoff and others were the first to study neural excitation activity in epileptogenic networks, using a hippocampal slice network model [163]. A small-world network was rewired with an increasing number of long-distance connections, making the network more random. Results showed that excitation levels changed from normal to seizure-like activity to bursting activity. Bursting activity was also found in interictal electrophysiology recordings, indicating that epilepsy patients may have more random interictal networks compared to healthy individuals. Dhyrfield-Johnsen and colleagues simulated medial temporal sclerosis in a computational model network by removing long-distance connections [82]. This initially increased the local clustering of the network as well as hyperexcitability. Local clustering decreased when the number of long distance connections was further decreased. Morgan and Soltesz hypothesize that networks of epilepsy patients are characterized by 'pathological hubs' that increase epileptic activity [161]. They showed that the incorporation of a small number of highly interconnected hub cells greatly increases synchronizing network activity in a rat dentate gyrus model. The network became hyperexcitable and possibly seizure-prone.

These modeling studies together with mathematical network modeling studies suggest that several factors of network topology contribute to the vulnerability for seizures, including path length, clustering and the number of hubs. Further research is needed to elucidate the interactions between measures such as overall connectivity levels, degree distribution, and synchronizability measures such as the eigenvalue ratio. Studying these interactions should lead to a integrated model for epilepsy and network topology.

Epilepsy patient studies

Several imaging techniques have been used to study alterations in functional brain networks of epilepsy patients during the interictal phase. Bettus and colleagues found a general decrease of connectivity in an fMRI study comparing mesial temporal lobe epilepsy (MTLE) patients to healthy controls [25]. Temporal connectivity on the contralateral side of the lesion seemed to be increased, which was interpreted as a possible compensation mechanism. Liao and others showed increased connectivity in the lesioned area but decreased connectivity between inferior frontal triangular and opercular regions correlated with epilepsy duration in fMRI recordings of MTLE patients [141]. Frontal and parietal within region connectivity was decreased as well as connectivity between frontal and parietal regions. The default mode network seemed to have less connectivity with other regions in patients. Network analysis showed lower path length and clustering in patients compared to healthy controls, indicating network randomization in MTLE epilepsy patients.

We recently studied the feasibility of functional connectivity of interictal EEG recordings as a diagnostic tool for epilepsy after a first seizure-like collapse [74] . We found that theta band connectivity of interictal EEG recordings was already increased in epilepsy patients after their first seizure. Moreover, increased theta band connectivity was predictive for a second seizure while visual inspection of the EEG showed no abnormalities. Horstmann and others compared interictal EEG recordings of anti-epileptic drug (AED) resistant epilepsy patients to healthy controls. Increased functional connectivity levels were found in patients in the delta, theta, and beta frequency bands of EEG recordings [110]. Weighted networks of the EEG recordings

showed increased path lengths and clustering in patients in several frequency bands.

In two recent studies we analysed MEG recordings of focal epilepsy patients with different lesion types, and compared them to healthy controls [78, 238]. Functional connectivity levels showed no alterations in patients compared to controls, but theta band PLI was correlated with seizure

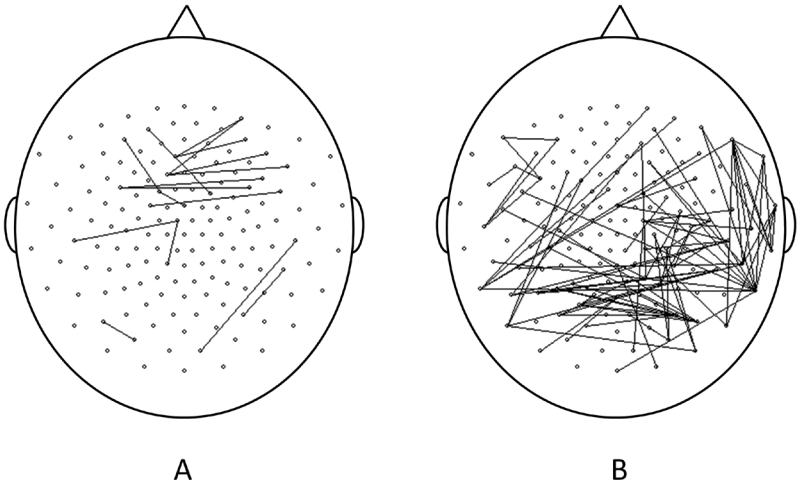

Figure 3. Altered functional connectivity in lesional epilepsy patients. Theta band (4-8 Hz) functional connectivity differences ($p < 0.01$) between lesional epilepsy patients and healthy controls derived from MEG recordings [238]. Connections that are decreased in patients are shown in the left figure, connections with increased strength in patients are shown on the right. In general, connections in patients seem increased, especially in the central, occipital and parietal regions of the right hemisphere.

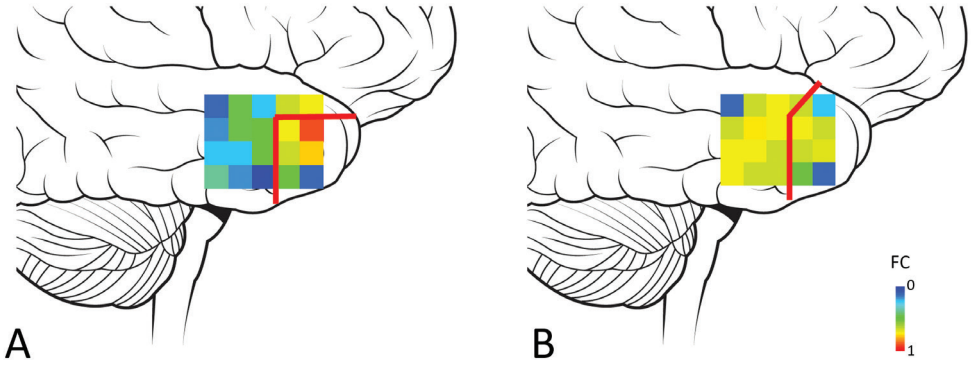

Figure 4. Functional connectivity and surgical outcome. Functional connectivity as measured on the temporal lobe with ECoG recordings during repilepsy surgery, based on Ortega and colleagues [173]. Resection borders are marked by red lines, the colored squares indicate functional connectivity levels of 4 x 5 grid electrodes. (A) Functional connectivity is shown to have a peak value in the resected area which is surrounded by lower connectivity levels. Resection of such a sharply defined connectivity peak is associated with good surgical outcome regarding seizure burden. (B) When no clear synchronization cluster is present or the synchronization cluster is not resected, the patient is less likely to be seizure-free after surgery.

frequency in the patient group. Clustering was higher in the theta and lower alpha band, while theta band path lengths tended to be longer in the patient group. Moreover, theta band path length was positively correlated with time since first seizure and seizure frequency. The correlation between epilepsy duration, functional connectivity and network topology was also found using fMRI and electrocorticography (ECoG) recordings of the lesioned area of MTLE patients [141, 237]. Our MEG and ECoG studies also showed differences in network topology between patients on AED polytherapy compared to patients on monotherapy. Finally, lesion type also had some effect on network topology in MEG recordings: networks showed more alterations in LGG and non-glioma patients than HGG patients [238].

Summarizing these findings, research has shown alterations of connectivity levels and network topology in lesional epilepsy patients. Altered connectivity patterns correlate with epilepsy duration in several studies. Increased theta band path lengths show correlations with several factors that determine epilepsy burden, such as epilepsy duration, seizure frequency, and AED monotherapy or polytherapy. Theta band connectivity analysis of EEG and MEG recordings seems promising as diagnostic tool for epilepsy patients.

Localization of the epileptic zone

Several studies have focused on more specific spatial alterations in functional networks of epilepsy patients in order to find markers of the epileptic zone from which seizures arise. Bettus and others compared functional connectivity patterns in EEG recordings of mesial temporal lobe epilepsy (MTLE) patients to those of patients with epilepsy of other origin (non-MTLE) [27]. A general increase of connectivity was found in the epileptic zone of the MTLE patients compared to the same areas in the non-MTLE group in the 3.4-97 Hz frequency range.

Ortega and colleagues used connectivity analysis of ECoG recordings to predict effectiveness of surgical intervention [173]. When sharply defined connectivity peaks were found in the preoperative recordings, resection of these peak areas was positively related to surgery outcome. More equally distributed functional connectivity patterns before surgery were related to poorer outcome. In a second study on five patients with similar pathology, the authors suggested that removal of hub nodes may be crucial for successful treatment, as these hub nodes seemed involved in the development of seizures [174].

A promising approach for the identification of seizure onset zones, even without the need for invasive electrophysiological recordings, is modularity analysis. Chavez and others studied modular structures in MEG recordings of five absence epilepsy patients and five healthy controls [52]. Networks were constructed in the 5-14 Hz frequency range, combining theta and alpha band ranges. Patients were shown to have less modules than healthy controls, and the connections between modules were stronger in the patient group. Connectivity levels within the module showed only minor differences between groups. This study indicates that especially intermodular (hub) connections may play an important role in absence epilepsy. Future research is needed to elucidate whether altered modular structures are a general feature of changing networks across epilepsy types. Moreover, it would be highly interesting to see whether provincial or interregional connector hub nodes can be used to identify epileptic zones in MEG recordings.

(IMPACT OF) SURGERY

Neurosurgical resection can be seen as the infliction of an acute brain lesion. It might be expected that lesions with a sudden occurrence in the brain have a different impact on brain networks than slowly developing lesions, such as tumors. How acute brain lesions directly affect functional connectivity and networks is difficult to study, as ideally one would like to have imaging of the same brain in a healthy and a lesioned state. We already mentioned our study of connectivity before and after tumor resection, in which networks seemed to return to a 'healthy' topology [71]. However, this study focused on patients in which the brain was already damaged due to a tumor. In this section, we will discuss some modelling and clinical studies that indicate how neurosurgical intervention affects network topology.

Model studies

Modelling studies on the impact of brain lesions on connectivity and network topology have shown that neural networks are most vulnerable for targeted attacks on hubs. It was found in a cat and macaque cortex connectivity model that random attacks have only minor effects on path lengths, while targeted attacks on important nodes have a major impact on the global integration of the network [119]. Scale-free networks had most similarities regarding robustness against lesions with the brain networks. A model based on human diffusion MRI maps with known structural connections showed that targeted attacks also cause great disturbance on functional interactions, whereas random attacks had relatively little impact. [4]. Moreover, some of the most disruptive lesion sites were found to be central nodes that corresponded to regions where lesions are known to produce complex cognitive disturbances, and were located within the 'default mode network'. Another modelling study on the effects of lesions found that the most densely connected neural regions synchronize most easily [109]. Again, lesioning the nodes with most connections, especially connector hubs, had the largest impact on cortico-cortical interactions. Given the importance of provincial and connector hubs in this model, findings also indicate that modular structure might affect robustness against targeted lesions.

A stroke is an acute brain lesion of the brain that may have similar impact on brain dynamics. Only one report describes a comparison of a (right capsula interna) stroke patient with 8 healthy controls before and during a motor task [67]. EEG recordings were used to construct unweighted networks, and the patient's network was compared to that of healthy controls. Unweighted networks were reconstructed from this functional connectivity data, and the patient's network was compared to that of healthy controls. Decreased local and long-distance network efficiency was found in the beta and gamma frequency range for the patient. This indicates that less optimal network topology may be related to neurological deficits in stroke patients. Further research in a larger population, possibly with more sophisticated network analysis would be of great interest in these patients.

Clinical studies

We used the Wada test as a model for acute brain lesions in patients in [72, 77]. The Wada test or intra-arterial amobarbital procedure (IAP) is used to assess functioning of the brain after 'shutting down' one hemisphere with amobarbital as part of pre-surgical screening in pharmaco-resistant epilepsy patients. Functioning of the non-anaesthetised hemisphere can

temporarily be assessed by means of neuropsychological testing, while the EEG is recorded. A consistent increase of connectivity was found in the injected hemisphere after injection. Contralateral and interhemispherical functional connectivity decreased in the delta and theta band after injection, while connectivity increased in the beta band. We recently performed graph analysis on the same data set [77]. Weighted clustering decreased after injection in the theta, alpha, and beta bands. There was also a decrease of the path length in the theta and alpha bands. Moreover, edge weight correlation decreased in the theta and beta band after injection. These alterations all indicate that the whole neural network becomes more random after sedation of one hemisphere, replicating the pattern observed in brain tumor patients. We also analysed the correlation between memory performance during the Wada test with network topology after injection. Increased small-world topology in the theta band, as well as longer path lengths in the alpha band, were correlated with better memory scores, indicating direct associations between network topology and cognitive functioning.

In the previous sections, we have shown that brain tumors and epilepsy are related to altered functional networks. Resective surgery may also lead to global changes in functional network topology, and should be seen in this respect as a targeted attack of brain networks. We will give our vision on the future use of network theory in surgical planning in the final section of this chapter.

CONCLUSIONS AND FUTURE PROSPECTS

In this chapter, we have shown that efficient brain network organization is crucial for optimal functioning. Moreover, network topology is disturbed in a wide range of neurological patients. Particularly brain tumor and lesional epilepsy patients may benefit from presurgical mapping of functional and structural networks. A better identification of the epileptic zone and target areas for surgical resection based on network analysis could in the future be used to guide surgical procedures and improve surgical outcome. It may also help to improve prediction cognitive deficits due to surgery, as well as post-surgical seizure burden in epilepsy patients. We consider the application of network analysis in the clinical setting an ultimate and feasible goal of this research.

The rising field of network analysis of the human brain brings a rapidly increasing understanding of neural network functioning, but improved methodology is still needed for clinical application. Several issues need to be addressed before findings in different studies can be properly compared. The size of the constructed networks is still limited by technical and computation power. Moreover, no paradigm exists to properly compare networks of different size. Finally, it remains to be studied how functional networks relate to structural networks, or even how networks constructed from neurophysiological recordings such as EEG and MEG relate to those based on fMRI [41, 181].

Connectivity characteristics may provide markers for specific cognitive tasks. A lot of research in large populations is needed to clarify these interactions and to make it possible to take inter-subject variations into account. However, findings in both structural and functional imaging

studies seem promising [34, 140, 242]. We speculate that advanced network analysis of functional modularity and path length and centrality per node may play an important role in the characterization of these markers.

The number of studies on the use of functional connectivity for the identification of epileptic onset zones and crucial areas for seizure spread has increased dramatically over the past years. Results of this increasing number of studies are not consistent yet, but begin to shape the prospects for clinical application. Theta band connectivity and networks based on MEG, EEG, and ECoG recordings seem to be essential in this respect, as it correlates with several factors determining epilepsy burden, including seizure frequency, duration and AED use [34, 71, 110, 237]. We have already demonstrated the possible value of theta band functional connectivity for diagnosing epilepsy after a first collapse in patients without visually detectable disturbances on EEG recordings [74]. Moreover, ECoG connectivity seems to have predictive value regarding seizure outcome [173, 174]. A properly funded definition of epileptic hub nodes seems to be a pivotal step towards clinical application of network analysis in the neurosurgical treatment of epilepsy.

CHAPTER 3

Long-term effects of temporal lobe epilepsy on local neural networks: a graph theoretical analysis of corticography recordings

E van Dellen, L Douw, JC Baayen, JJ Heimans, SC Ponten, WP Vandertop, DN Velis, CJ Stam, JC Reijneveld

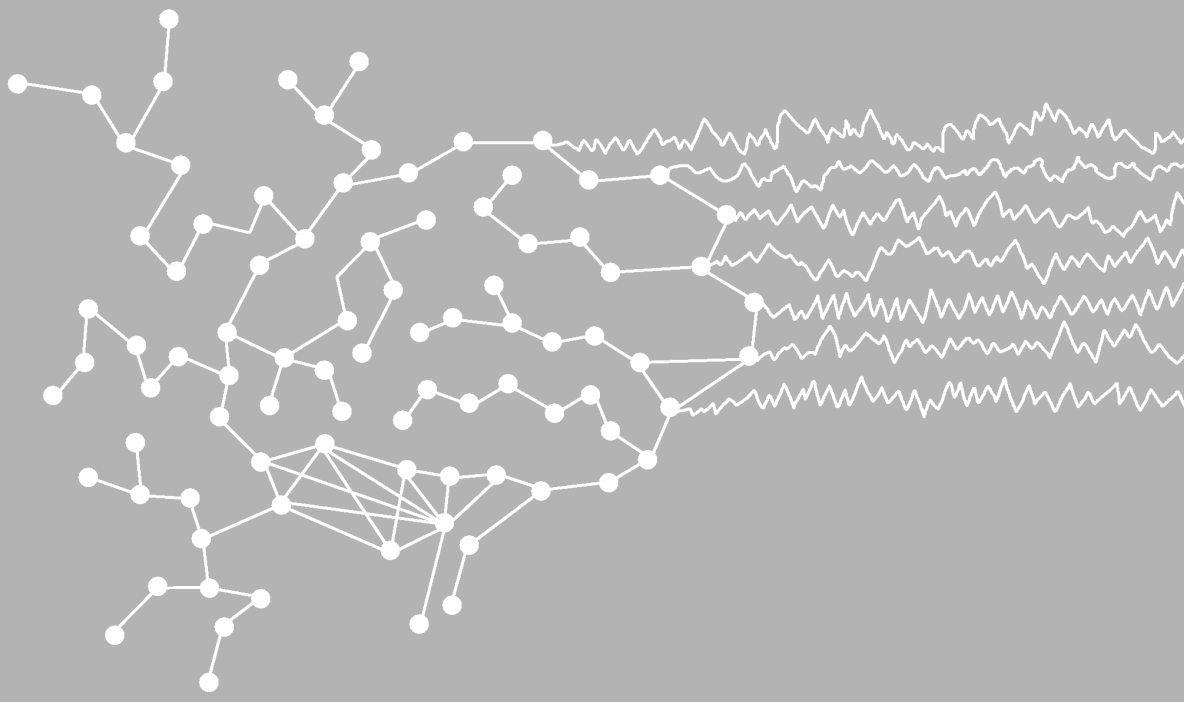

PLoS One (2009) 4(11), e8081.

ABSTRACT

Pharmaco-resistant temporal lobe epilepsy (TLE) is often treated with surgical intervention at some point. As epilepsy surgery is considered a last resort by most physicians, a long history of epileptic seizures prior to surgery is not uncommon. Little is known about the effects of ongoing TLE on neural functioning. A better understanding of these effects might influence the moment of surgical intervention. Functional connectivity (interaction between spatially distributed brain areas) and network structure (integration and segregation of information processing) are thought to be essential for optimal brain functioning. We report on the impact of TLE duration on temporal lobe functional connectivity and network characteristics. Functional connectivity of the temporal lobe at the time of surgery was assessed by means of interictal electrocorticography (ECoG) recordings of 27 TLE patients by using the phase lag index (PLI). Graphs (abstract network representations) were reconstructed from the PLI matrix and characterized by the clustering coefficient C (local clustering), the path length L (overall network interconnectedness), and the 'small-world index' S (network configuration). Functional connectivity (average PLI), clustering coefficients, and the small-world index were negatively correlated with TLE duration in the broad frequency band (0.5–48 Hz). Temporal lobe functional connectivity is lower in patients with longer TLE history, and longer TLE duration is correlated with more random network configuration. Our findings suggest that the neural networks of TLE patients become more pathological over time, possibly due to temporal lobe changes associated with long-standing lesional epilepsy.network analysis have shown to be a promising tool in studying epilepsy and brain tumor patients. Changes in network characteristics and functional connectivity have been associated with both epilepsy and brain lesions [9, 10, 132, 136]. We therefore consider that changes in functional connectivity and network configuration may be a marker of possible progression of TLE. We hypothesize that functional interactions in the brain are correlated to temporal lobe epilepsy duration. We expect to demonstrate a correlation between TLE duration and changes in network characteristics of the temporal lobe. We expect less functional connectivity and a more random configuration of the temporal neural networks as TLE duration increases.

INTRODUCTION

Epilepsy surgery is often a more effective way to treat temporal lobe epilepsy (TLE) than antiepileptic drugs (AEDs) [195, 261], but it is considered a last resort by many physicians. This reluctance can be explained by a failure of the surgical procedure to alleviate epileptic seizures in a considerable number of cases and by the risk of postoperative cognitive and visual deficits. Another reason for a delay in surgery is that TLE is often characterized by periods of remission with relative seizure freedom [22]. As a result, a history of epileptic seizures of 10 to 20 years prior to surgical intervention is not uncommon [23].

As most patients in whom surgery is considered suffer from TLE for a period of at least several years, it is important to understand how this ongoing disease interferes with brain functioning. If a prolonged disease course has a negative impact on brain functioning in TLE patients, this would support the importance of early surgical intervention. However, relatively little is known about the natural history of TLE. It is often preceded by an initial precipitating injury, of which a complex febrile seizure is the most common [151]. Hereafter, a latent period tends to occur, followed by recurrent, spontaneous seizures, indicating that TLE might be a progressive disease [28]. When looking at structural damage related to epileptic seizures, progressive volume loss of the hippocampus, amygdala and the entorhinal cortex has been described as a consequence of ongoing TLE [23]. A correlation between the number of brain structures with epileptogenic characteristics and epilepsy duration has been described in TLE patients [11]. It is not known how functional neural networks change during disease progression, and what the impact of changes is on seizure initiation and propagation. However, a contralateral increase of functional connectivity for TLE patients has been described [25].

In modern neuroscience, the brain is increasingly seen as a complex network of dynamical systems with interactions between local and further remote brain regions. A way to explore the interactions between brain regions is to look at functional interactions, also called functional connectivity. Functional connectivity refers to the statistical interdependencies that exist between neurophysiological time series [216]. Electrocorticography [132] and depth electrode [13, 181, 200] studies have shown that network synchronization in the temporal lobe increases during a seizure when compared to the interictal and postictal states. Several studies indicate that a predisposing state exists prior to a seizure, which is characterized by desynchronization or hypersynchronization in different surrounding brain areas [136, 143, 258]. The changing synchronization patterns may be explained by the impact of brain disease on the spatial network configuration of the brain. These changes can be studied using a ‘graph’ theory approach [216]. A ‘small-world’ network is thought to be the optimal network configuration for brain functioning [255]. In such a small-world network, local integration is high, while the overall integrity of the network is also maintained (see figure 1 in chapter 2). Social networks, the Internet, and the healthy brain are examples of networks that show these characteristic small-world features [216]. It is suggested that changes in network characteristics occur in epilepsy patients, leading to a pathological, more random structure in the interictal state, which is temporarily reversed during a seizure [9, 132, 178, 200]. These changes in configuration may lead to disturbed higher brain functions and further lower the brain’s threshold for epileptic seizures (for a review see reference [41]).

A better understanding of the effects of ongoing TLE on neural functioning might influence the timing of surgical intervention. Functional connectivity and neural network analysis have

shown to be a promising tool in studying epilepsy and brain tumor patients. Changes in network characteristics and functional connectivity have been associated with both epilepsy and brain lesions [9, 10, 132, 136]. We therefore consider that changes in functional connectivity and network configuration may be a marker of possible progression of TLE. We hypothesize that functional interactions in the brain are correlated to temporal lobe epilepsy duration. We expect to demonstrate a correlation between TLE duration and changes in network characteristics of the temporal lobe. We expect less functional connectivity and a more random configuration of the temporal neural networks as TLE duration increases.

METHODS

Patients and Data Selection

All pharmaco-resistant TLE patients who underwent temporal lobe surgery and intra-operative ECoG recordings at the VU University Medical Center in Amsterdam between October 2003 and September 2005 were eligible for inclusion in this study. The VU University Medical Center is a tertiary referral centre for epilepsy surgery as part of the nationwide Dutch Collaborative Epilepsy Surgery Program.

Intra-operative neocortical registrations were performed using 465 subdural electrode grids (interelectrode distance 1 cm; see figure 1) and recorded with a Brainlab digital EEG system (OSG, Rumst, Belgium). Sample frequency was 500 Hz. The grid was placed directly on the lateral temporal cortex, covering T1-T3. The grid position was documented during the procedure on schematic representations of the brain. For every patient, five artifact-free epochs of 4096 samples (8.19 s) were selected off-line by careful visual inspection [ED, CJS]. All selected epochs were recorded while patients were in an interictal state (as determined by the ECoG recording) and before resection of the lesion had taken place.

Patients were sedated with propofol during surgery. Due to the retrospective nature of this study, there was no standardized protocol to control the amount of anesthesia while recording ECoG. As the level of sedation might influence the ECoG, the burst suppression ratio (BSR) of the recordings was calculated and used as a covariate in the analysis (See Figure S1 for an example of used ECoG data). The BSR is the sum of all the regions showing at least 0.5 seconds of suppression, divided by the total length of the epochs (40.95 s). Suppression was defined as a region with very low ECoG activity, using 5 microV as threshold value [186].

Ethics statement

The data were obtained for clinical purposes with patient consent for all performed procedures. As a retrospective study this work was exempt from ethical approval. Data were analyzed anonymously. All clinical investigations were conducted according to the Declaration of Helsinki.

Functional Connectivity

Selected epochs were converted to ASCII files for further analysis with DIGEEGXP software, developed in our department [CJS]. Five selected epochs per patient were filtered in the broad frequency band (0.5–48 Hz). The phase lag index (PLI) was used to calculate functional connectivity of the selected epochs [215]. The PLI measures the asymmetry of the distribution

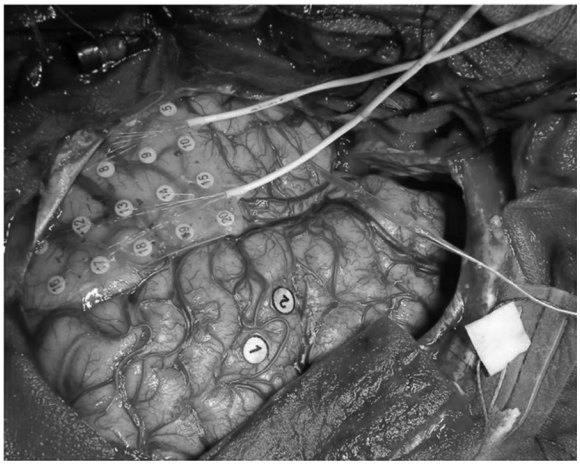

Figure 1. Intra-cranial corticography recording. Picture of a grid, placed directly on the cortex for intra-cranial recording.

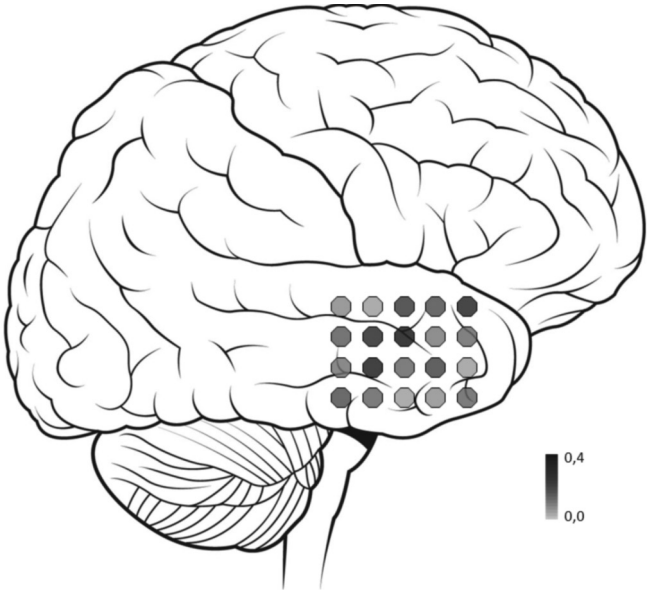

Figure 2. Visualization of the functional connectivity pattern over the temporal lobe. A grid of 4x5 electrodes is placed directly on the temporal lobe and the registered area is schematically documented. Five Epochs of representative ECoG recordings are selected per patient. The PLI values are calculated based on these recordings, resulting in a matrix with synchronization values for all possible electrode combinations. The figure shows a mean PLI value for each grid electrode based on this synchronization matrix, representing the average synchronization with the other channels.

of instantaneous phase differences between different electrophysiological signals, in this case ECoG recordings, that can be obtained from a time series of phase differences ΔΦ (tk), k=1 . . . N in the following way:

$$\mathrm{PLI} = \left| \left\langle sign\left[\sin\left(\Delta\phi(t_k) \right) \right] \right\rangle \right| \quad (1)$$

The PLI rules out volume conduction as a confounding factor, since the presence of a consistent, nonzero phase lag between two time series cannot be explained by volume conduction alone. The PLI is therefore less effected by common sources, while performing at least as well as the synchronization likelihood (SL) [160] in detecting true synchronization. The PLI ranges between 0 and 1. A PLI of more than 0 indicates phase locking to a certain extent, whereas a PLI value of 0 indicates no coupling or coupling with a phase difference centered around 0±π radians. For a detailed description of PLI calculation, see reference [214]. The PLI was calculated between all channels, resulting in a 20 by 20 channel matrix. The overall (whole-grid) PLI was computed by averaging all PLI values. To visualize functional connectivity, we projected the PLI scores per channel over a schematic grid representation,showing the average synchronization of the channel with the other channels of the grid (see figure 2).

Graph analysis

We hypothesize that network topology, and not just average strength of synchronization as indicated by PLI, is correlated with epilepsy duration in our study population. A graph is a basic topographical representation of a network that consists of nodes ('vertices') and connections between these nodes ('edges') [253]. Graphs are characterized by a clustering coefficient C and a characteristic path length L. The clustering coefficient C, which is the likelihood that neighbors of a vertex will also be connected, is a measure for the tendency of network elements to form local clusters. The characteristic path length L is the average of the shortest distance between pairs of vertices counted as a number of edges. The path length L indicates how well network elements are integrated or interconnected [253].

To compute the clustering coefficient C and the characteristic path length L from the PLI of the ECoG data, we used the methods described by reference [213]. The first step in applying graph theoretical analysis to synchronization matrices is to convert the NxN PLI matrix into a binary graph, with N as the number of channels used. A binary graph is a network that consists of vertices and edges (undirected connections between elements). The PLI matrix can be converted to an unweighted graph by considering a threshold T. If the PLI between a pair of channels i and j exceeds T, an edge is said to exist between i and j; otherwise no edge exists between i and j.

Differences between the patients in average PLI can influence C and L when it is computed for a threshold T, because a lower PLI trivially results in less edges. To control for the influence of the number of edges, we applied several fixed values of k (k=3, k=4, k=5), where k denotes the average number of edges per vertex. By using this method, graphs in both groups are guaranteed to have the same number of edges. We followed the suggestion of reference [253] for the minimal k value for a network with size N (here 20), such that a random network generated by using this k will still be fully connected: $N \geq k \geq L_n(N)$. In the current study, this was true for k≥3. K values between 3 and 5 have been used in previous studies with a similar network size [156, 213].

Once the PLI matrix has been converted to a graph, the next step is to characterize the graph in terms of its clustering coefficient C and characteristic path length L. The path length L

was calculated as 'harmonic mean' distance between pairs as described by reference [146], making it possible to deal with vertices that are not connected. The values of C and L for every k were compared to 1000 random surrogate matrices, generated as described by reference [149], by calculating the ratio between the C and L of the patient and the surrogate data (referred to as Cs and Ls). To analyze the small-world characteristics of the network we used the measure of small-world index S [112], which is defined as $S=(C/C_s)/(L/L_s)$. A network can be defined as a small-world network if $C/\langle C_s \rangle >>1$ and $L/\langle L_s \rangle \sim 1$, which means that any value of S greater than 1 is account for small-world network.

Statistical Analysis

All statistical analyses were performed using SPSS 15.0 for Windows (SPSS Inc., Chicago, USA). Possible correlations between age, age of epilepsy onset and epilepsy duration were analyzed by means of Pearson's correlation coefficients.

Analysis of the correlation between epilepsy duration and the type of lesion or type of epilepsy was done using independent t-tests (MTS versus tumor; partial versus generalized seizures) and one-way ANOVA (differentiated for multiple types of lesions and seizures).

In order to analyze correlations with seizure frequency, BSR, PLI and network variables, non parametric tests were used, because these variables were not normally distributed. Correlations between PLI and network characteristics and epilepsy duration, age, age of epilepsy onset, seizure frequency, and BSR, were analyzed by means of Kendall's Tau correlation coefficients. Possible effects of gender, seizure type (partial or generalized), nature of the lesion (tumor, vascular or mesial temporal sclerosis), and AEDs (monotherapy or polytherapy) on PLI and network characteristics were analyzed by means of Mann Whitney nonparametric U-tests.

Since multiple correlations were analyzed, a Bonferroni correction was performed.

RESULTS

Patient Characteristics

The files of a total of 27 TLE patients (mean age 40 years, 41% male) were analyzed (for patient characteristics, see table 1 and 2). Surgical outcome after one year was documented according to the modified Engel scale [85]. Three patients showed artifacts in the ECoG recordings, which occurred in one channel (one patient) or two channels (two patients). These artifacts were caused by bad contacts between the grid and the temporal brain surface. The artifact channels were excluded from further analyses in these patients.

Four correlation coefficients were calculated regarding epilepsy duration and its correlation with other patient characteristics (age, age of epilepsy onset, BSR, seizure frequency). A Bonferroni correction for multiple analysis was performed, determining that significant correlations were found only when $p<.013$ level was reached.

Functional Connectivity

The overall PLI was significantly correlated with the history of epilepsy: PLI was lower when epilepsy duration was longer (Kendall's Tau=20.389; p=.005; see figure 3). Correlations

with PLI are shown in table 3. We found a significant correlation between the PLI and BSR, indicating that a higher level of sedation was correlated with increased PLI. Also, higher PLI was correlated with a higher age of onset. No correlation was found between seizure frequency and PLI. The significance level was set at $p<0.013$ for correlations of patient characteristics (epilepsy duration, age of onset, BSR, seizure frequency) with PLI, because four correlations were calculated. The correlations between epilepsy duration and BSR with PLI, remained significant after the Bonferroni correction.

Group comparisons were made to analyze possible correlations between gender, lesion type or single versus multiple AED use and PLI. Mann-Whitney U Test showed a significantly lower PLI in patients using multiple AEDs (M=0.159) when compared to single AED use (M=0.207). No correlation was found between lesion type or gender and PLI. The PLI difference for single versus multiple AED use remained significant after Bonferroni correction ($p<.025$ as two comparisons were calculated).

Graph Analysis

The clustering coefficient C and small-world index S were correlated with history of epilepsy for an average degree k=3 (Kendall's Tau (C) =20.346; p=.013 and Kendall's tau (S)=20.360; p=.009 respectively; see figure 4). The correlation of epilepsy duration with the small-world index S remained significant after Bonferroni correction, determining correlations to be significant when p=.013 was reached. The clustering coefficient C showed a correlation with epilepsy duration at a significance level of p=.013, which was the same as the cut-off point for significance after Bonferroni correction. An example of a network distribution over the ECoG grid is shown in figure 5.

When using an average degree k=4, clustering coefficient and small-world index tended to be correlated to epilepsy duration (Kendall's tau (C)=20.236; p=.090 and Kendall's tau (S) =20.226; p=.103 respectively), but did not reach the significance level ($p<.013$). No group differences were found regarding graph analysis when using k=5.

There were no significant correlations between gender, age of epilepsy onset, AED use, or BSR with respect to clustering coefficient C, path length L, and small-world index S for the used values of k. However, a correlation was found between seizure frequency and clustering coefficient C and between seizure frequency and small-world index S for k=3: higher seizure frequency was associated with higher local clustering and a higher small-world index of the network. These correlations were still found to be significant after Bonferroni correction (significant correlation when $p<.013$). There were no correlations between seizure frequency and local clustering, path length, and small-world index for k=4 and k=5.

Several interactions between patient characteristics were analyzed, as mentioned in the methods section (table 2). A significant negative correlation was found between epilepsy duration and age of epilepsy onset (Pearson correlation=20.589; p=.001), indicating that patients with a longer epilepsy duration were younger at epilepsy onset. We also found a negative correlation between epilepsy duration and seizure frequency (Kendall's Tau =20.378; p=.009). This indicates that patients with a longer history of epilepsy had a lower seizure frequency. Epilepsy duration tended to be negatively correlated with the BSR (Kendall's Tau =20.307; p=.030), indicating a lower sedation level during ECoG recordings in patients with a longer epilepsy duration. However, the significance level for this interaction was no longer reached after Bonferroni correction. No other interactions were found between the patient characteristics.

Table 1. Clinical data

Patient	Gender	Age	Duration	Seizure type	Path	Outcome
1	F	36	22	Partial simple and complex	DNET	1A
2	M	41	5	Partial simple and complex	MTS	1B
3	F	35	3	Sec. generalized; partial complex	LGG	1A
4	M	49	42	Partial complex	MTS	1A
5	M	41	0	Partial simple and complex	LGG	1B
6	M	21	3	Generalized; partial complex	DNET	1A
7	M	18	12	Partial complex	MTS	1D
8	M	57	3	Partial complex	AVM	1A
9	F	68	32	Partial complex	MTS	1A
10	F	48	15	Partial complex	Unknown	1A
11	F	17	16	Generalized	MTS	1A*
12	M	38	36	Partial complex	MTS	1A
13	F	20	3	Partial simple	MTS	1A
14	F	37	30	Partial complex	MTS	1A
15	F	35	25	Generalized; partial complex	LGG	1A
16	F	52	50	Generalized; partial complex	MTS	1A
17	F	25	24	Sec. generalized; partial simple and complex	MTS	IIA
18	M	67	20	Generalized; absence, partial complex	HAEM	IID
19	F	42	15	Generalized, partial complex, partial simple	LGG	1A
20	M	50	4	Absence	HAEM	1A
21	M	33	21	(Sec.) generalized; partial complex	MTS	IIB
22	F	50	25	Sec. generalized; partial complex	MTS	IIB
23	F	41	4	Partial simple and complex	HAEM	1A
24	F	28	8	Sec. generalized; partial simple	MTS	1B
25	F	42	28	Generalized; partial complex	MTS	IID
26	M	41	25	Partial complex	Unknown	1B
27	F	43	15	Sec. generalized; partial simple and complex	MTS	1A

*F=female, M=male, Duration=epilepsy duration (years), Path=pathology, DNET=dysembryoplastic neuroepithelial tumor, MTS=mesiotemporal sclerosis, LGG=low-grade glioma, AVM=arteriovenous malformation, HAEM=haemangioma, Unknown=tumor of unknown pathology, Outcome=clinical outcome one year after surgery according to Engel's scale of epilepsy burden, 1A=seizure free, 1B=non-disabling partial seizures, 1C=some disabling seizures, 1D=generalized seizures only when AED is stopped, IIA=first seizure-free, now rare seizures, IIB=rare disabling seizures; IIC=more than rare disabling seizures since surgery, IID=nocturnal seizures only. * data were only available at 6 months after surgery.*

Table 2. Group characteristics

Characteristic	Total (N=27)	STLE (N = 9)	LTLE (N =18)	p
Age ± SD (years)	40 ± 13	37 ± 12	41 ± 14	.470
Gender (%)				.441
Male	41	56	33	
Female	59	44	67	
Type of lesion (%)				.217
MTS	56	33	67	
Other; of which	44	67	33	
LGG	15	22	11	
DNET	7	11	6	
Haemangioma	11	22	6	
AVM	4	11	0	
Unknown	7	0	11	
Age of onset ± SD (years)	22 ± 16	33 ± 13	16 ± 14	.004*
History of epilepsy ± SD (years)	18 ± 13	4 ± 2	25 ± 10	<.001*
Seizure frequency (per year) ± SD	348 ± 597	1147 ± 499 (N=8)	396 ± 687 (N=17)	.009*
Type of epilepsy (%)				1.000
Partial	56	56	56	
Generalized	44	44	44	
Antiepileptic drug use				.026*
Monotherapy	33	67	17	
Polytherapy	67	33	83	
BSR ± SD	0.15 ± 0.13	0.23 ± 0.14	0.11 ± 0.10	.020*

*The p-value mentioned in this table for difference between STLE and LTLE is calculated between MTS and the total number of tumor patients. * statistically significant difference (p<.05).*

DISCUSSION

Functional Connectivity

This study indicates that broad-band functional connectivity recorded intra-operatively over the temporal neocortex is lower in patients with a longer history of TLE. The association between pathology and lower functional connectivity is in line with other studies. Correlations between functional connectivity loss and pathological states such as epilepsy, brain tumors, and schizophrenia have been described previously [10, 135, 154]. Bartolomei and others found a correlation between duration of epilepsy and the number of cortical structures with epileptogenic characteristics by analyzing intracerebral EEG recordings of TLE patients [11]. A correlation has been reported between brain tumors and decreased broad-band functional connectivity [10]. It is hypothesized that pre-ictal hypersynchronized epileptogenic zones may be surrounded by

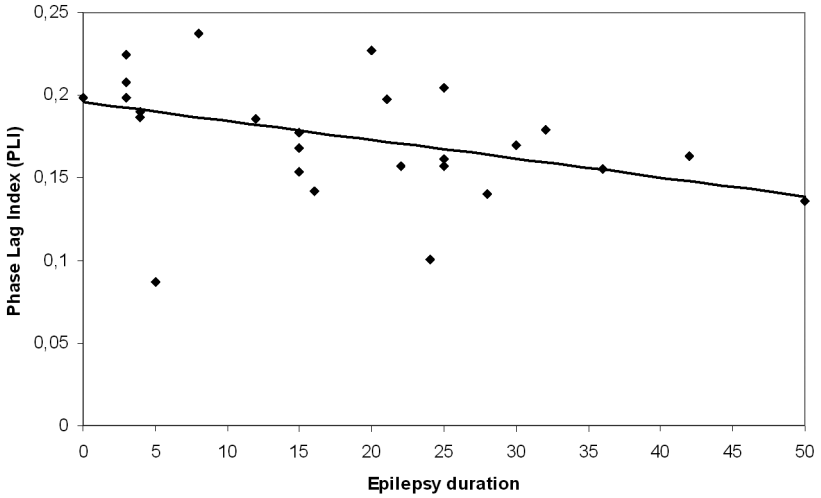

Figure 3. Correlation between epilepsy duration and functional connectivity. The Phase Lag Index (PLI) value is given as a function of epilepsy duration of each patient, showing a decreased PLI with longer epilepsy duration.

isolating zones of hyposynchronization [135]. Ponten and others found that synchronization increases during a seizure in TLE patients [180]. Based on these studies, it is hypothesized that epileptogenic zones might be identified by their synchronization pattern. Synchronization analysis may therefore be useful as a method to functionally map the temporal cortex of TLE patients, hereby locating specific sites that participate in the initiation and propagation of seizures [12, 173]. Furthermore, analyzing synchronization patterns might be a way to locate epileptic foci in TLE patients who are selected for epilepsy surgery. Ortega and colleagues have suggested that seizures might arise from specific regions that have synchronization patterns which are highly differentiated from patterns in the rest of the temporal cortex [173, 174].

Network Properties

This study shows that patients with a longer TLE duration have less small-world network properties in the temporal cortex, suggesting that a less optimal functional network configuration occurs in the course of TLE. This study is the first to show an association between changes in neural network characteristics and the duration of TLE.

The correlation between increased network randomization and increased TLE duration is found to be most pronounced when using a high threshold for the number of edges (k=3). The choice of a threshold is somewhat arbitrary, but also provides information about the connections that change over time. We speculate that in this study, more random networks in patients with a longer epilepsy duration reflect a randomization of the strongest local connections. This randomization results in a less optimal local network configuration, which might reflect a higher vulnerability for seizures. Morgan and Soltesz found that the incorporation of a small number of highly interconnected granule cell hubs into a rat dentate gyrus model greatly increases network activity [161]. In their model, this resulted in a hyperexcitable, potentially seizure-prone circuit.

Several other model studies describe the potential importance of network randomization

regarding the vulnerability to seizures. Netoff and co-workers found in a hippocampal slice model that seizures could be induced by changing the proportion of local versus long-distance connections [163]. As the neural network configuration was transformed into a more random network, seizure-like behavior was more likely to arise. Srinivas and others observed hippocampal rat neurons in vitro which were injured with an exposure to glutamate [206]. The neural network became hypersynchronous and fired bursts at high frequency after this injury, which they interpreted as induced epileptic activity. The network properties showed that the clustering coefficient decreased after injury: the network became more random as epileptic activity developed. Percha and others found that in a model of mesial TLE, epileptogenesis is characterized by structural changes in the neural network topology and axonal sprouting [177]. They showed in a two-dimensional model that an abrupt transition from an unordered local state to an ordered state of global coherence occurs when the network configuration changes from a small-world network to a more random network configuration. The authors speculated that a seizure arises as brain pathology causes the transition to a more random network beyond a critical point.

But what causes this randomization? The lesions in TLE patients result in cell loss, which might cause a reduction of the number of connected edges [179], as has been described in brain tumor patients [9]. Apart from cell loss, mossy fiber sprouting is a hallmark of seizure-induced sclerosis in TLE. Dyhrfjeld-Johnsen and others used a model with cell loss and sprouting to simulate network changes in TLE patients [82]. The value of L/L_{random}=1.19 found in the Dyhrfjeld-Johnsen study at baseline (without a sclerotic process) was the same as the average path length found in our study. When looking at progression of sclerosis, we see that one of their simulation models, based on mossy fiber sprouting, also has a pattern similar to ours. In this model, L/L_{random} remains stable while C/C_{random} becomes more random with increasing sclerosis. Mossy fiber sprouting might therefore explain our findings of a more random network with increased epilepsy duration.

Previous clinical studies have already shown a correlation between dynamic functional network properties and TLE. Wendling and others found that the interaction of local interneuron connections in TLE patients is involved in the interictal to ictal state transition [256]. Ponten and co-workers analyzed the network configuration of mesial TLE patients based on the synchronization likelihood [180]. They compared network topography before, during, and after a seizure. A more randomly organized network was present in the interictal state, which moved towards a more ordered configuration during seizures. Most changes occurred in the C/C_s ratio. Schindler and colleagues found a similar result in their analysis of EEG recordings of 100 epilepsy patients [199]. Their study showed an increase of C/C_s ratio and L/L_s ratio during seizure onset, and a decrease of these parameters during seizure end. Kramer and others also found a changing clustering coefficient and small-world index at seizure onset [131]. Our study suggests that a long history of seizures (which induces shifts in network topology) may be related to functional changes in interictal local clustering and small-world properties.

An unexplained phenomenon in TLE is its course, which is often characterized by a seizure-free latency period after initial onset, eventually ended by recurrence of seizures. Because of this course, it is suggested that TLE should be seen as a progressive disease. Bernasconi and others found progressive volume loss of the hippocampus, the amygdala, and the entorhinal cortex in TLE patients, which is the structural manifestation of progression [23]. The possible emergence of an epileptogenic network during the silent period of TLE has been described [36]. There seems to be a randomness threshold, beyond which a network is prone to seizure-like behavior. Neural networks of TLE patients may become more random during the latency

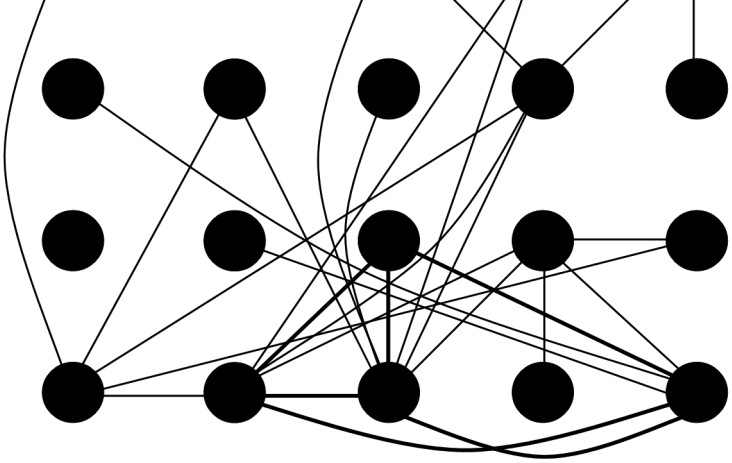

Figure 4. Network representation on the ECoG grid. Network representation of patient 13 for an average number of connections k=3. The characteristics of this network are: C/C_s=2.12, L/L_s=1.07 and S=1.98. Note that some edges are printed bold. These edges represent connections between three so-called 'hub' vertices (vertices with a relative high number of connections), which increase the small-world properties of the network in two ways. Firstly, the edges mark a local cluster, which increases the network characteristic C/C_s. Secondly, this particular cluster also increases the global integration of the network as almost all connected vertices in the network can be reached through these hubs, resulting in a lower L/L_s.

Furthermore, the recurrence of a single seizure might lower the threshold for new seizures to occur in TLE patients [19, 28]. From this perspective, it might be hypothesized that not only structural changes due to the lesion alter the functional network configuration, but the seizures do as well. We speculate that lesion and seizures affect the local neural networks in such a way that they become more prone to seizures, which might play an important role in the recurrence of epilepsy after a latency period in TLE patients.

Age of epilepsy onset, AED use, and level of anesthesia during surgery must be considered as possible confounders in this study regarding functional connectivity, as these factors were correlated with both epilepsy duration and functional connectivity. However, the found correlation remained a significant result after Bonferroni correction, indicating that the result was robust and was not explained by multiple testing. Age of onset was not correlated with network characteristics (C, L, and S). Likewise, AED use and level of anesthesia during surgery were related to synchronization, but not to network configuration measures. These findings show that network characteristics, although based on functional connectivity, measure different functional properties. Lesion volumes were not available and were therefore not included in our analysis.

In our study, we have found a correlation between higher seizure frequency and a higher clustering coefficient and small-world index. We also found, however, a higher seizure frequency to be correlated with the history of epilepsy. This could be expected because data were collected in the clinical setting of an epilepsy surgery program. Surgery is preferred as the epilepsy burden (of which seizure frequency is an important factor) becomes subjectively unacceptable; surgical intervention might therefore be evaluated earlier in the disease course when patients suffer from seizures more frequently. Seizure frequency must be considered as possible confounder in this study. However, a Bonferroni correction was performed and our results regarding small-world index remained significant, whereas the local clustering reached a p-value that was the same as the cut-off point for significance. We have found our results to be evidence of a robust correlation between epilepsy duration and these network characteristics. Apart from that, seizure frequency is reported as an extrapolation of the number of seizures patients suffered from at time of surgery, which does not truly represent

the total number of seizures patients have had. Due to the retrospective nature of this study, we were not able to trace the absolute total number of seizures that patients had suffered from. Future research should point out whether the number of seizures prior to surgery is of influence on network characteristics.

Recently, a correlation has been shown between small-world network topology and cognitive functioning [242]. Moreover, changed network characteristics in brain tumor patients may be responsible for cognitive decline [34]. Cognitive deficits are also an important quality of life limiting factor in temporal lobe epilepsy patients [84]. The correlation between disturbed functional networks and lesional epilepsy should therefore be subject of future studies.

CONCLUSION

In the present study we have shown that there is both a decrease in connectivity of functional networks in the temporal lobe and that those same networks are more random in TLE patients having a long history of epilepsy. In particular we speculate that the functional neural networks of TLE patients become more random due to the influence of ongoing seizures on the structure of the network, irrespective of the presence of a structural lesion. Therefore our findings suggest that, as far as neural network functioning is concerned, surgical intervention might be more effective if performed earlier on in the course of TLE. Further investigations should address the course of epilepsy in TLE patients from the perspective of plasticity of network characteristics that accompany this process.

CHAPTER 4

MEG network differences between low- and high-grade glioma related to epilepsy and cognition

E van Dellen, L Douw, A Hillebrand, IHM Ris-Hilgersom, MM Schoonheim, JC Baayen, PC de Witt Hamer, DN Velis, M Klein, JJ Heimans, CJ Stam, JC Reijneveld

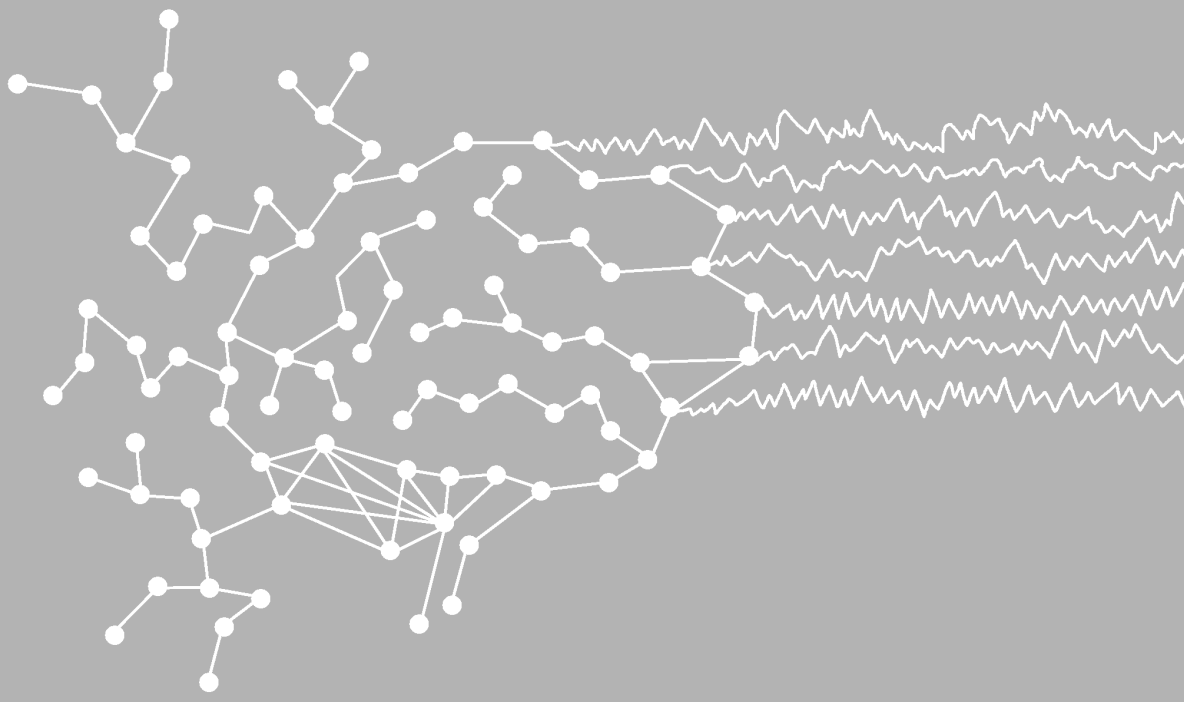

PLoS One (2012) 7(11), e50122.

ABSTRACT

Objective: To reveal possible differences in whole brain topology of epileptic glioma patients, being low-grade glioma (LGG) and high-grade glioma (HGG) patients. We studied functional networks in these patients and compared them to those in epilepsy patients with non-glial lesions (NGL) and healthy controls. Finally, we related network characteristics to seizure frequency and cognitive performance within patient groups.

Methods: We constructed functional networks from pre-surgical resting-state magnetoencephalography (MEG) recordings of 13 LGG patients, 12 HGG patients, 10 NGL patients, and 36 healthy controls. Normalized clustering coefficient and average shortest path length as well as modular structure and network synchronizability were computed for each group. Cognitive performance was assessed in a subset of 11 LGG and 10 HGG patients.

Results: LGG patients showed decreased network synchronizability and decreased global integration compared to healthy controls in the theta frequency range (4-8Hz), similar to NGL patients. HGG patients' networks did not significantly differ from those in controls. Network characteristics correlated with clinical presentation regarding seizure frequency in LGG patients, and with poorer cognitive performance in both LGG and HGG glioma patients.

Conclusion: Lesion histology partly determines differences in functional networks in glioma patients suffering from epilepsy. We suggest that differences between LGG and HGG patients' networks are explained by differences in plasticity, guided by the particular lesional growth pattern. Interestingly, decreased synchronizability and decreased global integration in the theta band seem to make LGG and NGL patients more prone to the occurrence of seizures and cognitive decline.

INTRODUCTION

Symptoms in patients with brain tumors and in other lesional epilepsy patients are to some extent correlated with histological characteristics of the lesion. For example, most low-grade glioma (LGG; WHO grade 2) patients suffer from seizures. The faster and more invasively growing high-grade gliomas (HGG; WHO grade 3 and 4) more often lead to focal neurological deficits and symptoms due to raised intracranial pressure [18, 38]. Moreover, patients with cerebral lesions suffer from cognitive deficits, for example in the attention domain, that cannot be explained by local disturbance due to infiltration of the lesion [100].

Cerebral lesions such as brain tumors can lead to global alterations in functional interactions, even between brain regions remote from the tumor [9, 10]. This recent insight may increase our understanding of the symptoms in these patients. Differences in symptom patterns might be explained by specific neural network alterations induced by these lesions, possibly depending on pathological background and growth patterns. The brain can be approached as a complex network of interacting brain regions [209]. Functional networks can be studied using neurophysiological recordings such as magnetoencephalography (MEG). Once functional connections between brain areas have been estimated, the resulting brain network can be characterized by concepts originating from graph theory [41, 187, 209]. Several studies have shown that small-world networks, which combine local segregation with global integration, facilitate optimal (brain) network functioning [14, 76, 209, 253].

Loss of small-world characteristics, particularly in the theta frequency range (4-8 Hz), have been shown to correlate with seizure frequency, duration of disease, and cognitive decline in patients with brain tumors and/or epilepsy [9, 34, 74, 78, 180, 182, 215, 237, 247]. However, at this point the picture is far from complete. Previous studies on functional networks in brain tumor patients were mostly based on MEG recordings obtained after neurosurgical intervention or biopsy, while tumor resection has been described to alter functional connectivity [71]. Moreover the contributions of other factors on these network changes, such as genetic predisposition [202], the duration of epilepsy [78, 237], but also the pathology of the underlying lesion, are largely unknown, let alone their interactions. Other network measures than the small-world characteristics described above may yield additional crucial information related to brain functioning in healthy controls and patients suffering from brain diseases. Synchronizability, defined as the stability of the synchronous state [7], , may be of special interest in lesional epilepsy patients, because a seizure can be seen as a temporary transition to a global synchronized state. Indeed, it has been shown that network synchronizability is dynamically altered during epileptic seizures [199]. Synchronizability is related to the topology of the underlying network, but this interaction is complex [5]. The loss of small-world characteristics in the functional networks of brain tumor patients can therefore not be seen as a direct explanation for the vulnerability for epileptic seizures in these patients. Characterization of synchronizability during interictal MEG may provide additional insights on the relation between epilepsy and altered functional networks. Furthermore, functional modules have been identified in the human brain that change during the aging process [152, 153]. Dynamic changes in modularity are related to learning ability, suggesting that the underlying modular structure determines cognitive performance [15]. It has recently been shown that modularity is altered in patients with absence seizures during interictal MEG recordings [52], but no previous work has studied modular characteristics in relation to brain tumors and lesional

epilepsy.

In this paper we investigate functional brain networks in LGG and HGG patients. We compare these patients to healthy controls and epilepsy patients with non-glial lesions (NGL). Since epilepsy burden is a known correlate of altered network topology [78, 237], we only studied glioma patients suffering from epilepsy. We hypothesize that networks differ between LGG and HGG patients. We speculate that plasticity effects are reflected in the networks of patients with relatively slow growing lesions such as LGG, in such a way that their networks are more similar to networks of NGL patients than to those in healthy controls or in patients with rapidly growing lesions such as HGG [68]. We expect that changes are mostly seen in the theta band, as functional connectivity in this frequency range is most constantly described to be altered in brain tumor and epilepsy patients [34, 71, 74, 78]. Finally, we aim to show that a change in synchronizability is related to higher seizure frequency, and that disrupted modular network organization is related to poorer cognitive performance.

METHODS

Subjects

Patients were referred for MEG recordings as part of presurgical evaluation by the Neurosurgical Center Amsterdam between January 2006 and October 2009. Inclusion criteria were: (i) age 18 years or older, (ii) a radiologically identified cerebral lesion confirmed by neuropathology, (iii) a history of seizures. Exclusion criteria for patients and healthy controls were i) prior neurosurgical treatment and ii) a history of neurological disease (other than the inclusion criteria). MEG recordings were obtained prior to neurosurgical intervention. MEG recordings of healthy control subjects were obtained. We divided the patient group into three subgroups according to the subsequent pathological diagnosis of the lesion after surgery: low-grade glioma (LGG; WHO classification grade II), high-grade glioma (HGG; WHO classification grade III and IV) and non-glioma. Seizure frequency (defined as number of seizures per month) and epilepsy duration (defined as time in months since first seizure) at time of MEG recording were calculated to determine the burden of these factors for every patient.

Ethics statement

Ethical approval was granted by the VU University Medical Ethics Committee. All data were analysed anonymously. Subjects who underwent MEG recordings for research purposes had given written informed consent before participating. All clinical investigations were conducted according to the Declaration of Helsinki.

Neuropsychological screening

We preoperatively assessed the Stroop color-word test (attention, executive functioning, mental flexibility, mental processing speed), categoric verbal fluency (executive functioning), and the visual verbal learning test (storage and retrieval of verbal memory) in a subset of patients. Scores were compared to those of a healthy control subject (individually matched for age, sex, and educational level) derived from a normative sample [117]. Educational level

was assessed with an 8-point scale scoring system, ranging from not having finished primary education (level 1) to having obtained a university degree (level 8) [126]. Patients' cognitive performance z-scores were calculated for each neuropsychological test score by comparing each person's score with the mean and standard deviation of the matched healthy controls. In order to obtain a single score on each subtest, different aspects of each test were averaged after conversion to z-scores.

Magnetoencephalography (MEG)

MEG recordings were obtained using a 151-channel whole-head MEG system (CTF Systems Inc., Port Coquitlam, BC, Canada). Subjects were seated inside a magnetically shielded room during MEG recordings (Vacuumschmelze GmbH, Hanau, Germany). A third-order software gradient was used, with a recording pass band filter of 0.25-125 Hz. Recordings were made during a no-task, eyes closed resting-state condition with a 625 Hz sampling frequency. The headposition relative to the coordinate system of the helmet was recorded at the beginning and end of each recording by leading small alternating currents through three head position coils attached to the left and right pre-auricular points and the nasion on the patient's head. Changes up to 0.5 cm during recordings were accepted. Recordings of 136 channels were found suitable for analysis in this study; the other 15 channels malfunctioned in at least one of the MEG recordings. For each subject, five artifact free epochs of 4096 samples (6.554 seconds) were carefully selected by visual analysis [L.D./E.D.] and further analysed with the Brainwave software v0.8.83 [authored by C.S.; available at http://home.kpn.nl/stam7883/brainwave.html]. Artifacts were typically due to (eye) movements, drowsiness or technical issues. The length of the epochs was chosen to be 4096 samples as this has proven to be sufficient to detect clinically relevant differences in functional connectivity in previous studies [10, 78, 237]. MEG registrations were converted to datafiles with a coded filename before epoch selection, so the investigators were blind to the subjects' diagnosis during this process. The selected epochs were filtered in seven frequency bands: delta (0,5-4Hz), theta (4-8 Hz), lower alpha (8-10 Hz), upper alpha (10-13 Hz), beta (13-30 Hz), lower gamma (30-45 Hz) and higher gamma (55-80 Hz) [212].

Functional connectivity

Functional connectivity was calculated by means of the phase lag index (PLI), a measure that is insensitive to the effects of volume conduction (see [214] for a detailed description). The PLI calculates synchronization between time series based on the consistency with which one signal is leading or lagging with respect to another signal. It uses the asymmetry of the distribution of instantaneous phase differences between two signals, since a nonzero phase lag between these signals cannot be explained by volume conduction. The PLI ranges between 0 (no asymmetric phase distribution) and 1 (completely asymmetric phase distribution), and has proven to be a useful measure of functional connectivity in several recent MEG studies in our department [34, 78, 210]. An index of the asymmetry of the phase distribution is obtained as described in formula (1) in chapter 3. For each subject, the PLI was calculated between all MEG channels. The overall level of functional connectivity was then computed by averaging all PLI values over all channels. This overall PLI value was used to analyze correlations between the average level of connectivity and lesion pathology.

Graph analysis

We constructed weighted graphs, in which the edge weight represents the strength of the connection between the vertices. The MEG sensors were considered as vertices (nodes) and the PLI between sensors as edge weights. We calculated the most fundamental network

measures, as described by Watts and Strogatz [253], namely the average weighted clustering coefficient C_w and average weighted shortest path length L_w [210]. The unweighted clustering coefficient describes the likelihood that neighbours of a vertex are also connected, and it quantifies the tendency of network elements to form local clusters. We used the weighted equivalent of this measure to characterize local clustering.

For each vertex i, it is defined as:

$$C_{w,i} = \frac{\sum_{k \neq i} \sum_{\substack{l \neq i \\ l \neq k}} w_{ik} w_{il} w_{kl}}{\sum_{k \neq i} \sum_{\substack{l \neq i \\ l \neq k}} w_{ik} w_{il}} \tag{2}$$

where w_{ik} and w_{il} is the weight between vertex i and vertices k and l, respectively, and wkl is the weight between vertices k and l. The average weighted clustering coefficient is computed by averaging $C_{w,i}$ over all vertices.

The average (weighted) shortest path length indicates the level of global integration of the network. In unweighted networks, it depends on the average number of edges used to connect any two vertices in the network [253]. The average weighted shortest path length (L_w) is defined as the harmonic mean of shortest paths between all possible vertex pairs in the network, where the shortest path L_{ij} between vertices i and j is defined as the path with the largest total weight [210].

$$L_w = \frac{1}{\left(1/N(N-1)\right) \sum_{i=1}^{N} \sum_{j \neq i}^{N} \left(1/L_{ij}\right)} \tag{3}$$

with *N* the number of vertices.

Network properties are determined not only by edge weights and network topology, but also by network size. In order to facilitate comparison of results with other studies, we compared the calculated C_w and L_w values to a reference, C_{ws} and L_{ws}, derived from 1000 surrogate networks of the same size. The surrogate networks were constructed by randomly shuffling the edge weights over the network. The resulting C_w/C_{ws} and L_w/L_{ws} are thus the normalized average weighted clustering coefficient and normalized average weighted shortest path length of the network.

Modularity quantifies how a network can be optimally divided in subgroups or modules and was calculated as described by [97], modified for weighted networks by [211]:

$$Q_m^w = \sum_{s=1}^{m} \left[\frac{W_s}{W_{total}} - \left(\frac{d_{w,s}}{2W_{total}} \right)^2 \right] \tag{4}$$

where m is the number of modules, W_s is the sum of the weights of all links in the module s, W_{total} is the total sum of all weights in the network, and $d_{w,s}$ is the sum of the weighted degrees of the vertices in module s.

Simulated annealing

The optimal way to divide the network into modules was then determined using a simulated annealing algorithm [97, 211]. Simulated annealing is an optimization technique that can be used to find an optimal network configuration while considering a cost C. An optimal modularity Q_m^w which consists of the largest possible modules, is found for the configuration with the lowest cost C, which is therefore defined as Q_m^w. Each of N vertices was randomly assigned to one of m possible clusters, where the initial m was taken as the square of N. At each step one of the vertices was randomly chosen and assigned to a different random module number from the interval [1, N]. The new partitioning was preserved with probability:

$$p = \begin{cases} 1 & \text{if} \quad C_f \le C_i \\ e^{(-\frac{C_f - C_i}{T})} & \text{if} \quad C_f > C_i \end{cases} \tag{5}$$

where C_f is the final cost and C_i is the initial cost, and the temperature T describes to what extent the system allows the exploration of high-cost regions. The temperature T was initially set at 1, and was lowered every 100 steps with T_{new} = 0.995 T_{old}. The simulated annealing algorithm ran for 10^6 steps in total.

Within-module degree and participation coefficient

We can describe the role of a vertex within a module by calculating its connectivity within that module. The within-module degree (z_i^w) was used to describe to what extend vertex i is connected to other vertices in the same module [63]. A high z_i^w reflects a high within-module degree. The weighted within-module degree is defined as follows:

$$z_i^w = \frac{k_i^w(m_i) - \bar{k}^w(m_i)}{\sigma^{k^w(m_i)}} \tag{6}$$

where mi is the module containing node i, $k_i^w(m_i)$ is the within module degree of node i (the sum of all links between node i and all other nodes in module m_i, and $\bar{k}^w(m_i)$ and $\sigma^{k^w(m_i)}$ are the respective mean and standard deviation of the within-module degree distribution.

We can also determine to what extend a vertex connects different modules, [63]. The participation coefficient P_i^w describes how the connections of vertex i are distributed among all modules. The participation coefficient P_i^w is defined as:

$$P_i^w = 1 - \sum_{m \in M} \left(\frac{k_i^w(m)}{k_i^w} \right)^2 \tag{7}$$

where M is the set of modules, $k_i^w(m)$ is the sum of all links between node i and all other nodes in module m_i, k_i^w and P_i^w is the sum of all links between i and all other nodes in the network. The P_i^w ranges from 0 to 1.

Between-module connectivity P_w for the whole network was calculated by averaging all P_i^w, which was used as a measure of connectivity between modules.

Network synchronizability

We calculated network synchronizability as measured by the eigenvalue ratio $R = \lambda N/\lambda 2$ to characterize the stability of the synchronous state [7]. For a detailed description we refer to [7], and [29]. In brief, we determined the spectrum of eigenvalues of the graph Laplacian L, which is the difference between the diagonal matrix of vertex degrees and the adjacency matrix. The eigenvalues are then ordered from largest to smallest, being $\lambda 1 = 0$. Networks are more synchronizable when the eigenvalue ratio R is smaller [7]. In order to make results easier to interpret, we define synchronizability $S = R^{-1}$. The synchronizability S is higher for networks with a more stable synchronous state, and S ranges between 0 and 1.

Statistical analysis

All statistical analyses were performed using PASW 18.0 for Windows (SPSS Inc., Chicago, USA). A one-way ANOVA was performed to test for differences in age between groups. Pearson's Chi square test was performed to test for differences in gender between groups. The PLI and network variables do not follow a normal distribution, hence Kruskal-Wallis tests were performed to explore differences concerning these variables between patients and healthy controls for each frequency band. We corrected for multiple testing using the false discovery rate (FDR) because we performed tests for 5 network characteristics. When a Kruskal-Wallis test showed significant results ($p < 0.05$), post-host analysis was performed by means of Mann-Whitney U tests. Correlations with epilepsy characteristics and cognitive performance were calculated using Kendall's tau tests.

RESULTS

Subject characteristics

We included 35 patients (20 male; 13 LGG, 12 HGG, 10 NGL) and 36 healthy controls (18 male). Patient characteristics are shown in table 1. There was a difference in age between groups ($F(3,67) = 6.59$; $p = 0.001$); NGL patients were significantly younger than patients in the other groups. No significant differences in gender were found between groups (Pearson's chi square = 5.49; $p = 0.145$). No significant differences regarding epilepsy duration and seizure frequency were found between LGG and HGG patients (Mann-Whitney $U = 44.5$; $p = 0.069$ and $U = 64.5$; $p = 0.473$, respectively), although epilepsy duration tended to be longer in LGG patients. NGL patients had longer epilepsy duration than LGG (Mann-Whitney $U = 12$; $p < 0.001$) and HGG patients (Mann-Whitney $U = 5$; $p < 0.001$). Similarly, NGL patients had higher seizure frequency than LGG (Mann-Whitney $U = 28,5$; $p = 0.022$) and HGG patients (Mann-Whitney $U = 17.5$; $p = 0.004$). We found no group differences in the number of anti-epileptic drugs (AEDs) used (Pearson's chi square = 5.90; $p = 0.207$).

Neuropsychological assessment

Cognitive test scores were available for 11 LGG and 10 HGG patients. Cognitive data for NGL patients were available for only 2 patients due to different test paradigms in other patients, and we therefore excluded this group from further analysis. Cognitive performance z-scores based on healthy controls matched for age, gender and educational level are given in table 1. No significant differences in cognitive performance were found between LGG and HGG patients.

Lesion pathology and functional connectivity

No significant differences were found between any of the patient groups and healthy controls regarding overall PLI level. A non-significant trend was found of higher overall PLI in the theta band in LGG patients compared to HGG patients (Mann Whitney U = 44.5; p = 0.068).

Lesion pathology and network characteristics

Kruskal Wallis tests showed that lesion type had a significant effect on normalized weighted clustering coefficient (C_w/C_{ws}), normalized average weighted path length (L_w/L_{ws}), synchronizability (S), modularity (Q_m^w) and between-module connectivity (P_w) in the theta band (Table 2; Figure 1 and 2). Analysis for other frequency bands showed no significant differences between groups. Post-hoc analyses were performed to reveal how the groups differed on these theta band parameters (Table S1). Normalized average weighted clustering was higher in LGG than in healthy controls and HGG patients. Also, LGG patients had lower between-module connectivity than healthy controls, HGG and NGL patients. NGL patients showed higher theta band normalized weighted path length than healthy controls and HGG patients, as well as higher modularity than healthy controls. We found no difference between HGG patients and healthy controls regarding network characteristics.

The number of modules ranged between 5 and 10 for all subjects depending on frequency band, and showed no significant differences between patients and controls (Table S2). Upper alpha band normalized average weighted clustering coefficient (Kendall's tau = -0.214; p = 0.009) and normalized weighted shortest path length (Kendall's tau = -0.184; p = 0.024) were found to be negatively correlated with age, but we found no significant correlations between age and theta band network characteristics.

As is shown in figure 1, the findings suggest that differences between patient groups regarding network characteristics may be (partly) explained by differences in average PLI levels. We therefore analyzed possible correlations between PLI and theta band C_w/C_{ws}, L_w/L_{ws}, and P_w (Table S3). Theta band C_w/C_{ws} and L_w/L_{ws} were indeed positively correlated to theta band PLI, whereas a negative correlation was found between P_w and theta band PLI.

Epilepsy, cognition and network characteristics

Post-hoc analysis was performed on network characteristics in the theta band. Higher seizure frequency was associated with lower synchronizability (Kendall's tau = -0.448; p = 0.036) in LGG patients, but not in HGG patients (Kendall's tau = 0.048; p = 0.833) or NGL patients (Kendall's tau = 0.000; p = 1.000) (Figure 3).

Average cognitive test scores correlated positively with theta band synchronizability (Kendall's tau = 0.661; p = 0.005) in LGG patients, but not in HGG patients (Kendall's tau = 0.200; p = 0.421). Further analysis showed that in LGG patients, theta band synchronizability correlated positively with attention (Stroop test) and executive functioning (verbal fluency test) (Kendall's tau = 0.697; p = 0.003 and Kendall's tau = 0.559; p = 0.020, respectively; Figure 4). Executive functioning was also negatively correlated with normalized average weighted clustering coefficients (Kendall's tau = -0.544; p = 0.025), while verbal memory (visual verbal learning test) was positively correlated with modularity (Kendall's tau = 0.477; p = 0.042) in LGG patients. In HGG patients, we found that higher between-module connectivity correlated positively with better attention test scores (Kendall's tau = 0.511; p = 0.040).

Table 1. Patient characteristics

Characteristic	LGG	HGG	non-Glioma	Controls
N	13	12	10	36
Age (years)	44,1 (±SD 9,7)	50,3 (±SD 11,5)	30,1 (±SD 6,8)	43,9 (±SD 11,9)
Gender				
Male	6		4	18
Female	7	102	6	18
Lesion type	Grade II: 13	Grade III: 4	DNET: 3	
		Grade IV: 8	MTS: 4	
			HEM: 1	
			HAM: 1	
			DYS: 1	
Lateralization (lesion)				
Left	5	3	6	
Right	8	9	4	
Seizure frequency	8,2 (±SD 9,9)	17,4 (±SD 43,6)	28,9 (±SD 31,1)	
Epilepsy duration	44 (±SD 64)	20 (±SD 39)	228 (±SD 141)	
Seizuretype				
Part. simple	4	2	1	
Part. complex	0	0	2	
(Sec.) Generalized	9	10	7	
AED use				
None	2	0	0	
Single AED	5	9	4	
Multiple AEDs	2	3	6	
Cognitive performance	-0,5 (±SD 1,1)	-0,2 (±SD 0,8)		
Attention	-1,1 (±SD 1,8)	-0,5 (±SD 1,1)		
Executive functioning	-1,2 (±SD 1,1)	-1,0 (±SD 0,8)		
Verbal memory	0,0 (±SD 0,9)	0,0 (±SD 0,7)		

Seizure frequency is given per month; Epilepsy history is defined as months passed since first seizure. Cognitive performance scores are presented as z-scores based on individual matched healthy controls. Also, cognitive performance is presented of the domains attention (Stroop test), executive functioning (Verbal Fluency test) and verbal memory (Visual Verbal Learning test). Abbreviations: AED = anti-epileptic drug; DNET = Dysembryoplastic Neoepithelial Tumor; MTS = Mesiotemporal Sclerosis; HEM = Hematoma; HAM = Hamartoma; DYS = Dysplasia.

We found correlations between several theta band network parameters and both cognitive performance and seizure frequency in LGG patients, and it may therefore be that these clinical parameters are also correlated. We calculated the correlation between seizure frequency and cognitive performance in LGG patients and found a non-significant negative trend (Kendall's tau = -0.419; p = 0.081).

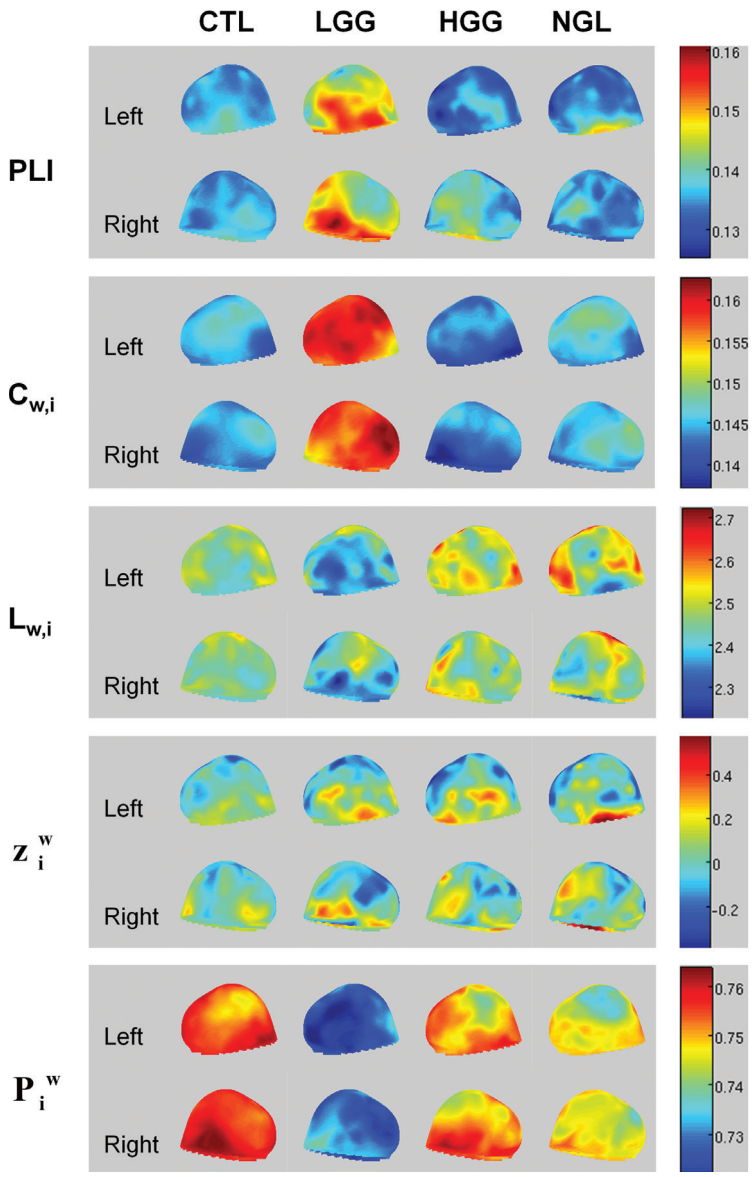

Figure 1. Theta band PLI and network characteristics for patients and healthy controls. Parameters were averaged for each sensor on a group level and displayed on a helmet-shaped surface to show global patterns of differences between patient groups. Note that particularly in LGG patients, theta band clustering and participation coefficients show global alterations irrespective of local PLI values. Abbreviations: CTL = healthy controls; LGG = low-grade glioma patients; HGG = high-grade glioma patients; NGL = non-glioma patients; PLI = phase lag index; Cw,i = nodal clustering coefficient; Lw,i* = nodal path length;* z_i^w *= within-module degree z-score;* P_i^w *= participation coefficient. * In the analysis we use normalized average weighted clustering coefficient (Cw/Cws) and normalized average weighted shortest path length (Lw/Lws) instead of the unnormalized values for each vertex i, Cw,i and Lw,i which are visualized here. Cw/Cws and Lw/Lws are calculated by first averaging over nodes and then dividing Cw and Lw by a reference value Cws and Lws, in order to get normalized values. However, this normalization does not affect the spatial distribution of Cw,i and Lw,i, and therefore the original data is presented.*

Table 2. Differences between patients and healthy controls regarding theta band network characteristics

Measure	LGG	HGG	NGL	Controls	p-value
PLI	0.146	0.133	0.136	0.136	0.216
Cw/Cws	1.072 ↑	1.058	1.066	1.058	*0.019
Lw/Lws	1.105	1.084	1.101 ↑	1.087	*0.023
S	0.343 ↓	0.374	0.355 ↓	0.367	*0.009
Q_m^w	0.071	0.072	0.075 ↑	0.070	*0.025
Pw	0.727 ↓	0.750	0.745	0.756	*0.005

Results are given as mean values of network characterstics and p-values of Kruskall-Wallis tests. P-values were considered significant for ($p < 0.05$) after correction using the false discovery rate. Note that the within-module degree z-score (not shown) did not differ significantly. Results are marked (↑ or ↓) when significantly different from other groups based on post-hoc analyses using Mann-Whitney U tests. Significance levels are given in table S1. Abbreviations: NGL = non-glial lesion; LGG = low-grade glioma; HGG = high-grade glioma; PLI = phase lag index; Cw/Cws = normalized average weighted clustering coefficient; Lw/Lws = normalized average weighted shortest path length; S = synchronizability; Q_m^w *= modularity; Pw = between-module connectivity.*

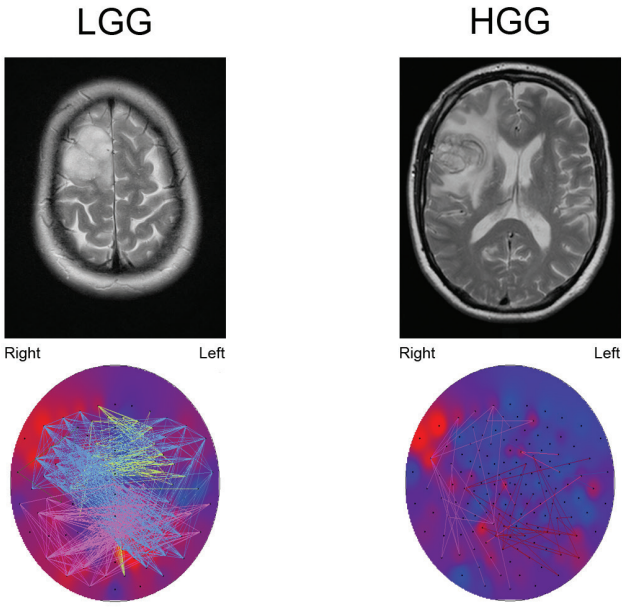

Figure 2. Example of theta band connection differences between a LGG patient and a HGG patient, both suffering from a tumor located in the right frontal lobe. The upper images show T2-weighted MRI images of the tumor. The lower images show theta band PLI levels (background colors; red colors represent high PLI levels, blue colors represent low PLI levels). Note that the tumor region seems to have the highest theta band PLI. The colored lines represent connections between sensors, each color representing another module. Connections are shown when their strength passes an arbitrary threshold chosen for optimal connection visualization. In HGG patients, only few connections exist above the threshold. Note that especially connections to the tumor region in LGG patients pass the threshold. However, two other modules are also clearly shown that are not found in the HGG patient, suggesting that the differences between LGG and HGG patients networks are not restricted to the tumor region.

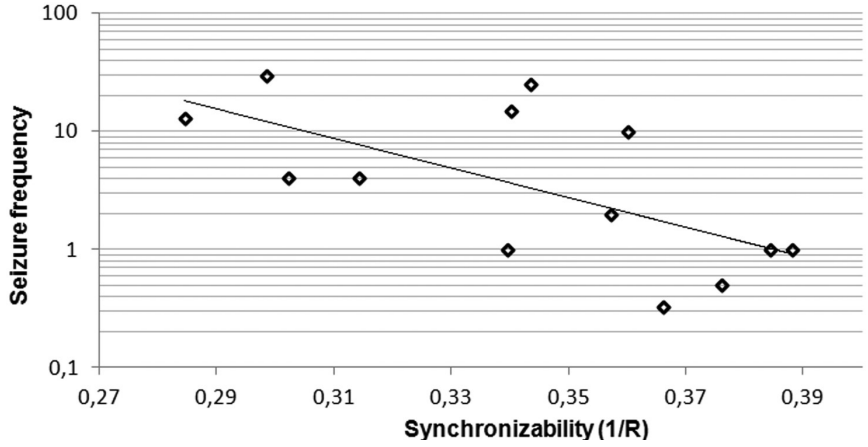

Figure 3. Theta band synchronizability and seizure frequency in low grade glioma patients. Note that seizure frequency is plotted on a logarithmic scale. See tables S4 and S5 for seizure frequency and synchronizability values for each patient.

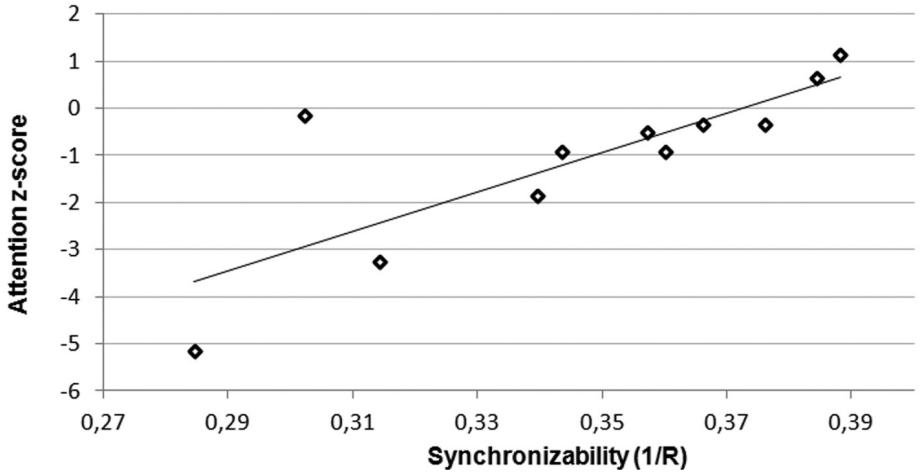

Figure 4. Theta band synchronizability and attention as measured by Stroop tests. Attention scores are presented as z-scores gained by comparison with healthy controls matched for age, gender and educational level. See table S4 for attention scores and synchronizability values for each patient.

DISCUSSION

Our study is the first to show that LGG patients have different neural network characteristics compared to HGG patients (table 3). Functional networks in LGG patients show theta band alterations similar to lesional epilepsy patients with non-glial lesions, while networks in HGG patients are more similar to those in healthy controls. Interestingly, we found topological network differences but no significant differences in general connectivity levels. We observed increased normalized theta band path lengths in NGL patients. In contrast, two previous functional MRI studies found smaller normalized average path lengths and lower clustering coefficients in localization-related (non-glioma) epilepsy patients compared to healthy controls [141, 247]. Another MEG study did not find any consistent network differences between NGL patients with epilepsy and healthy controls [110]. As was shown in the current study, differences in lesion pathology between the patient populations in these studies may partially explain these contradictory findings, as well as effects of anti-epileptic drug use and duration of disease [237].

Previous MEG studies comparing functional networks in post-operative glioma patients to those in healthy controls also reported contradicting findings (summarized in table 3). It is important to note here that these studies, especially when reporting on network analysis, were performed after surgical intervention, which has been shown to affect (theta band) connectivity patterns [71]. Patient heterogeneity as well as differences in (network) analysis approaches between these MEG studies and the current study make it even harder to compare results. Some of those previous studies used the synchronization likelihood (SL) as a measure of functional connectivity, which is less conservative than the PLI used in our study, or performed unweighted network analysis. It may thus be that previous studies revealed different aspects of functional network organization in different stages of disease and treatment, rather than being contradictory.

We found the aforementioned differences between LGG and HGG patients in the theta band, while average PLI levels showed a non-significant trend towards higher PLI in LGG patients. The network characteristics were significantly correlated to the overall PLI, even after normalization using random networks of the same size. The possibly higher PLI levels in LGG patients may therefore partly explain the observed differences in network measures. There is currently no optimal method of network construction from functional connectivity matrices that is completely free from biases [243]. The purpose of this study was to find sensitive measures based on functional connectivity between brain areas to differentiate between LGG and HGG patients. We therefore suggest that the network parameters presented here are of additional value compared to the calculation of overall PLI only, and may also provide additional information about the type of connections that are strengthened in LGG patients.

It is hypothesized that plasticity is guided by the particular lesional growth pattern [68]. A recent computational modeling study allowing both growth- and synchronization-dependent plasticity showed that acute lesioning of functional networks leads to increased local clustering levels [211]. Although the model only considered an acute lesion which limits comparability with our study, this is consistent with the increased clustering that we found in LGG patients. However, we found no network differences between HGG patients and healthy controls. A possible explanation is that it might take time before plasticity effects become evident on a global scale, and HGG patients tended to have shorter time between first symptoms and

Table 2. Differences between patients and healthy controls regarding theta band network characteristics

Study	Population	Methods	Findings
Bartolomei 2006a[1]	17 brain tumor patients vs 15 healthy controls	SL	broad and γ band: disconnected points in brain tumor patients after thresholding SL values
Bartolomei 2006b[1]	17 brain tumor patients vs 15 healthy controls	SL; unweighted networks (k=10)	Δ, θ and α band: local SL ↑ Δ, α and β band: long-distance SL ↑ θ, β, and γ band: L/Ls ↓ θ, and γ band: C/Cs ↓
Bosma 2008[1]	17 LGG patients vs 17 healthy controls	SL	Δ band: interregional SL ↑ or ↓ θ and lower γ band: interregional SL ↑ lower α band: interregional SL ↓
Guggisberg 2008[2]	15 focal brain lesion patients and 14 healthy controls	Imaginary coherence	Decreased α band coherence
Douw 2008[3]	15 brain tumor patients	PLI	θ band: PLI ↓ after resection; higher decrease correlated with lower post-surgery seizure burden
Bosma 2009[1]	17 LGG patients vs 17 healthy controls	PLI; unweighted networks (k=10)	θ band: PLI and C/Cs ↑ β band: C/Cs and S ↓ upper γ band: degree cor. ↓
Horstmann 2009[4]	21 MTLE patients vs 23 healthy controls	cross-correlation; phase sync.; various methods for network construction	broad, Δ, θ and β band: mostly C ↑, but also C ↓ or = depending on methodology
Douw 2010[1]	17 glioma patients	PLI; weighted networks	θ band: PLI and L/Ls related to higher seizure frequency

Overview of functional connectivity and network studies based on MEG recordings in brain tumor and TLE patients. The measure for functional connectivity used in the study is given in the Methods column. Abbreviations: SL = Synchronization Likelihood; PLI = Phase Lag Index; L/Ls = normalized average path length; C/Cs = normalized average clustering coefficient; degree cor. = degree correlation (measure for the tendency of vertices to connect to other vertices with a similar degree).

[1] MEG recordings used in these studies were obtained after surgery, which might also have had an impact on functional connectivity levels and network topology.

[2] No information available on epilepsy incidence in these patients.

[3] This study did not compare patients to healthy controls, but compared MEG recordings of patients before and after resection of the brain tumor.

[4] This study analyzed patients with non-glial lesions, and should therefore be considered only as a reference for patients with NGL in the present study.

MEG recordings [68]. In the model of Stam and others, however, increased path lengths and decreased modularity were particularly found directly after emergence of the lesion, subsequently normalizing over time [211].

Alternatively, our results may also have been affected by epilepsy characteristics and use of AEDs [78, 237, 247]. Patient groups in our study were relatively small to analyze within group correlations between epilepsy and network characteristics, but we did find a correlation between network synchronizability and seizure frequency in LGG patients. It would be interesting to compare glioma patients with and without epilepsy, and find possible differences

in the functional networks of these patients. However, since we found no significant differences between LGG and HGG patients regarding epilepsy duration, seizure frequency and AED use, we consider it unlikely these characteristics would explain differences between these groups.

We found decreased theta band synchronizability, defined as the stability of the synchronous state, in both LGG and NGL patients, and found that lower synchronizability correlated with higher seizure frequency and poorer attention test-scores in LGG patients. Although extremely interesting, these results should be interpreted with caution, as synchronizability was characterized as the stability of the synchronous state, where others use the same terminology to characterize the threshold value of a network for global synchronization [5]. Schindler and others showed that at seizure onset, synchronizability decreases, and increases again at seizure termination [199]. These changes coincided with increased clustering coefficients and path lengths. We suggest that modeling studies on the interaction between network structure and dynamics during seizures are needed to clarify the exact meaning of our observed correlations. The existence of hub nodes with a pathologically increased central role should also be taken into account, as this may be crucial for spreading of epileptic synchronized activity over the network [5, 32, 161, 173, 260]. Future work in which MEG functional networks may be reconstructed in source space is crucial in this respect, which would also allow the identification of anatomical correlates of these pathological hubs, and would increase comparability between subjects [104, 110, 113, 148, 247].

Our findings suggest that in glioma patients a modular brain organization, less local clustering, higher stability of the synchronized state and high between-module connectivity favor cognitive performance. A previous study using post-operative MEG recordings in LGG patients showed that a shorter path length in the delta band was related to better performance in the attention and executive functioning domain, while less local clustering in the lower alpha band was related to better verbal memory test scores, in line with our results [34]. However, another previous study in healthy controls showed an opposite correlation of better attention, working memory and processing speed performance in subjects with higher theta band clustering coefficients [76]. Although that study found correlations with different cognitive domains as compared to our study, and, moreover, healthy subjects instead of brain tumor patients were studied, these findings appear to be contradicting ours. Several other studies have been performed in healthy controls. The most consistent finding seems to be that of a correlation between shorter path lengths and better memory performance or higher intelligence, as this has been established in DTI, MRI and MEG studies [76, 140, 242]. However, an EEG study showed that people with lower education have networks with higher small-world characteristics during a memory task compared to higher educated subjects [154]. This may be interpreted as a reflection of the bigger effort made by subjects with lower education to deliver an equal performance as the subjects with higher education on the task. In general, it could be hypothesized that a small-world topology may be the optimal resting-state organization of healthy brain networks, but that this is not automatically the case for networks in the damaged brain. It could also be that other network characteristics of network topology, such as hierarchical modularity, need to be taken into account in order to capture all the complex interactions between network topology and cognitive performance [219].

The studied domains (attention, executive functioning and verbal memory) specifically require global integration of information. We speculate that modularity and between-module connectivity reflect the facilitation of functional communication. Interestingly, we observed correlations between these network parameters and cognition in the same frequency range, the theta band, as where we observed network differences between LGG patients and healthy controls. The network alterations therefore seem to reflect the less optimal communication

within the brain that leads to the impaired cognitive performance in patients with brain lesions. Other cognitive deficits in these patients may also be expected, but no standardized test scores were available in the current study.

We found a non-significant trend towards a negative correlation between epilepsy frequency and cognitive performance. Epilepsy itself can lead to cognitive deficits in brain tumor patients [61]. It might thus be that the network characteristics that we found in these patients are related to either one of these symptoms. Another hypothesis is that the network characteristics may contain information about how recurrent seizures lead to cognitive deficits. The non-parametric distribution of the parameters synchronizability and seizure frequency and the relatively small sample size make the current dataset unsuitable for a regression analysis to clarify these interactions more thoroughly. Also, We corrected for multiple testing per frequency band, as the connectivity matrices provide different information for each frequency band. We performed a Kruskall Wallis test in order to find possible differences regarding any of the metrics, and post-hoc analysis were performed to further interpret results. We suggest that stronger statistical correction would lead to an underestimation of possible group differences and correlations. We note that a correction for multiple testing is not commonly performed for multiple network measures, or average connectivity per frequency band [110, 148, 247].

In conclusion, this study shows that theta band functional networks based on MEG recordings differ in epileptic glioma patients depending on histopathology of the lesion. Lesion type effects are more explicitly seen in LGG and NGL (e.g. MTS) patients when compared to HGG patients, possibly due to plasticity effects that alter brain networks over time. Interestingly, seizure frequency and cognitive decline also correlate with these network alterations. Future studies with larger patient groups should elucidate in more detail the interactions between these clinical characteristics, plasticity and network topology.

ACKNOWLEDGEMENTS

The authors thank G.W.G.A de Vos and the MEG technicians of the Department of Clinical Neurophysiology, P.J. Ris, K. Plugge, N. Sijsma and S. Oudkerk, for technical assistance. E. van Dellen is supported by the Dutch Epilepsy Foundation (NEF) grant 09-09. L. Douw is supported by the Dutch Epilepsy Foundation (NEF) grant 08-08. M. Schoonheim is supported by the Dutch MS Research Foundation grant 08-650.

SUPPLEMENTARY INFORMATION

Table S1. Network differences between patients and healthy controls.

Gamma (Cw/Cws)	
LGG > Controls	(U = 111.5; p = 0.005)
LGG > HGG	(U = 31.5; p = 0.010)
Lambda (Lw/Lws)	
NGL > Controls	(U = 73; p = 0.003)
NGL > HGG	(U = 19; p = 0.005)
Synchronizability (S)	
LGG < Controls	(U = 119.5; p = 0.008)
LGG < HGG	(U = 33; p = 0.014)
NGL < Controls	(U = 100.5; p = 0.033)
NGL < HGG	(U = 24.5; p = 0.018)
Modularity (Q)	
NGL > Controls	(U = 70; p = 0.003)
Between-module connectivity (Pw)	
LGG < Controls	(U = 86; p < 0.001)
LGG < HGG	(U = 36; p = 0.022)
LGG < NGL	(U = 33; p = 0.049)

Results are given as for each patient group based on Mann-Whitney U tests.

Table S2. Overview of modularity analysis of patient groups and healthy controls.

		LGG		HGG		non-Glioma		Controls		p-value
Characteristic	Freq. range	Mean	SD	Mean	SD	Mean	SD	Mean	SD	
Modularity (Q)	delta	0.073	.0053	0.070	.0061	0.075	.0080	0.071	.0074	0.222
	theta	0.071	.0051	0.072	.0049	0.075	.0038	0.070	.0051	0.025*
	lower alpha	0.070	.0055	0.073	.0076	0.075	.0065	0.074	.0075	0.406
	upper alpha	0.072	.0062	0.071	.0073	0.076	.0056	0.071	.0072	0.180
	beta	0.070	.0046	0.070	.0074	0.070	.0051	0.068	.0054	0.502
	lower gamma	0.055	.0065	0.053	.0048	0.056	.0060	0.054	.0039	0.739
	upper gamma	0.044	.0015	0.048	.0061	0.047	.0071	0.045	.0017	0.190
No. of modules	delta	6.4	.50	6.7	.39	6.5	.48	6.7	.59	0.434
	theta	6.7	.46	7.1	.74	6.8	.51	7.1	.48	0.143
	lower alpha	6.6	.42	6.4	.87	6.7	.45	6.6	.66	0.643
	upper alpha	6.7	.73	7.0	.75	6.7	.67	6.8	.52	0.853
	beta	7.1	.58	7.0	.41	7.3	.60	7.2	.62	0.561
	lower gamma	8.2	.93	8.6	.75	8.2	.92	8.1	.78	0.236
	upper gamma	9.8	.78	9.5	1.15	9.2	.91	9.7	.59	0.265

Table S3. Correlations between PLI and several network characteristics in the theta band for all subjects (N=71).

Correlation between PLI and:	Kendall's tau	p-value
Cw/Cws	0.459	<0.001
Lw/Lws	0.341	<0.001
Pw	-0.252	0.002

Table S4. Theta band synchronizability values.

Patient	Healthy controls	LGG	HGG	NGL
1	0,3998	0,3022	0,3756	0,3722
2	0,3056	0,3882	0,3652	0,3704
3	0,3592	0,3436	0,3486	0,3476
4	0,367	0,2846	0,3908	0,3458
5	0,4058	0,3844	0,3722	0,3384
6	0,339	0,3602	0,3536	0,3374
7	0,392	0,3144	0,4054	0,3466
8	0,412	0,3572	0,3244	0,3520
9	0,3512	0,3662	0,3876	0,3744
10	0,4232	0,3396	0,3896	0,3696
11	0,3838	0,3762	0,3930	
12	0,4088	0,2986	0,3848	
13	0,3752	0,3402		
14	0,369			
15	0,3614			
16	0,3192			
17	0,4202			
18	0,3256			
19	0,3824			
20	0,4062			
21	0,3734			
22	0,4088			
23	0,0722			
24	0,3572			
25	0,3238			
26	0,3414			
27	0,3848			
28	0,38			
29	0,3744			
30	0,4078			
31	0,3898			
32	0,3678			
33	0,3678			
34	0,3812			
35	0,38			
36	0,3862			

CHAPTER 5

Epilepsy is related to theta band brain connectivity and network topology in brain tumor patients

L Douw, E van Dellen, M de Groot, JJ Heimans, M Klein, CJ Stam, JC Reijneveld

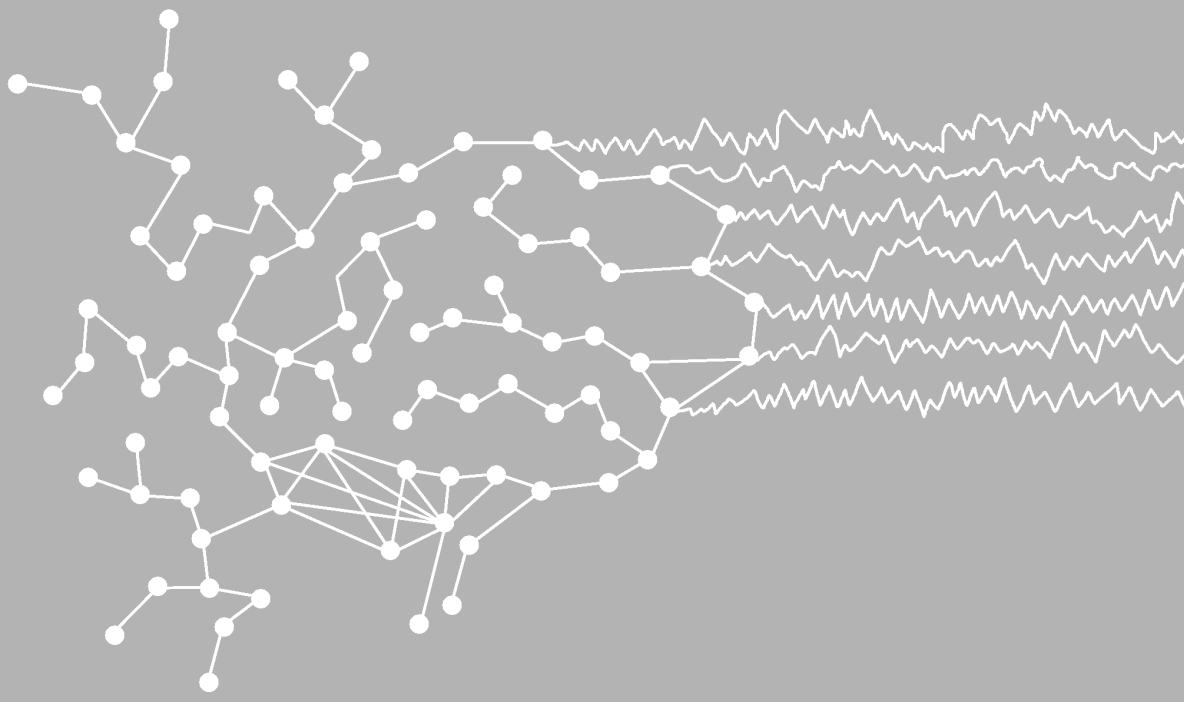

BMC neuroscience (2010). 11(1), 103.

ABSTRACT

Both epilepsy patients and brain tumor patients show altered functional connectivity and less optimal brain network topology when compared to healthy controls, particularly in the theta band. Furthermore, the duration and characteristics of epilepsy may also influence functional interactions in brain networks. However, the specific features of connectivity and networks in tumor-related epilepsy have not been investigated yet. We hypothesize that epilepsy characteristics are related to (theta band) connectivity and network architecture in operated glioma patients suffering from epileptic seizures. Included patients participated in a clinical study investigating the effect of levetiracetam monotherapy on seizure frequency in glioma patients, and were assessed at two time points: directly after neurosurgery (t1), and six months later (t2). At these time points, magnetoencephalography (MEG) was recorded and information regarding clinical status and epilepsy history was collected. Functional connectivity was calculated in six frequency bands, as were a number of network measures such as normalized clustering coefficient and path length. At the two time points, MEG registrations were performed in respectively 17 and 12 patients. No changes in connectivity or network topology occurred over time. Increased theta band connectivity at t1 and t2 was related to a higher total number of seizures. Furthermore, higher number of seizures was related to a less optimal, more random brain network topology. Other factors were not significantly related to functional connectivity or network topology. These results indicate that (pathologically) increased theta band connectivity is related to a higher number of epileptic seizures in brain tumor patients, suggesting that theta band connectivity changes are a hallmark of tumor-related epilepsy. Furthermore, a more random brain network topology is related to greater vulnerability to seizures. Thus, functional connectivity and brain network architecture may prove to be important parameters of tumor-related epilepsy.

INTRODUCTION

Gliomas are primary brain tumors arising from the supporting tissue of the brain. The presenting symptoms in glioma patients include epileptic seizures in 20-45% of patients [255]. Another 15-30% of patients develop seizures during their disease [132]. Multiple factors may contribute to epileptogenesis (for a review, see reference [16]), but all possible factors that have been studied up till now do not suffice when trying to clarify the course of tumor-related epilepsy. Possibly, a better understanding of tumor-related epilepsy could be achieved using a relatively new concept in neuroscience: 'functional connectivity' refers to the statistical interdependencies between neurophysiological time series such as EEG, MEG, or fMRI-BOLD signals [3, 220]. Functional connectivity is thought to reflect communication between different brain areas, thus having a major impact on brain functioning [41, 187]. Furthermore, the brain can be seen as a complex integrated network, in which focal changes influence the integrity and status of the brain as a whole. An 'optimal' brain network probably includes concepts that are pivotal in many types of complex networks, such as localized segregation combined with overall integration [204]. Watts and Strogatz proposed a theoretical framework for such a network, the so-called 'small-world' network [253]. The small-world network is an intermediate type of network in between the 'random' network, in which all connections between nodes are randomly drawn, and the 'regular' network, in which connections between nodes are present in an ordered fashion and all nodes have the same number of connections. Several studies have shown that both structural and functional brain networks in healthy humans and animals can be characterized by the small-world principle [99, 196, 208, 253].

Previous studies using magnetoencephalography (MEG) recordings show that functional connectivity and network topology are significantly altered in brain tumor patients when compared to healthy participants: lower frequency connectivity (in particularly the theta band) is pathologically increased, and the normal small-world configuration is disturbed [9, 10, 33, 34]. These differences are not only limited to the area around the tumor, but involve brain-wide networks and are related to cognitive deficits. Altered connectivity and network topology have also been reported in epilepsy patients, even in the inter-ictal period. Increased theta, but also delta, frequency EEG connectivity in between seizures was found in two studies investigating epilepsy patients [74, 110]. Furthermore, therapy-resistant epilepsy patients have been reported to have a more regular network topology than healthy controls as measured with EEG [110].

Changes over time in connectivity and network patterns in neuro-oncological or epilepsy patients have only been sparsely reported. In a previous study, we investigated a patient group with varying types of primary brain tumors with MEG before and after tumor resection [71]. After tumor resection, functional connectivity in the theta band significantly decreased in these patients, suggesting 'normalization' of the previously reported pathologically increased connectivity. Moreover, this decrease was related to better postsurgical outcome in terms of seizure-freedom. Studies using both fMRI and acute corticography recordings in mTLE patients suggest that prolonged therapy-resistant epilepsy is related to decreases in broadband functional connectivity [141, 237]. Furthermore, the small-world architecture is more disrupted in the temporal cortical networks of TLE patients with longer epilepsy history [237].

Previous studies suggest that both epilepsy and brain tumors are related to changes in connectivity, which may be most prominent in the theta band. Furthermore, brain networks

of both epilepsy patients and brain tumor patients display a loss of small-world features when compared to healthy controls. In the current study, we first aimed to investigate the relation between functional connectivity, network topology, and tumor-related epilepsy in a group of glioma patients. We hypothesized increased connectivity and less optimal network topology in the theta band to be related to epilepsy characteristics. Secondly, we studied the longitudinal changes in connectivity and network architecture during the first six months after neurosurgery in relation to changes in epilepsy features. The patients participated in a clinical study investigating levetiracetam monotherapy (an anti-epileptic drug (AED)), which implicates that patients were homogeneous with respect to AED use.

METHODS

Patients

This study was performed on patients who were included in a study primarily investigating the effect of levetiracetam monotherapy in brain tumor patients. Between April 1st 2007 and June 1st 2009, patients were recruited from two tertiary referral centers for brain tumor patients in The Netherlands (VU University Medical Center and Academic Medical Center, Amsterdam). Inclusion criteria were: (1) a diagnosis of novel or recurrent glioma confirmed by pathological diagnosis, (2) age ≥ 18 years, and (3) generalized or partial seizures with or without secondary generalization. All patients had undergone surgery and were treated with levetiracetam monotherapy at the time of inclusion. Exclusion criteria were: (1) lack of a basic proficiency of the Dutch language, or (2) the inability to communicate adequately. The first MEG recordings took place within six weeks after neurosurgery (t1). Follow-up took place after six months (t2) and one year (t3). Data regarding medical status, physical examination, and laboratory investigations were collected at these time points, as well as Karnofsky performance status [120] and Barthel index [250]. Patients were excluded during follow-up if their treating neurologist decided to discontinue levetiracetam monotherapy or if another antiepileptic drug (AED) was added to their regime. All patients gave written informed consent before participating, and study approval was obtained from both centers' ethics committees.

Magnetoencephalography (MEG)

Magnetic fields were recorded while subjects were seated inside a magnetically shielded room (Vacuumschmelze GmbH, Hanau, Germany) using a 151-channel whole-head MEG system (CTF Systems Inc., Port Coquitlam, BC, Canada). A third-order software gradient was used with a recording pass band of 0.25–125 Hz [248]. Fields were measured during a no-task eyes-closed condition, with a sample frequency of 625 Hz. At the beginning and end of each recording, the head position relative to the coordinate system of the helmet was recorded by leading small alternating currents through three head position coils attached to the left and right pre-auricular points and the nasion on the patient's head. Head position changes up to approximately 1.5 cm during a recording condition were accepted. During the recording, patients were instructed to close their eyes to reduce artifact signals due to eye movements. MEG channels that were defect or contained artifacts in at least one patient were excluded in the entire group, leaving 140 of the 151 MEG channels to be included.

Power analysis

Relative power was calculated by means of Fast Fourier Transformations in six frequency bands (respectively delta (0.5-4 Hz), theta (4-8 Hz), lower alpha (8-10 Hz), upper alpha (10-13 Hz), beta (13-30 Hz), and gamma (30-45 Hz).

Functional connectivity

Functional connectivity was assessed with the phase lag index (PLI) [214]. The PLI calculates synchronisation between time series by reflecting the consistency with which one signal is phase leading or lagging with respect to another signal. The PLI exploits the asymmetry of the distribution of instantaneous phase differences between two signals. It assumes that the presence of a consistent, nonzero phase lag between two time series cannot be explained by volume conduction alone. Thus, finding true interactions instead of volume conduction effects is more likely when using this method. The PLI ranges between 0 and 1, and a PLI of more than 0 indicates phase locking to a certain extent, whereas a PLI of 0 indicates no coupling or coupling with a phase difference centered around 0 ± π radians. See chapter 3, formula (1) for a mathematical description of the PLI.

Five artifact free epochs of 4096 samples (6.552 seconds) during resting-state with eyes closed were carefully selected by visual analysis from each patient at each time point [ED]. PLIs between each pair of MEG sensors were computed after filtering the MEG signals in six frequency bands (respectively delta (0.5-4 Hz), theta (4-8 Hz), lower alpha (8-10 Hz), upper alpha (10-13 Hz), beta (13-30 Hz), and gamma (30-45 Hz) [212]. Computation of the PLI was done offline with DIGEEGXP software, developed at our department [CJS]. PLI for all sensor pairs was averaged over each set of the selected five epochs, after which graph analysis took place.

Graph analysis

A graph is a topographical representation of a network, constructed by nodes (‘vertices’) and links (‘edges’) between them. Graphs can be unweighted (binary) or weighted; in the former case, a threshold is applied for every edge. When the connectivity value is higher than the threshold, the edge is present and gets a value of 1; if not, the edge is not and thus is given a value 0. In this study, we used undirected weighted graphs, in which the weight of every edge was the PLI value of the link between the two nodes it connects.

A wide range of network measures can be calculated after representing MEG data as a graph (see references [41, 193] for recent reviews). In this study, the most commonly used measures are employed. The first measure is the weighted clustering coefficient C, which refers to the likelihood that neighbors of a vertex will also be connected. The clustering coefficient characterizes the tendency of nodes to form local clusters and is thus a measure of local segregation of the graph. The second measure is the average weighted path length L, signifying the average highest connectivity of edges connecting any two vertices, and is a measure for global integration of the network. The combination of high local clustering and a short average path length seems to be the optimal configuration for efficient communication in a network [253]. A small-world network, which is thought to be a feasible model for human brain networks, has such a configuration. The (weighted) clustering index of vertex i with edge w with other vertices is defined as described in chapter 4, formula (2). The weighted characteristic path length L was defined as described in chapter 4, formula (3). For a more detailed description of calculation of the weighted clustering coefficient C_w and weighted average shortest path length L_w in this study see reference [210]. We normalized all network

characteristics to those of 1000 surrogate random networks of the same size, resulting in the measures C_w/C_{ws}, L_w/L_{ws}. The surrogate networks were obtained from the original networks by randomly reshuffling the edge weights, hereby preserving the symmetry of the matrix.

A second-order graph property has been proposed: the ratio between C_w/C_{ws} and L_w/L_{ws}, which is an index of 'small-worldness' [112]. Graphs with a small-world index>1 are considered small-world, since C_w/C_{ws}>1 and L_w/L_{ws}~1 apply in small-world networks.

Finally, we calculated the 'edge weight correlation'. This is a measure for the correlation between weights of neighboring edges, i.e. edges that connect to the same vertex [184]. The edge weight correlation is calculated as the range between the highest and lowest weight of all edges per vertex:

$$r_i = \frac{W_{max}(i) - W_{min}(i)}{W_{max}(i) + W_{min}(i)} \quad (8)$$

W_{max} accounts for the maximum weight and W_{min} for the minimum weight of the edges of node i. This range is then compared to that of the random equivalent of the network, in which the edges are randomly redistributed over the vertices while their weights are kept unchanged (as described above for other network characteristics). When the resulting value Wr lies between 0 and 1, a positive weight-weight correlation exists (because the range of neighboring weight values is smaller than in a random network), whereas the weights are anti-correlated when W_r>1. It has been shown that a positive weight correlation (thus: W_r<1) dramatically increases transport over the network, and edge weight correlation and thus transport increase further as W_r approaches 0 [184].

Statistical analysis

All statistical analyses were performed using SPSS 15.0 for Windows. Functional connectivity and network variables usually do not follow a normal distribution, warranting non-parametric testing. Correlations between connectivity, network features, and seizure-related variables were tested using Kendall's Tau. Differences in connectivity and network topology according to seizure-related variables were tested using Mann-Whitney U-tests. Changes in seizure characteristics, functional connectivity, and network features between the three time points were tested with Wilcoxon signed rank tests. When applicable, we corrected for the number of comparisons with the false discovery rate (FDR) [168].

RESULTS

Patients

A total of 24 patients were included, but 7 patients had to be excluded due to MEG artifacts at t1. Further analyses were performed using the remaining 17 patients. All patients had undergone surgical intervention and histopathological diagnoses were obtained (see table 1). Patients' mean age was 44 years (SD=12 years) and four patients were females. The majority of patients was diagnosed with glioblastoma multiforme (GBM, nine patients). The tumor was localized in the right hemisphere in 12 patients. These tumors were all localized in the frontal or temporal lobe. Five patients had left-sided tumors, which were localized in the frontal lobe

in most patients. Most patients (11 of 17) had at most one seizure per month in the last month before t1 (i.e. seizure frequency in table 1), while three patients had more than one seizure per day. Seizures were likely to be due to the tumor in all patients. At t2, 12 patients underwent a second MEG recording: two patients were excluded because they switched to another AED, while one patient had died due to disease progression. In two patients, no artifact-free MEG epochs were available. Of these 12 patients, 10 patients did not have seizures anymore, while 2 patients still had occasional seizures. At t3, only 6 patients were tested. Due to the small number of patients available at t3, no further analysis was performed on these measurements. Patient characteristics at t2 are displayed in table 2.

Power analysis

Relative power in each frequency band was calculated. No significant changes in relative power occurred between t1 and t2. There were also no correlations between relative power in each frequency band and clinical characteristics, such as seizure frequency and total number of seizures.

Functional connectivity

Significant correlations were found between functional connectivity and the total number of seizures, which refers to the total number of seizures that patients had experienced from the first to the last seizure before MEG measurement at the first time point. At t1, a higher number of seizures since diagnosis was significantly associated with higher theta band PLI (Kendall's Tau=.501, p=.008; see figure 1A). This correlation remained significant when excluding an outlier patient, who had experienced a total of 120 seizures. At t2, the same association was found, although significance was lost after correcting for the number of comparisons (Kendall's Tau=0.538, p=.020; see figure 1D). The total number of seizures significantly dropped between t1 and t2 from on average 11 seizures at t1 to less than one seizure between t1 and t2 (Wilcoxon signed rank test, Z=-2.81, p=.003). There were no significant changes in functional connectivity between the two time points (see figure 2).

In order to explore which type of theta band connectivity was related to the total number of seizures at t1, we summarized connectivity into three values: (1) short-distance PLI, (2) long-distance intrahemispheric PLI, and (3) long-distance interhemispheric PLI (see reference [71]). There were highly significant correlations between the total number of seizures at t1 with both short-distance theta band PLI (Kendall's Tau=.531, p=.005) as well as with long-distance intrahemispheric theta band PLI (Kendall's Tau=.563, p=.003). Theta band functional connectivity in the temporal lobe seemed to have the strongest relation to the number of seizures: left temporo-occipital PLI (Kendall's Tau=.563, p=.003), right fronto-temporal PLI (Kendall's Tau=.610, p=.001), right temporo-occipital PLI (Kendall's Tau=.531, p=.005), and left temporal PLI (Kendall's Tau=.515, p=.006).

Several possible confounders for the reported results were explored in post-hoc analyses. There were no significant associations between functional connectivity and patients' age, the total daily dose of levetiracetam, anti-tumor treatment (chemotherapy, radiotherapy, or dexamethasone), performance status, and the duration of epilepsy at t1. Furthermore, there were no differences in functional connectivity between men and women (gender differences have been reported previously with respect to anatomical and functional connectivity [91, 92]), patients with disease recurrence versus newly diagnosed patients, patients suffering from partial or generalized seizures, patients with low-grade versus high-grade tumors, left-sided and right-sided tumors, and type of resection (biopsy or (sub)total resection), although only two patients underwent biopsy.

Table 1. Patient characteristics at t1.

	Age	Gender	Seizure type	Epilepsy duration [months]	Seizure freq. [month]	Total no. seizures	Type of surgery	PA	Tumor localization	CT	RT	DEX	KPS	Barthel
1	57	M	PS	65	4-30	10	R	OIII	RF	N	Y	N	90	20
2	43	M	GS	19	>30	120	R	AII	RF	Y	N	N	70	19
3	46	F	GS	163	0	11	R	OII	LF	Y	N	N	90	20
4	49	M	GS	30	>30	20	R	GBM	LF	Y	Y	N	80	20
5	68	M	PS	61	>30	2	R	GBM	RT	Y	N	Y	100	20
6	36	M	GS	5	0	1	R	AIII	RF	N	Y	N	90	20
7	30	M	GS	21	1	2	R	AII	RF	N	N	N	100	20
8	50	M	GS	11	1	1	B	AIII	LPO	Y	Y	Y	90	20
9	25	F	GS	15	4-30	8	B	GBM	RT	Y	Y	Y	90	20
10	61	M	GS	32	0	1	R	GBM	RF	Y	Y	Y	100	20
11	45	M	GS	117	1	1	R	OIII	RT	N	Y	N	90	20
12	37	F	GS	33	1	2	R	GBM	RFT	Y	Y	N	90	20
13	47	M	GS	38	1	3	R	AIII	LF	N	Y	N	70	19
14	29	M	GS	22	1-4	3	R	GBM	RF	Y	Y	N	90	20
15	49	F	PS	9	1	2	R	GBM	LF	Y	Y	Y	80	16
16	48	M	GS	10	0	1	R	GBM	RT	Y	Y	N	100	20
17	25	M	GS	16	1	3	R	GBM	RT	Y	Y	N	100	20

M=male, F=female, PS=partial seizures, GS=generalized seizures, R=(sub)total resection, B=stereotactic biopsy, PA=histopathological diagnosis, OII or III=oligodendroglioma WHO grade II or III, AII or III=astrocytoma WHO grade II or III, GBM=glioblastoma multiforme, RF=right frontal, LF=left frontal, RT=right temporal, LPO=left parieto-occipital, RFT=right fronto-temporal. CT=chemotherapy, RT=radiotherapy, DEX= dexamethasone, KPS=Karnofsky performance status, N=no, Y=yes.

Graph analysis

Increasing theta band edge weight correlation (i.e. lower value of Wr) was significantly related to higher total number of seizures at t1 (Kendall's Tau=-.507, p=.008; see figure 1C). Higher total number of seizures at t1 was related to higher theta band path length, although this correlation was not significant after correcting for multiple comparisons (Kendall's Tau=.404, p=.031; see figure 1B). There were no significant changes in network features between time points (see figure 3).

Table 2. Patient characteristics at t2.

	Seizure frequency (per month)	Total number of seizures	CT	RT	DEX	KPS	Barthel
1	0	10	N	N	N	100	19
3	0	11	N	N	N	90	20
4	1	22	Y	N	Y	80	20
6	0	1	N	N	N	90	20
7	0	2	N	N	N	100	20
8	1	3	Y	N	Y	100	20
9	0	8	N	N	Y	90	20
10	0	1	Y	N	N	90	20
11	0	1	N	N	N	90	20
12	0	2	Y	N	N	80	20
15	0	2	N	N	N	80	18
16	0	1	Y	N	N	90	20

CT=chemotherapy, RT=radiotherapy, DEX=dexamethasone, KPS = Karnofsky performance status, N = no, Y = yes.

Again, confounders were explored. There was no correlation between network features and duration of epilepsy, tumor treatment (radiotherapy, chemotherapy, dexamethasone), performance status, and daily dose of levetiracetam. There were no differences in network features between male and female patients, patients with recurrent disease or newly diagnosed brain tumors, patients who had undergone resection versus biopsy, patients with tumors in the left and right hemisphere, and patients with partial seizures and patients with generalized seizures. However, higher age was related to lower edge weight correlation (Kendall's Tau=.502, p=.006).

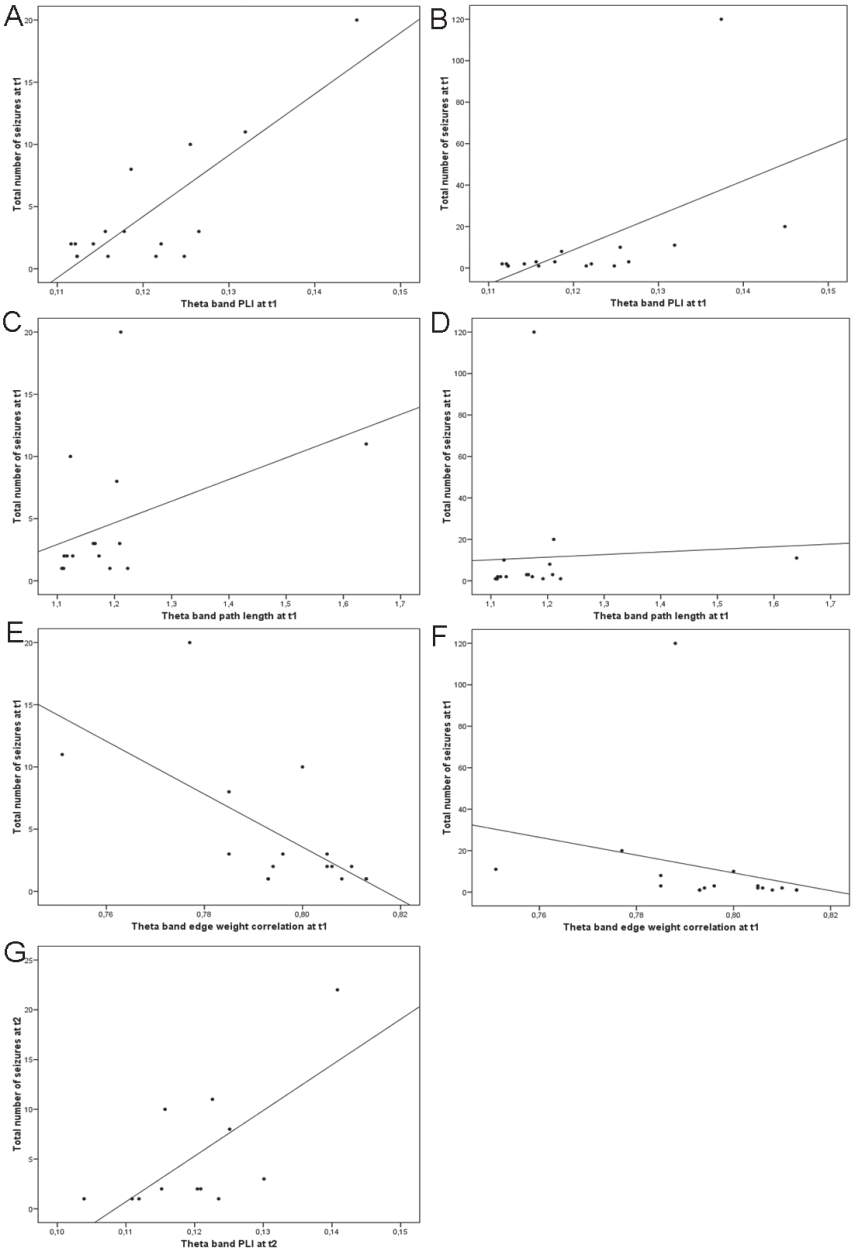

Figure 1. Scatterplots of correlations between functional connectivity, network characteristics, and total number of seizures at both t1 and t2. Left column: scatterplots excluding outlying patients (patient 2 in table 1), right column: scatterplots including this patient. (A) correlation between theta band phase lag index (PLI) at t1 without outlying patient, (B) correlation between theta band PLI at t1 with outlying patient, (C) correlation between theta band path length and total number of seizures at t1 without outlying patient, (D) correlation between theta band path length and total number of seizures at t1 with outlying patient, (E) correlation between theta band edge weight correlation and total number of seizures at t1 without outlying patient, (F) correlation between theta band edge weight correlation and total number of seizures at t1 with outlying patient, and (G) correlation between theta band PLI and total number of seizures at t2.

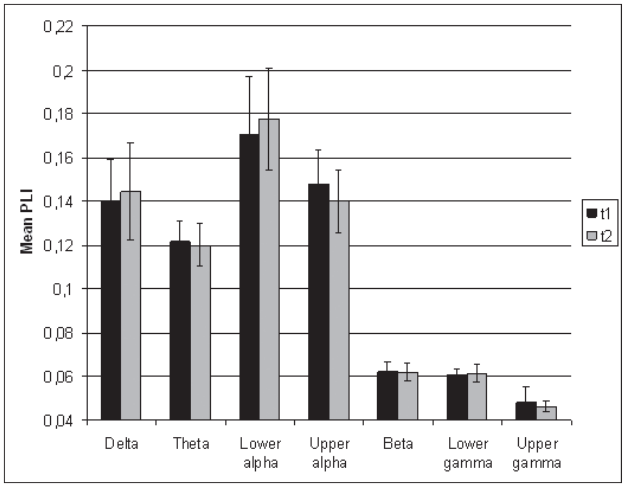

Figure 2. Mean PLI at both time points. PLI = phase lag index.

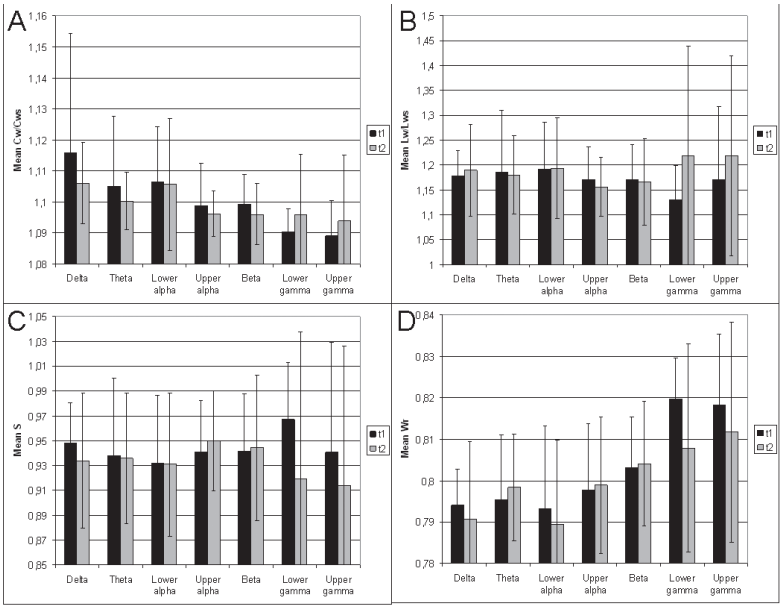

Figure 3. Mean network characteristics at both time points. C_w/C_{ws}=weighted normalized clustering coefficient, L_w/L_{ws}=weighted normalized clustering coefficient, S=small-world index, W_r=edge weight correlation.

DISCUSSION

Significant associations exist between epilepsy characteristics and both functional connectivity and network topology in brain tumor patients directly after neurosurgical intervention: increased theta band phase lag index (PLI) is related to a greater total number of seizures. This association mostly concerns theta band connectivity within the temporal lobe, and between the temporal and other lobes. There is also a correlation between higher total number of seizures and higher theta band edge weight correlation (W_r). No significant changes in functional connectivity or network variables were observed over time. Furthermore, the total number of seizures from the first seizure to both time points seemed to be the only factor related to differences in connectivity and network variables (except age), while other variables such as treatment characteristics, type of tumor, and lateralization of the tumor were not significantly related to connectivity and network topology.

Our findings concerning the association between theta band functional connectivity and number of epileptic seizures corroborate several lines of previous research and confirm our initial hypothesis. Earlier studies in brain tumor patients have shown that these patients have increased connectivity in lower frequency bands, and particularly in the theta band [10, 33]. Furthermore, theta band functional connectivity significantly decreased after tumor resection in a group of mixed brain tumor patients, suggesting 'normalization' of the previously reported pathologically increased connectivity [71]. In epilepsy, increased theta band connectivity has also been reported in the inter-ictal EEG [74]. Increased theta band functional connectivity seems to be a hallmark of epilepsy, tumor-related epilepsy, and/or brain tumors, and the current results support further investigations into this hypothesis.

Brain tumor patients have been found to have disrupted small-world- brain networks when compared to healthy controls [9, 34]. In the current study, there was a significant relation between higher number of seizures and higher edge weight correlation in the theta band. Although high edge weight correlation has been thought to be beneficial to functional status of the network, because of increased transport of information [184], correlations that are too high may increase vulnerability to seizures due to an abnormally high synchronisability of the brain network. Using a model of rat hippocampus, it has been shown that adding highly connected hubs increases network vulnerability to seizures [161]. Furthermore, single-cell recordings in rats also show that hubs are highly influential throughout the network, and may or may not promote synchronizability [32]. At seizure onset, epilepsy patients also show increases of average interconnectedness of the network [131, 180, 198]. Thus, it seems as though there is a critical threshold of connectivity and synchronisability. There was also a near-significant correlation between higher number of seizures and longer theta band path length. This increased path length in epilepsy patients has been found with EEG [110].

The associations between connectivity and seizures in this study were mainly due to connectivity with and within the temporal lobe. This result could be due to the relatively high number of patients with temporal tumors (6 of 17), but may also be related to the origins of theta band oscillations and its relation with epilepsy. The theta band contains an oscillatory pattern that has for long been thought to emanate from the hippocampal structures, after which it spreads to the outer layers of the brain. However, later studies have shown that other regions of the brain may also generate theta oscillations in certain cognitive states

[159]. Power, amplitude, and synchronization of the theta band has mainly been linked to cognitive functioning, particularly processes involved in learning and memory [118, 127, 216]. Microscopically, theta band oscillations may be regulated by GABAergic interneurons [122, 123]. Moreover, blockade of GABA receptors in induced epilepsy alters patterns of theta activity [144], and hubs consisting of GABAergic interneurons may determine network synchronization [32]. Also, neuronal changes associated with temporal lobe epilepsy can disrupt hippocampal theta function [145]. These studies point towards a possible link between epilepsy and the theta band. In human neurophysiological data, the association between the theta band and epilepsy has increasingly been studied over the past two decades. Pathological thalamo-cortical theta oscillations have been described in absence seizures [55], and increased theta band absolute spectral power is related to absence epilepsy [158] and generalized epilepsies [56]. Another study reports increased theta band power to be related to the severity of epilepsy [54]. Moreover, interhemispheric theta band coherence proved to be a selective feature of patients with generalized epilepsy [55].

Functional connectivity and network topology did not change significantly over the two time points in this study, although seizure frequency did change over time. The limited sample size in this study may have impacted significance, but the lack of change may also be due to the possibility of a stable plateau phase in connectivity and network topology. Possibly, resection of the tumor induces a great change in functional connectivity, after which this stable phase is reached at t1, approximately 6 weeks after neurosurgical intervention. Future studies should aim at elucidating this possibility. A number of explored variables also did not have a significant impact on connectivity and network features, although this intuitively may have been expected. This could be due to the small sample size and heterogeneous group, but the impact of radiotherapy, chemotherapy, and dexamethasone on the background EEG is largely unknown. A study investigating epilepsy patients receiving add-on levetiracetam treatment reports no changes in background EEG, although they did not look at connectivity [246]. Furthermore, there was no significant influence of the type (i.e. WHO grade) and lateralization (left or right hemisphere) of the tumor on functional connectivity or network characteristics, corroborating previous research that has also pointed out that the location of the tumor does not determine the pattern of connectivity changes in the brain, although patients with right-sided tumors were generally better off in terms of alterations in connectivity [10]. Another possible explanation for the lack of change may also be the high heritability of both functional connectivity and network topology [183, 203]. The effect of factors such as tumor treatment may not be great enough to overcome the constancy of the genetically determined network architecture.

This study has some limitations, one of which is the small sample size, limiting statistical power. Although patients were homogeneous with respect to brain tumor type (glioma) and AED, variation was present regarding a number of variables. These variables were not significantly related to functional connectivity or network features, but future studies should aim to investigate more homogeneous subgroups of brain tumor patients to elucidate more specific effects. Furthermore, all MEG experiments have the limitation of the inverse problem, common sources and volume conduction. However, the PLI is very strict in this respect and disregards all zero-lagged correlations, which means that our results are not the result of spurious correlations because of common sources or volume conduction.

CONCLUSION

Our results suggest that theta band connectivity and network topology may be important for tumor-related epileptic seizures. These findings bring up thoughts about possible mechanisms of epileptogenesis in brain tumor patients. Functional connectivity and network characteristics in the theta band seem most important in tumor-related epilepsy. Future research should focus on elucidating this correlation between epilepsy and the theta band.

CHAPTER 6

Connectivity in MEG resting-state networks increases after resective surgery for low-grade glioma and correlates with improved cognitive performance

E van Dellen, PC de Witt Hamer, L Douw, M Klein,
JJ Heimans, CJ Stam, JC Reijneveld, A Hillebrand

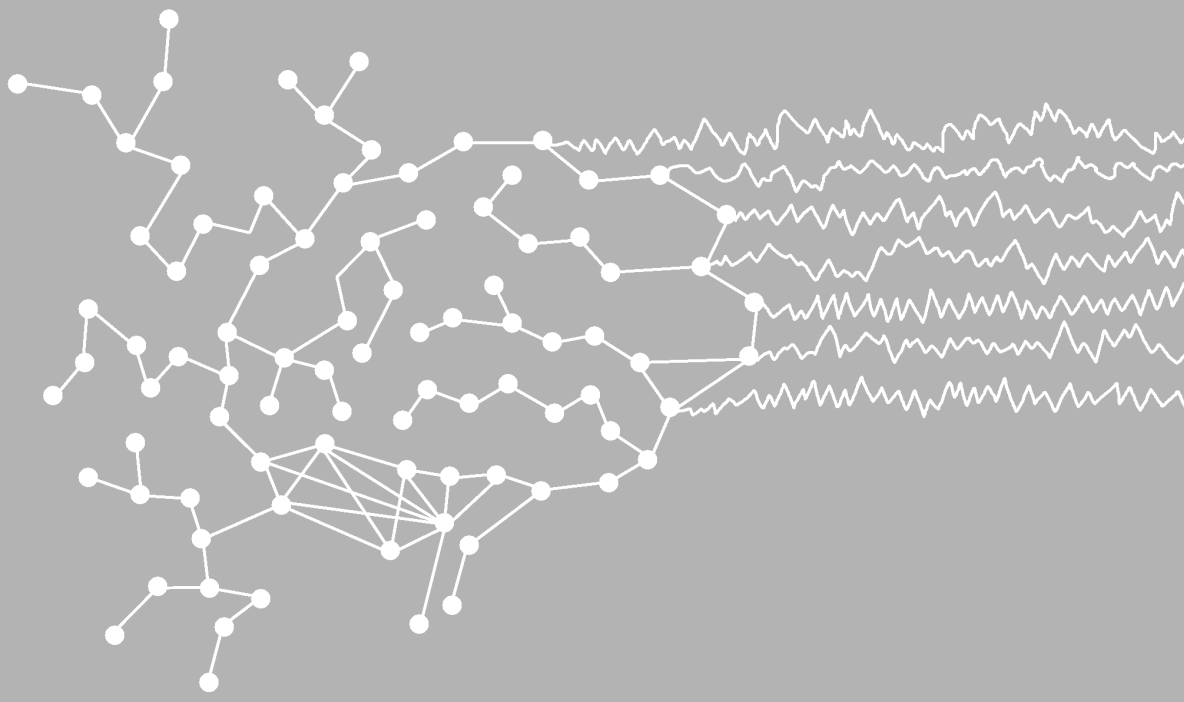

NeuroImage: Clinical (2013), 2, 1-7

ABSTRACT

Purpose: Low-grade glioma (LGG) patients often have cognitive deficits. Several disease- and treatment related factors affect cognitive processing. Cognitive outcome of resective surgery is unpredictable, both for improvement and deterioration, especially for complex domains such as attention and executive functioning. MEG analysis of resting-state networks (RSNs) is a good candidate for presurgical prediction of cognitive outcome. In this study, we explore the relation between alterations in connectivity of RSNs and changes in cognitive processing after resective surgery, as a stepping stone to ultimately predict postsurgical cognitive outcome.

Methods: Ten patients with LGG were included, who had no adjuvant therapy. MEG recording and neuropsychological assessment were obtained before and after resective surgery. MEG data were recorded during a no-task eyes-closed condition, and projected to the anatomical space of the AAL atlas. Alterations in functional connectivity, as characterized by the phase lag index (PLI), within the default mode network (DMN), executive control network (ECN), and left- and right-sided frontoparietal networks (FPN) were compared to cognitive changes.

Results: Lower alpha band DMN connectivity was increased after surgery, and this increase was related to improved verbal memory functioning. Similarly, right FPN connectivity was increased after resection in the upper alpha band, which correlated with improved attention, working memory and executive functioning.

Discussion: Increased alpha band RSN functional connectivity in MEG recordings correlates with improved cognitive outcome after resective surgery. The mechanisms resulting in functional connectivity alterations after resection remain to be elucidated. Importantly, our findings indicate that connectivity of MEG RSNs may be used for presurgical prediction of cognitive outcome in future studies.

INTRODUCTION

Low-grade glioma (LGG) patients often have cognitive deficits that limit their quality of life. Cognitive performance in these patients is affected by several factors, related to both the disease itself and to its treatment [124]. The preservation and possibly restoration of cognitive performance is particularly important for this patient population with a relatively long life expectancy. Resective surgery may result in cognitive improvement or deterioration, as the resection removes infiltrative tumor tissue that disturbs the surrounding normal brain tissue, and at the same time disrupts connections to surrounding normal brain that can be critically functional [124]. Especially the surgical outcome of complex cognitive processes such as attention, executive functioning and memory processing is unpredictable. Improved presurgical prediction of cognitive outcome would significantly contribute to patient counseling and surgical management decisions.

Mapping of functional connectivity patterns may be worthwhile for this purpose. An optimal organization of functional brain networks is required for proper cognitive processing [42, 219]. These networks can be analyzed by characterizing functional connectivity between brain areas, using magnetoencephalography (MEG), electroencephalography (EEG) and fMRI recordings [219]. In glioma patients, like in most patients with neurological and psychiatric diseases, the organization of functional networks is globally disturbed [42, 100, 219]. We have shown that MEG functional connectivity patterns change after brain resective surgery [71]. Moreover, other studies have shown that preoperative functional connectivity may be of value to guide surgical management decisions in these patients. An MEG study showed that in healthy subjects, especially alpha band connectivity is high in functionally critical brain areas such as somatosensory and language areas, and that this connectivity is altered in glioma patients [96]. Two consecutive studies showed that areas with decreased alpha band connectivity could be resected without neurological deficits [148, 226]. Connectivity analysis of large-scale brain networks therefore seems promising as a tool to predict surgical outcome.

Increased MEG connectivity in the delta, theta and gamma frequency bands has been associated with poorer cognitive performance in brain tumor patients [33]. Similarly, glioma patients with a more locally clustered and less integrated network organization (of MEG recordings filtered in the delta and lower alpha frequency bands) perform worse during neuropsychological assessments [34]. However, these studies describe global alterations in network organization rather than communication between anatomically defined regions. The current study pertains to specific subnetworks, and not the global network. In healthy subjects, several so-called resting-state networks (RSNs) have been linked in fMRI studies to performance in cognitive domains such as attention, memory processing and motor functioning [39, 59, 105, 190]. The default mode network (DMN), which is deactivated during tasks, is the most consistently described RSN, and its resting-state activity has been related to performance in several cognitive domains including attention and working memory [40]. Also, a left-sided and right-sided frontoparietal network (FPN) are thought to be crucial for attention, language and memory processing, while a frontal-cingulate network was described as the executive control network (ECN) [57, 190]. Correlations between decreased RSN activity and cognitive deficits have been described in several neurological disease states such as Alzheimer's disease, stroke, and epilepsy [40, 169]. Our study provides novel longitudinal information of both alterations in MEG RSN connectivity and cognitive changes in a population

which is not exposed to disease or therapy-related factors associated with these changes, other than resective surgery.

In this study, we aim to determine alterations in RSN connectivity after resective surgery in LGG patients, and relate this to changes in cognition. For this purpose, we study a relatively small but homogenous group of LGG patients that underwent resection without any other interventions or medication changes. We focus on the DMN, FPN and ECN, since these RSNs are involved in complex cognitive domains, which are especially relevant for this patient population. We apply a recently developed beamformer method in combination with the phase lag index (PLI), a phase synchronization measure that is relatively insensitive to common sources [104, 214], to MEG recordings. Based on studies in patients with other neurological pathology, we hypothesize that higher RSN network connectivity after tumor resection in LGG patients is related to better cognitive performance outcome [40, 169, 200].

METHODS

Patients

Consecutive patients were referred for MEG recordings by the Neurosurgical Center Amsterdam between April 2010 and April 2011. Data were collected as part of the LESION study, which is a prospective longitudinal observational study of patients eligible for tumor surgery. Inclusion criteria were (1) adult (≥ 18 years) patients who (2) had resective surgery for a histopathologically confirmed LGG (WHO grade II) and (3) had no other oncological therapy, and (4) had given written informed consent. MEG recording and neuropsychological assessment was obtained at 2 time points: prior to neurosurgical intervention (T1), and within six months after surgery (T2).

Ethics statement

Ethical approval was granted by the VU University Medical Ethics Committee. All patients had given written informed consent before participating. All clinical investigations were conducted according to the Declaration of Helsinki.

Neuropsychological screening

Based on previous studies in LGG patients, six cognitive domains were defined (Table 1), and each subtest of the neuropsychological assessment was used as a measure for functioning in one or more cognitive domains [75, 125]. A performance z-score for each domain was calculated by comparing each person's score with the mean and standard deviation (SD) of all patients' test scores at T1. The same mean and SD value were used to calculate z-scores at both time points. A delta-score was calculated for each patient by subtracting the z-scores for both time points in order to quantify change in cognitive performance.

Magnetoencephalography (MEG)

MEG recordings were made in a magnetically shielded room (VacuumSchmelze GmbH, Hanua, Germany) using a 306-channel whole-head neuromagnetometer (Elekta Neuromag Oy, Helsinki, Finland). Five minutes of MEG data were recorded during a resting-state eyes-closed condition with a sample frequency of 1250 Hz. An anti-aliasing filter and high-pass filter

of 410 Hz and 0.1 Hz were applied, respectively. Other artefacts were removed from the data with an offline spatial filter, namely the temporal extension of Signal Space Separation (tSSS) [227, 228] in MaxFilter software (Elekta Neuromag Oy, version 2.2.10). A sliding window of 10 seconds was

Table 1. Cognitive test battery and corresponding domains

Neuropsychological test	**Corresponding cognitive domain**
Concept Shifting Test	Executive functioning, Psychomotor speed
Categoric Word Fluency Task	Executive functioning
Rey Auditory Verbal Learning Test	Verbal memory
Stroop Color-Word Test	Attention
Memory comparison test	Working memory
Letter-Digit Substitution Test	Information processing, Psychomotor speed

Tests were assessed as described by [139], except for the Concept Shifting Test [111].

used. Channels that were malfunctioning during the recording, for example due to excessive noise, were automatically discarded before estimation of the SSS coefficients. Additionally, malfunctioning channels were identified by visual inspection of the data, and excluded before applying tSSS. The number of excluded channels varied between one and eight. The tSSS filter was then used to remove noise signals that SSS failed to discard, typically from noise sources near the head, using a subspace correlation limit of 0.9.

The head position relative to the MEG sensors was recorded continuously using the signals from four head-localisation coils. The head-localisation coil positions were digitized, as well as the outline of the participants scalp (~500 points), using a 3D digitizer (3Space FastTrack, Polhemus, Colchester, VT, USA). This scalp surface was used for co-registration with the patient's anatomical MRI.

Anatomical MRI

Structural Magnetic Resonance Images (MRI) were made for co-registration with a sagittal slice distance of 0.5-1.5 mm. Co-registration of these T1-weighted MRIs with the MEG data was achieved using surface matching software developed by one of the authors (AH), resulting in an estimated co-registration accuracy of approximately 4 mm [258]. A single best fitting sphere was fitted to the outline of the scalp as obtained from the co-registered MRI, which was used as a volume conductor model for the dipole fitting and beamformer analysis described below. The co-registered MRI was then spatially normalized to a template MRI using the SEG-toolbox in SPM8. The new segmentation toolbox [254] is an extension of the unified segmentation algorithm [6], which incorporates additional tissue priors for improved matching of the subject's MRI to the template. The AAL atlas was used to label the voxels in a subject's normalized co-registered MRI [232]. Subcortical structures were removed, and the voxels in the remaining 78 cortical regions of interest (ROIs) were used for further analyses [90], after inverse transformation to the patient's co-registered MRI.

Time-series estimation for regions-of-interest

We used the beamformer approach as described by Hillebrand and others [104]. In summary, neuronal activity in the labeled voxels in the ROIs was reconstructed using a scalar beamformer implementation (Elekta Neuromag Oy, beamformer, version 2.1.27) similar to Synthetic

Aperture Magnetometry [188]. This beamformer sequentially reconstructs the activity for each voxel in a predefined grid covering the entire brain (spacing 2 mm) by selectively weighting the contribution from each MEG sensor to a voxel's time-series. Each ROI contains many voxels and the number of voxels will be different for each ROI. In order to represent a ROI by a single time-series, we selected, for each ROI and frequency band separately, the voxel with maximum pseudo-Z value in that frequency band [188]. For the computation of the pseudo-Z values we estimated the data covariance for, on average, 325 seconds (range: 144-694 sec.) of data, and used a unity matrix for the noise covariance. The broad-band (0.5-48Hz) time-series for these selected voxels were used for further analysis. This resulted in 78 time-series for each frequency band. Six frequency bands were analyzed: delta (0,5-4Hz), theta (4-8 Hz), lower alpha (8-10 Hz), upper alpha (10-13 Hz), beta (13-30 Hz), and lower gamma bands (30-48 Hz). Time-series were downsampled 4 times, and for each subject, five artifact free epochs of 4096 samples (13.1072 seconds) were selected (EvD) and further analysed using Brainwave v0.9.58 [authored by C.S.; available at http://home.kpn.nl/stam7883/brainwave.html].

Functional connectivity

The phase lag index (PLI) was used to assess functional connectivity between the reconstructed signals in source space. The PLI is a measure that is relatively insensitive to the effects of volume conduction [214]. The synchronization between time series is based on the consistency of the nonzero phase lag with respect to another signal. The instantaneous phase difference for each time sample is computed using the analytical signal concept and the Hilbert transform. The PLI characterizes the asymmetry in the distribution of instantaneous phase differences between two signals. The reason for using the asymmetry of this distribution as a measure of functional interactions, is that a nonzero phase lag between these signals cannot be explained by volume conduction. The PLI ranges between 0 (no phase locking) and 1 (total synchronization). See chapter 3, formula (2) for a mathematical description of PLI. For each subject, the PLI was calculated for all possible ROI pairs. The functional connectivity within one of the predefined RSNs described below was then computed by averaging all PLI values between the ROIs within that sub-network.

Resting-state networks

Most RSNs described in literature are based on independent component analysis (ICA) applied to resting-state fMRI data. These ICA analyses suggest that the regions within each RSN are functionally closely coupled, at least at the level of BOLD-fMRI. Based on the assumption that such coupling should have a correlate in the MEG data [39, 46, 66, 105, 167], we defined MEG RSNs by selecting only those connections between the ROIs within literature-based RSNs. The review by Rosazza and Minati was used to define the RSNs, as it presents a complete overview of the RSNs with detailed information about their anatomical definitions [190]. We selected four RSNs that are of interest for cognitive functioning in the domains that are frequently affected in LGG patients [124], namely the default mode network (DMN), the left and right frontoparietal network (FPN), and the executive control network (see table S1 for included ROIs). An overview of all RSNs and their definitions in terms of ROIs is provided in the supplementary material, as well as an analysis for a different definition of the RSNs (table S1).

Statistics

Statistics were computed using IBM SPSS statistics 18.0. The PLI is typically non-parametrically distributed between subjects, and the analyzed patient group contained a relatively small

number of subjects. Wilcoxon signed ranks tests were therefore used to test whether PLI levels differed between T1 and T2 for mean PLI over all connections, and for the mean PLI within each RSN. Results were considered significant for $p < 0.05$, corrected for multiple testing using the false discovery rate (FDR) per frequency band. Possible differences between T1 and T2 regarding cognitive performance in any of the six domains were determined using Wilcoxon signed ranks tests because of the small sample size. When a significant RSN PLI alteration was found, we

Table 2. Patient characteristics

Patient	Age	Gender	Lat.	Localization	Preop. vol.	Postop. vol.	EOR
1	20	F	R	Temp	7	0	99%
2	48	F	R	Front-Temp-Ins	72	8	89%
3	29	M	L	Front-Temp	68	4	94%
4	53	F	L	Temp	106	5	95%
5*	29	M	R	Front-temp	78	25	68%
6	52	M	L	Temp	49	5	90%
7*	46	M	R	Front-temp	80	19	76%
8	18	M	L	Front-temp	37	1	98%
9	28	F	L	Front-temp-Ins	56	10	82%
10	30	M	L	Front	30	11	63%

Patient characteristics. Lateralization and localization of the tumor are given, as well as tumor volumes (as determined with iPlan software, BrainLAB, Feldkirchen, Germany) and the extent of the resection. Abbreviations: Preop. vol = preoperative tumor volume (mL); Postop. vol. = preoperative tumor volume (mL); EOR = extent of resection; F = female; M = male; lat = lateralization of tumor; temp = temporal; front = frontal; ins = insula; NA = not available. * = no neuropsychological evaluation data available.*

Table 3. Changes in cognitive performance

Patient	Overall	Executive functioning	Verbal memory	Working memory	Information processing	Attention	Psychomotor speed
1	0.45	-0.28	-0.05	0.20	0.47	2.59	0.45
2	-0.06	-0.39	-0.38	0.14	-0.23	0.18	-0.59
3	-0.09	-0.28	-0.03	-0.36	-0.17	0.14	0.56
4	-0.79	-0.40	-2.15	-0.17	-0.01	-0.23	0.16
5	NA	NA	NA	NA	NA	NA	NA
6	-0.02	-0.51	0.35	0.06	0.57	-0.29	-0.86
7	NA	NA	NA	NA	NA	NA	NA
8	-1.33	-1.65	-1.00	-1.02	-1.07	-2.88	-0.15
9	-0.09	0.29	-0.04	-0.09	0.08	0.09	-0.11
10	0.34	-0.14	0.35	0.12	0.43	0.75	0.55

Individual cognitive performance scores are presented per domain. Values represent the difference of the z-scores between T1 and T2 (positive values indicate better performance after resection).

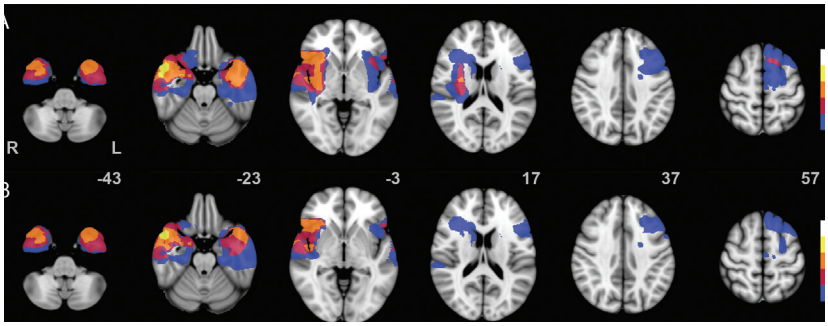

Figure 1. Localization of gliomas and resection cavities. Heatmap of lesion load for (A) glioma localization and (B) resection cavity localization of the study population on MNI standard brain template (MNI z-coordinates are given for each cross section). The legend shows the number of gliomas and resection cavities, respectively, that are represented by the colors in the figure. Note that most lesions are remote from the default mode network and right frontoparietal network shown in figures 2 and 3.

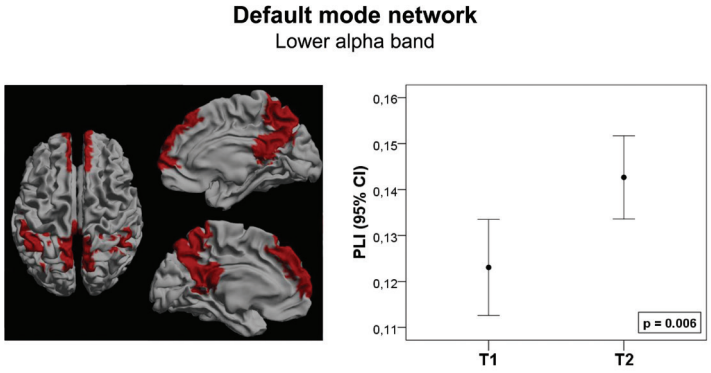

Figure 2. The default mode network, marked red in the left frame, showed increased connectivity in the lower alpha band after resection. Connectivity increase is presented as a 95% confidence interval at both timepoints. The p-value marks the significance of a Wilcoxon signed ranks test.

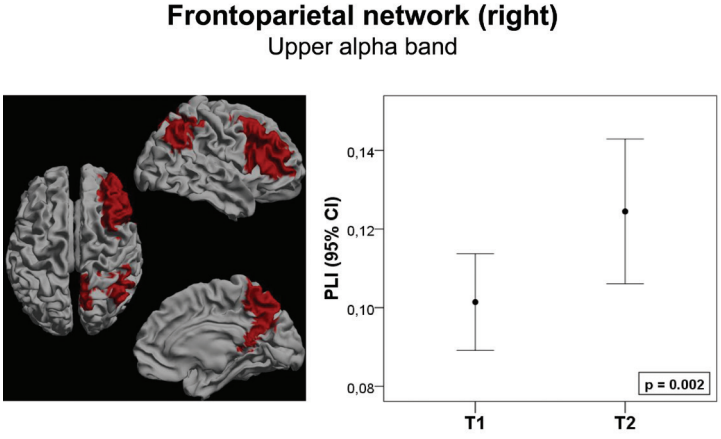

Figure 3. The frontoparietal network of the right hemisphere, marked red on the left frame, showed increased connectivity in the upper alpha band after resection. Connectivity increase is presented as a 95% confidence interval at both timepoints. The p-value marks the significance of a Wilcoxon signed ranks test.

assessed possible correlations with cognitive performance in each of the six domains as a post-hoc analysis using Kendall's tau tests.

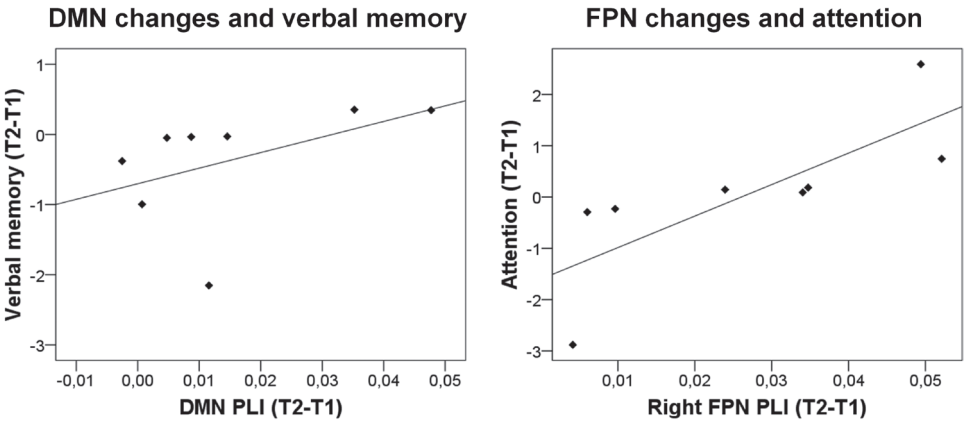

Figure 4. Correlations between lower alpha band DMN changes and verbal memory (left; tau = 0.571; R2 = 0.215; p = 0.048), and upper alpha band FPN changes and attention (right; tau = 0.857; R2 = 0.602; p = 0.003). Most patients show only small increases in RSN connectivity and small improvement in cognitive performance. Especially patients with no increase of RSN connectivity show deterioration of cognitive performance scores.

RESULTS

Ten patients with a WHO grade II glioma were included (table 2; figure 1). Mean time between resection and T2 was 16 weeks (range 11-25 weeks). Neuropsychological data at both T1 (pre-resection) and T2 (post-resection) were available in eight patients. Wilcoxon signed ranks tests showed no differences in cognitive performance between T1 and T2 on a group level in any of the six cognitive domains (table 3; table S2).

Functional connectivity analysis

First, we studied whether changes in global connectivity or connectivity of specific subnetworks after resective surgery can be detected using MEG. Therefore, global alterations in average PLI were determined using Wilcoxon paired signed ranks tests. No significant differences were found in any of the six frequency bands between T1 and T2. Furthermore, we determined PLI alterations for each frequency band in the four RSNs as defined by [190]. After resection, patients showed higher PLI in the default mode network in the lower alpha band ($z = -2.599$; $p = 0.006$; figure 2). Patients also showed higher PLI in the right FPN after resection in the upper alpha band ($z = -2.803$; $p = 0.003$; figure 3). In this right FPN, a higher PLI was also found in the theta ($z = -2.191$; $p = 0.027$) and lower alpha ($z = -2.191$; $p = 0.027$) bands after resection,

but only alteration in the upper alpha band remained significant after FDR correction. No significant alterations were found in the left FPN or in the ECN. This demonstrates that changes in connectivity can be detected using MEG.

Second, to determine the relation between the MEG alterations in connectivity of specific subnetworks and changes in the corresponding cognitive domains, we assessed correlations (Kendall's tau) between cognitive performance and the RSNs that showed significant MEG connectivity changes after resection. In the lower alpha band, we found a positive correlation between DMN connectivity and verbal memory scores (tau = 0.571; p = 0.048; figure 4A). Similarly, upper alpha band right FPN connectivity correlated positively with attention (tau = 0.857; p = 0.003; figure 4B), working memory (tau = 0.571; p = 0.048) and executive functioning (tau = 0.643; p = 0.026). Of interest, patients with a relatively large cognitive improvement demonstrated a large increase of RSN connectivity (figure 4).

DISCUSSION

The organization of the human brain can be described as a globally integrated network, in which local segregation is found in several subnetworks that are involved in different cognitive tasks [41, 57, 66, 190]. In this study, surgical resection of LGG increased the connectivity of two of these networks, namely the default mode network (DMN) and the right frontoparietal network (FPN). Importantly, a large increase of resting-state network (RSN) activity was related to better post-surgical cognitive performance regarding attention, memory functioning, and executive functioning. This provides proof of principle that cognitive changes after resective surgery correspond with connectivity alterations in RSNs.

Resting-state networks and cognitive functioning

Previous cross sectional studies in healthy controls and stroke patients have elucidated the cognitive processes in which the RSNs that we analyzed are involved. Indeed, activity in the FPNs for memory and attention functioning was established in healthy controls [58, 70, 88]. Two previous studies describe the effects of ischemic stroke on the FPN. Nomura and colleagues showed that the amount of damage to the FPN correlated with lower functional connectivity in that network, while connectivity in a control network was preserved [169]. This indicates that lesions in the FPN cause functional disturbances within this particular network, also to regions that were not directly damaged due to the lesion. Dubovik and colleagues showed in an EEG study that higher alpha band connectivity of the fronto-opercular cortex in stroke patients was related to verbal fluency and verbal working memory performance, while connectivity of the right inferior parietal cortex was related to spatial memory performance [79]. Both these regions are part of the FPN. In the present longitudinal study, we found that increased alpha band right FPN connectivity was related to better performance in the attention, working memory, and executive function domains.

Our finding of better verbal memory in patients with increased DMN connectivity is somewhat different from previous findings. The DMN has mainly been described in fMRI studies as a network that is deactivated during task performance, while the resting-state level of connectivity is correlated to attention and working memory performance (see Broyd for an extensive review [40]); decreased DMN connectivity was found in several diseases such as

ADHD, autism and Alzheimer's disease. In contrast, increased connectivity in schizophrenia patients was related to excessive alertness [40]. Although increased connectivity within the DMN could thus be seen as a normalization after resection of the glioma, the correlation with verbal memory is not yet clear. We postulate that alterations in the DMN can have global effects on cognitive functioning because of its central role in the network, and we expect the correlation found between DMN connectivity and verbal memory to reflect this global effect.

Connectivity changes and resective surgery

To the best of our knowledge, this is the first study to show alterations in RSN connectivity after resective brain surgery. One previous study on the effects of tumor resection described that functional connectivity patterns after resection change in a complex way, demonstrating a decrease in interhemispheric theta band connectivity [71]. Other work focused on the predictive value for surgical outcome of presurgical connectivity of the tumor region. When the resected area has a high alpha band functional connectivity, this suggests eloquence for language or motor functioning [96, 148, 226]. On the other hand, a central role or high connectivity in the presurgical network can also predict seizure freedom after resection, depending on the frequency of the analyzed oscillations [173, 260]. In our study, patients that showed highest increase of alpha band RSN activity after surgery were also the ones with improved neuropsychological test scores.

In this study, patients demonstrated varying increase in connectivity of the DMN and the right FPN after a local surgical intervention. An important question is which factors determine why some patients show larger connectivity increases than others after resection, or, in a broader perspective, what determines the impact of a lesion or resection on the global brain network. One tempting hypothesis is that the level of increase in connectivity after resective surgery depends on the level that structures involved in the DMN and FPN are (directly or indirectly) affected by tumor infiltration or tumor mass effect. Many infiltrative gliomas in these patients involved long projection fibers, which are candidate structures subserving these networks. Alternatively, distant disinhibitive effects on the functional status of these networks cannot be ruled out until the structures substantiating these network have been identified. Previous work based on MEG, EEG and fMRI has revealed global alterations in connectivity in the presence of a lesion, including the contralateral hemisphere [10, 72, 77, 93]. Moreover, the impact of lesions in an anatomically realistic model of the human brain relied to a large extent on the importance, or 'hub' status, of the lesioned area in the anatomical network [4]. These studies therefore suggest that the preoperative connectivity of the region that is to be resected contains information on the postoperative functional changes that can be expected. In support of this hypothesis is previous work that has demonstrated that preoperative local connectivity is predictive for postoperative neurological functioning [96, 148, 226]. Future work should focus on the connectivity between the tumor region and RSNs to predict postoperative functional changes to guide surgical management decision.

Methodological considerations

The study of MEG functional connectivity and RSNs in source-space is a relatively new methodological approach. Combined EEG/fMRI registrations in healthy controls have indicated that particularly synchronized activity in the alpha band has a spatial correlate with RSNs such as the DMN, which was also the frequency range where our results were found [116]. Previous MEG studies have validated these networks using Independent Component Analysis (ICA) applied to the Hilbert envelope of the MEG timeseries [39, 66, 105]. We used the PLI to measure interactions between these validated predefined ROIs. Previous MEG studies have shown that the PLI is a valid measure of synchronization that is useful to

characterize functional interactions related to cognitive processing in both healthy controls and glioma patients [34, 76]. An important advantage of source space MEG functional connectivity analysis is that it measures neuronal activity directly with a high temporal resolution, which is done in a standardized anatomical space using the beamformer approach, while functional MRI studies estimate neural activity based on an indirect measure of metabolic changes.

This study has some limitations. As part of our analysis approach we normalized the patients' MRIs to a template brain (and then labeled voxels using a standard (AAL) atlas), while our patients had altered anatomy due to the tumor, which may have influenced results. Moreover, for the postoperative beamformer analysis, data were projected to voxels at locations where no actual cortical tissue was present anymore due to the resection. However, we expect this to have minimal effects, as we used the voxel with highest power as a representative source for each ROI, and voxels at locations without cortical tissue are not likely to show any activity apart from 'leakage' from surrounding sources (e.g. [8]). Although a small number of patients was used, a correlation between the connectivity changes and cognitive changes was nevertheless detected. A larger cohort will be subject of future studies to further assess this relation.

In conclusion, improvement in cognitive performance was related to increased functional connectivity in resting-state networks after resective surgery of LGG, as detected by source space MEG analysis. An increase in DMN connectivity in the lower alpha band was related with an increase in verbal memory performance, and an increase in FPN connectivity in the upper alpha band was related with an increase in attention, executive functioning, and working memory performance. This provides proof of principle that MEG functional connectivity is linked with cognitive outcome of resective surgery. These findings may be utilized in future studies to elucidate whether presurgical MEG resting-state connectivity can predict cognitive outcome, which would aid patient counseling and surgical management decisions.

ACKNOWLEDGEMENTS

The authors would like to thank G. Engels and N. Sijsma for their assistance with data analysis; W. Cleijne for her assistance with neuropsychological assessments; P. Tewarie and K. Olde Dubbelink for their input on the definition of resting-state networks; and the MEG technicians of the Department of Clinical Neurophysiology, P.J. Ris and K. Plugge, for technical assistance. E. van Dellen is supported by the Dutch Epilepsy Foundation (NEF) grant 09-09. L. Douw is supported by the Rubicon grant of the Netherlands Organisation for Scientific Research (NWO).

The authors have no conflicts of interests to report.

SUPPLEMENTARY INFORMATION

Table S1. Resting-state networks

Resting-state network	Corresponding AAL atlas ROIs (Rosazza and Minati, 2011)	Corresponding AAL atlas ROIs (1 ROI overlap)
Default mode network	Precuneus, posterior cingulate gyrus, inferior parietal gyrus, medial prefrontal gyrus	Precuneus, posterior cingulate gyrus, anterior cingulate gyrus*, inferior parietal gyrus, medial prefrontal gyrus
Executive control	Medial frontal cortex, superior frontal gyrus, anterior cingulate gyrus	Medial frontal cortex, superior frontal gyrus, anterior cingulate gyrus
Frontoparietal (left/right)	Inferior frontal gyrus pars triangularis, inferior frontal gyrus pars opercularis*, medial frontal gyrus, precuneus*, inferior parietal gyrus, angular gyrus	inferior frontal gyrus pars triangularis, medial frontal gyrus, inferior parietal gyrus, superior parietal gyrus*, angular gyrus

*Definitions of the analyzed RSNs. Data that were presented as main results in the paper were based on the ROI definition of Rosazza and Minati. However, a slight modification to this definition was proposed by Tewarie and others (in preparation), which prevents overlap of connections between RSNs (right column). Our data were also analyzed using this definition. Differences between both definitions were marked with *.*

Table S2. Differences in cognitive performance scores between T1 and T2

Cognitive domain	Mean	SD	p-value
Executive functioning (T2-T1)	0.420	0.55	0.055
Verbal memory (T2-T1)	0.368	0.84	0.250
Working memory (T2-T1)	0.140	0.40	0.641
Information processing (T2-T1)	-0.008	0.53	0.844
Attention (T2-T1)	-0.043	1.50	0.945
Psychomotor speed (T2-T1)	-0.001	0.53	1.000

Wilcoxon signed ranks tests comparing patients' cognitive performance z-scores before and after tumor resection. No significant differences were found.

CHAPTER 8

The lesioned brain: still a small-world?

E van Dellen*, L Douw*, JC Baayen, M Klein, DN Velis,
WCJ Alpherts, JJ Heimans, JC Reijneveld, CJ Stam
*** Both authors contributed equally**

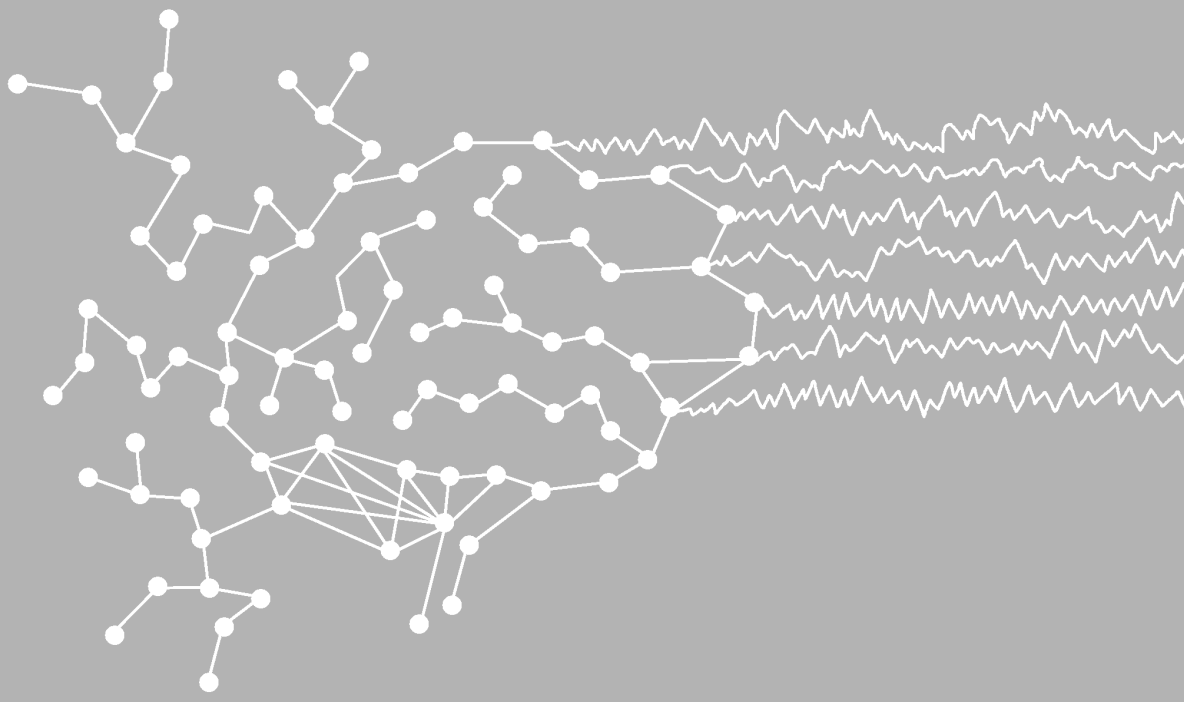

Frontiers in Human Neuroscience (2010) 4, 174.

ABSTRACT

The intra-arterial amobarbital procedure (IAP or Wada test) is used to determine language lateralization and contralateral memory functioning in patients eligible for temporal lobe resection because of pharmaco-resistant epilepsy. During selective sedation of one hemisphere, functioning of the contralateral hemisphere can be assessed by means of neuropsychological tests. We use the IAP as a reversible model for the effect of lesions on brain network topology. The dataset used, existing of EEG recordings during IAP, has been analyzed previously. Three artifact free epochs (4096 samples) were selected from each EEG record before and after amobarbital injection. Functional connectivity was assessed by means of the synchronization likelihood (SL). The resulting functional connectivity matrices were constructed for all six epochs per patient in four frequency bands, and weighted network analysis was performed. The clustering coefficient (C_w), average path length (L_w), small-world index (S), and edge weight correlation (W_r) were calculated. Recordings of 33 patients (18 males) were available. Most patients had a tumor (58%), while others had mesial temporal sclerosis (MTS; 39%), and one had gliosis due to trauma. The lesion was located in the left hemisphere in 52% of patients. Network topology changed significantly after amobarbital injection: clustering decreased in all frequency bands, while path length decreased in the theta and lower alpha band, indicating a shift towards a more random network topology. Likewise, the edge weight correlation decreased after injection of amobarbital in the theta and beta bands. Network characteristics after injection of amobarbital were correlated with memory score: higher theta band small-world index and increased upper alpha path length were related to better memory score. The whole-brain network topology in patients eligible for epilepsy surgery becomes more random and less optimally organized after selective sedation of one hemisphere, as has been reported in studies with brain tumor patients. Furthermore, memory functioning after injection seems related to network topology, indicating that functional performance is related to topological network properties of the brain.

INTRODUCTION

The Wada test (intra-arterial amobarbital procedure, IAP) is a commonly used test to determine language dominance and memory capacity in surgery candidates with temporal lobe epilepsy (TLE) [191, 249]. During the IAP, functioning of the non-anaesthetized hemisphere can temporarily be assessed by means of standardized neuropsychological testing, while sodium amobarbital selectively suppresses neural activity in the barbiturate-perfused cerebral regions of the hemisphere ipsilateral to the internal carotid artery catheterized. The IAP has for long been a clinically essential tool in determining patients' eligibility for epilepsy surgery, since it determines language dominance and whether the non-sedated hemisphere has sufficient reserve capacity to sustain memory functions after resection of (parts of) the affected temporal lobe.

In addition to its clinical application, the IAP can be considered a research model of reversibly 'shutting down' the greater part of one hemisphere of the brain. Functional connectivity refers to the statistical interdependencies between time series [3], and may change when lesions occur in the brain. Functional connectivity is thought to reflect communication between different brain areas, thus having a major impact on optimal brain functioning [37, 187, 201, 231, 244]. Previous research at our department showed that functional connectivity of the electroencephalogram (EEG) changed dramatically after amobarbital injection [72]. Changes in connectivity were found not only in the injected and contralateral hemispheres themselves, but also in the interaction between both hemispheres. These results suggest that connectivity throughout the whole brain immediately reacts to changes in activity level in one part of the brain.

The brain functions as a complex integrated network, in which focal changes influence the integrity and functional status of the brain as a whole. Patterns of connectivity between brain areas may change when suppressing activity in one hemisphere. Visual representations of these patterns can be constructed from neurophysiological time series, such as recorded with EEG. The electrodes or brain areas are nodes in the network, while functional connectivity is the strength of the link between these vertices. The application of complex network theory or 'graph theory' to the brain has proven to be relevant for brain functioning [41, 187]. Not only does graph theory provide information about the level of communication throughout different parts of the brain, it may also prove possible to define an 'optimal' network for brain functioning. This optimal network would include concepts that are pivotal in many types of complex networks, such as localized segregation combined with overall integration. Watts and Strogatz proposed a theoretical framework for a network that may contain two of the essential features of brain networks, the so-called 'small-world' network [253]. This network combines both high local 'clustering' with short 'path length', which refers to the average number of links or 'edges' that have to be crossed to reach any other node or 'vertex' in the network. Another important feature of brain network topology may be the edge weight correlation, referring to the extent to which connections to one node have similar weights. A network consisting of nodes with high edge weight correlation seems to be most beneficial to information processing [184]. Although a complete model of brain functioning does not exist at this point, exploration of the small-world topology does help us understand networks in the brain, using relatively simple measures such as clustering and path length.

Several studies have shown that both structural and functional brain networks in healthy

humans and animals can be characterized by the small-world principle [2, 99, 102, 196, 223, 253]. Network theory is also increasingly applied to patients with brain disease, for instance in Alzheimer's disease [210] and schizophrenia [154]. However, investigations regarding the impact of circumscribed lesions on network features in the human brain are rather sparse up till now. Studies in brain tumor patients have shown that these patients display a loss of the small-world configuration of the brain when compared to healthy controls [9, 34]. Moreover, network topology in these patients was related to poorer cognitive functioning [34].

The reversible IAP is a highly useful model to investigate acute adaptation of global functional brain networks after lesioning. In this study, we use the IAP as a simulation of the acute effects of a lesion on graph theoretical features of the brain. We hypothesize that 'shutting down' parts of one complete hemisphere has significant effects on functioning and network topology of the whole brain, possibly having an impact similar to brain tumors. Furthermore, we investigate the association between these network properties and cognitive performance during the Wada test.

METHODS

Patients

EEG data from all patients who underwent the IAP between November 2003 and October 2007 at the VU University Medical Center were visually inspected for this retrospective study. Functional connectivity in these patients has been described earlier [72]. All patients suffered from pharmaco-resistant epilepsy and were selected for temporal lobe epilepsy surgery, warranting a preoperative IAP. Only patients of whom three artifact-free epochs of eight seconds directly before and after amobarbital injection could be selected were included. The EEGs and neuropsychological data that were used were recorded as part of regular patient care, and data were analyzed anonymously in this study. The medical ethical committee approved this retrospective study and decided informed consent was not needed.

Intra-arterial amobarbital procedure

In order to inject the amobarbital selectively into the internal carotid artery, a 4F catheter was placed via a femoral artery approach, guided by angiography. In order to observe flow patterns through the circle of Willis, selective angiography of the internal carotid artery and visualization in posterior-anterior and lateral projection was performed in all patients before injection of the sodium amobarbital. None of the patients showed cross-flow into the contralateral arteria cerebri media. The injections of amobarbital were administered by hand through a catheter which was removed immediately after injection. Patients were typically injected with a bolus of 125 mg sodium amobarbital in 2.5 cc. Patients had their eyes open, and were instructed to lie still as much as possible during the procedure. The aim of the IAP is to assess language lateralization and memory functioning of the hemisphere contralateral to the temporal lobe that is to be resected. Approximately 2.5 minutes after amobarbital injection, the patients are visually presented with five pictures of random objects, which they must try to remember. When the amobarbital effects wear out after on average 15 minutes (as seen on the EEG recording), recognition of the objects patients have been presented with during the sedated period is assessed. This yields a correct percentage of 0, 20, 40, 60, 80, or 100%.

A score above 60% indicates that enough memory functioning is present in the contralateral presumed healthy hemisphere, rendering the patient eligible for resection.

EEG recording & data selection

Electroencephalography was performed continuously from approximately one hour before to half an hour after the Wada procedure. EEGs were recorded with a digital EEG apparatus (Brainlab, manufactured by OSG) from Fp2, Fp1, F8, F7, F4, F3, A2, A1, T4, T3, C4, C3, T6, T5, P4, P3, O2, O1, Fz, Cz and Pz with tin electrodes. Impedance was kept below 5 kOhm. Initial filter settings were: time constant 1 s and high frequency cut-off 70 Hz. Sampling frequency was 500 Hz per channel, no data skew with a 16 bit AD conversion precision. As reference for the EEG, an average montage was used during measurements.

During the Wada procedure, patients are firstly injected with amobarbital in the lesioned side of the brain. Some patients also undergo sedation of the contralateral hemisphere after the effect of the first injection has faded. However, in order to ensure that no delayed sedation effects could account for our results, we only used first injection epochs, which were all performed in the lesioned hemisphere. The amobarbital effect is maximal up to the first minute after starting the injection. Therefore, the three most artifact free epochs of eight seconds (i.e. 4096 samples) were visually selected [LD] both from the 40 seconds directly before and directly after injection. The two frontoparietal (Fp2,1) as well as the auricular (A2,1) electrodes were excluded to minimize artifacts due to eye movements. Further analyses of functional connectivity were performed off-line with software developed at the department of clinical neurophysiology of the VU University Medical Center (DIGEEGXP [CJS]).

Functional connectivity & graph analysis

In order to calculate graph theoretical variables, the synchronization likelihood (SL, see references [160, 217]), a non-linear measure of synchrony between two time series, was used as an index of functional connectivity. Synchronization likelihoods between all combinations of the 17 included electrodes were determined, providing us with a 17x17 matrix of SL values. These matrices were calculated in the following four frequency bands: theta (4-8 Hz), lower alpha (8-10 Hz), upper alpha (10-13 Hz), and beta (13-30 Hz), see reference [212]. The delta and gamma bands were not analyzed, because these frequency bands are sensitive to sedation effects and movement artifacts, respectively. The results of our functional connectivity analysis in this patient group have been published previously [72].

Graph theory was used to analyze the effects of IAP on neural network topology. A graph is a topographical representation of a network, constructed by vertices and edges between these nodes. Various measures can be used to characterize a graph, three of which were used in this study (see references [41, 193] for recent reviews). The clustering coefficient C, which is the likelihood that neighbors of a vertex will also be connected, characterizes the tendency of nodes to form local clusters. The average path length L, which is the average shortest path length connecting two vertices counted as a number of edges, is a measure for global integration of the network. The combination of high local clustering and a short average path length seems to be the optimal configuration for efficient communication in a network [253]. A small-world network, which is thought to be a feasible model for human brain networks, has such a configuration. In our analysis, we constructed weighted graphs, in which a certain weight is given to each edge that reflects the importance or strength of the edge [210]. The strength of each edge was defined as the SL between the pair of vertices. Based on these weights, the clustering coefficient C_w and average shortest path length L_w were calculated while assuming networks to be symmetric. Clustering coefficient was defined following formula

(2) in chapter 4, while path length was calculated using formula (3) in chapter 4. For a more extensive description of the procedures see reference [210].

All network properties depend not only on edge weights and network structure but also on network size. The use of a certain reference which corrects for network size would increase comparability of network characteristics. We therefore compared all characteristics to those of 1000 surrogate random networks of the same size, resulting in the measures C_w/C_{ws}, L_w/L_{ws}. The surrogate networks were obtained from the original networks by randomly reshuffling the edge weights, which produces an equal probability over the whole matrix. Symmetry was retained in this network, but node strength is not retained exactly in these weighted random networks. The small-world characteristics of the network were measured using the small-world index S, which is defined as $S=(C_w/C_{ws})/(L_w/L_{ws})$. A network is considered a small-world network if $C_w/C_{ws}>1$ and $L_w/L_{ws}\sim1$. Any value of $S>1$ thus is account for small-world network.

Finally, we calculated the edge weight correlation. This is a measure for the correlation between weights of neighboring edges, i.e. edges that connect to the same vertex [184]. The weight correlation is calculated as the range between the highest and lowest weight of all edges per vertex. This range is then compared to that of the random equivalent of the network, in which the edges are randomly redistributed over the vertices while their weights are kept unchanged (as described above for other network characteristics). When the resulting value $W_r<1$, a positive weight correlation exists (because the range of neighboring weight values is smaller than in a random network), whereas the weights are anti-correlated when $W_r>1$. It has been shown that a positive weight correlation dramatically increases transport over the network, and especially as W_r reaches 0; a positive correlation indicates that highly connected paths are present [184].

Statistical analysis

All statistical analyses were performed using SPSS 15.0 for Windows (SPSS Inc., Chicago, USA). Since the data regarding network characteristics did not show a normal distribution, non-parametric tests were used to analyze differences between groups. Wilcoxon signed rank tests were used to compare within subject C_w/C_{ws}, L_w/L_{ws}, S, and W_r values before and after amobarbital injection. Non-parametric Mann-Whitney Tests were performed to explore differences regarding network characteristics between patients with left or right hemisphere lesions, patients with MTS or a tumor, and male and female patients. The false discovery rate (FDR) was applied per frequency band to correct our results for multiple testing and avoid type I error when investigating network properties [168]. This method is less conservative than for example the Bonferroni correction, and it is used frequently in imaging experiments.

In our analysis of the correlation between topological features and test performance during the IAP, we used the non-parametric Kendall's Tau. Because of the exploratory nature of these analyses, no correction for multiple testing was applied, and significance was set at $p<.05$.

RESULTS

Patient characteristics

Fifty-seven patients underwent the IAP during the inclusion period. Artifact free epochs from the first injection into the lesioned hemisphere were not available in 24 patients.

Table 1. Test statistics of all comparisons between network characteristics before and after injection of amytal

	Z	P-value
Theta band		
Normalized clustering coefficient (C_w/C_{ws})	-3.39	< .001*
Normalized path length (L_w/L_{ws})	-3.32	< .001*
Small-world index (S)	-1.81	.07
Edge weight correlation (W_r)	-2.95	.002
Lower alpha band		
Normalized clustering coefficient (C_w/C_{ws})	-2.71	.005*
Normalized path length (L_w/L_{ws})	-2.98	.002*
Small-world index (S)	-0.96	.34
Edge weight correlation (W_r)	-2.01	.044
Upper alpha band		
Normalized clustering coefficient (C_w/C_{ws})	-3.00	.002*
Normalized path length (L_w/L_{ws})	-1.76	.08
Small-world index (S)	-1.70	.09
Edge weight correlation (W_r)	-1.48	.14
Beta band		
Normalized clustering coefficient (C_w/C_{ws})	-2.60	.008*
Normalized path length (L_w/L_{ws})	-1.56	.12
Small-world index (S)	-1.65	.10
Edge weight correlation (W_r)	-3.31	< .001*

*Note. Wilcoxon signed rank tests were used. P-values are before correcting for multiple testing, * indicate significance after applying the false discovery rate for controlling chance capitalization.*

All statistical analyses were performed on the remaining 33 patients. These 33 patients (18 male) had a mean age of 37 years (SD=12.2). The cause of localization-related epilepsy was a histopathologically confirmed tumor in 19 patients (58%), of whom 13 had the tumor in the left hemisphere.

Thirteen patients (39%) had mesial temporal sclerosis (MTS), left-sided in 4 patients. One patient (2%) suffered from gliosis in the right hemisphere due to trauma. In total, 17 patients suffered from a lesion in the left hemisphere and had amobarbital injected into this hemisphere. The other 16 patient had right-sided lesions and underwent the IAP with injection in the right hemisphere. The lesion was located in the temporal lobe in 30 patients (91%), while a fronto-temporal lesion was present in 3 patients (9%). The 24 patients who could not be included due to artifacts in EEG recordings and non-lesioned first injection side did not differ from the included patients with respect to age, sex, lesion type, and lesion lateralization. Seventeen of the 33 analysed EEGs were recorded during first injection into the left hemisphere.

Network changes

Neural network characteristics after injection of amobarbital were compared to the resting state before injection by means of Wilcoxon signed rank tests (see table 1). Results for clustering coefficient, path length, and small-world index are shown in figure 1A, while changes in edge weight correlation are depicted in figure 1B.

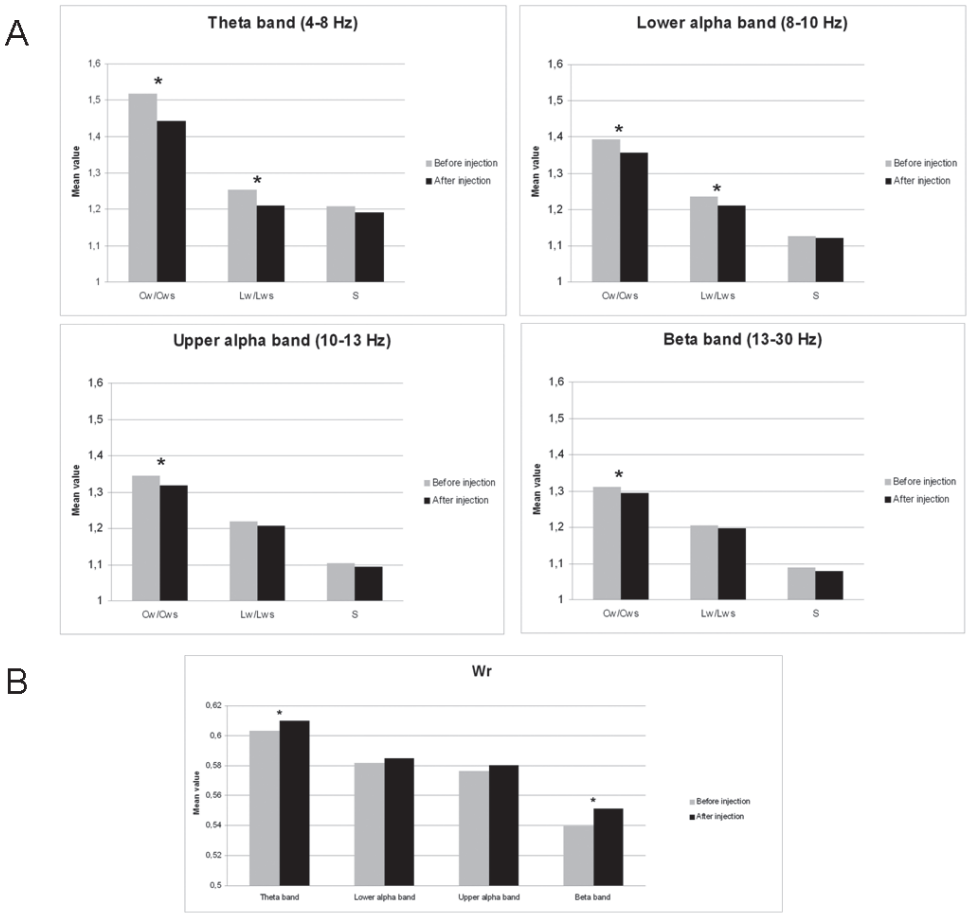

*Figure 1. Mean changes in network features after injection of sodium amobarbital. * = p< .05 (corrected for multiple comparisons). (A) C_w/C_{ws}=normalized clustering coefficient, L_w/L_{ws}=normalized average path length, S=small-world index. (B) W_r=edge weight correlation.*

The normalized clustering coefficient significantly decreased after injection of amobarbital across all frequency bands: the theta band (p<.001), lower and upper alpha band (p=.006 and p=.002 respectively), and in the beta band (p=.008; note that the given p-values are uncorrected, but pass the FDR multiple comparisons test for p<0.05). The post-injection theta band average path length also decreased when compared to resting state (p=.001), as it did in the lower alpha band (p=.002). Furthermore, edge weight correlation decreased significantly after injection in the theta band (p=.002) and in the beta band (p=.001). These findings indicate that amobarbital generally caused a more random and less optimal network topology after injection, while results are not inherent to changes in synchronization likelihood due to the normalization of all network measures with random networks. To confirm this finding, correlations between SL levels and memory scores were also explored, but no significant correlations were found. An example of synchronization strength per node is shown in Figure 2A, while connectivity within both hemispheres, between the central areas and the hemispheres, and between the two hemispheres is depicted in the Figures 2B–D, respectively.

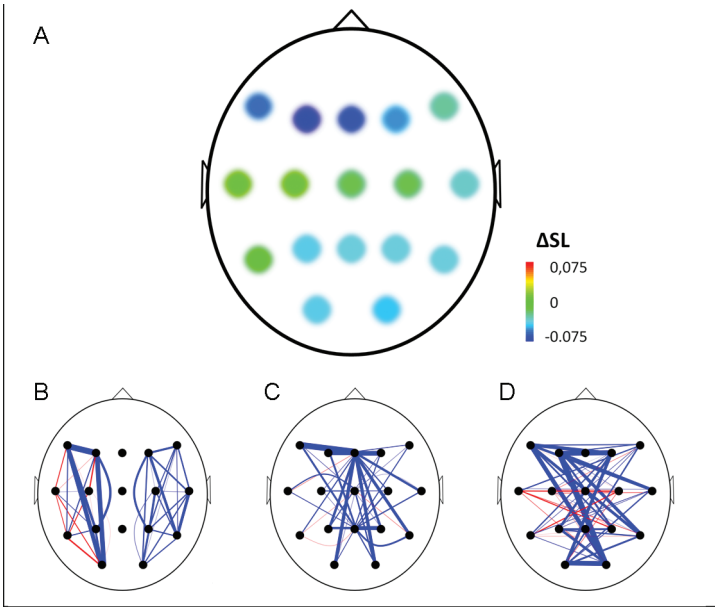

Figure 2. Example of changes in synchronization from before to after injection of amobarbital in the right hemisphere of one representative subject. (A) Mean changes in synchronization for each electrode with all other electrodes, ΔSL = difference in mean synchronization likelihood between before and after injection of amobarbital. (B–D) Blue line indicates decrease of synchronization likelihood between two electrodes, red line indicates increase. Thickness of lines indicates extent of change after injection (thin = small, thick = large). Three types of edges are depicted: (B) within hemisphere edges,(C) edges between the central (midline) electrodes and the other electrodes, and (D) interhemispheric edges.

Patients differed on a number of clinical variables, which could influence network topology. Because of the small sample size and non-parametric distribution of network properties, multivariate analyses of several covariates was not performed. Instead, possible differences in network topology change were explored by means of post-hoc non-parametric Mann-Whitney tests, with which differences between property deltascores between patient groups (i.e. subtraction of the after injection value from the before injection value) were tested. Instead, possible differences in network topology change were explored by means of post-hoc non-parametric Mann-Whitney tests, with which differences between property deltascores between patient groups (i.e. subtraction of the after injection value from the before injection value) were tested. Differences between patients with tumors (n=19) and MTS (n=13) were tested, excluding the one patient with gliosis due to trauma. No significant differences in deltascores were found (see table 2). The possible impact of lesion lateralization and thus side of injection (left n=17, right n=16) was also explored. Changes in network properties were not significantly influenced by lateralization of the lesion (see table 2). We were also interested in possible gender effects on our results, so the same methods were used to explore differences between men (n=18) and women (n=15). In the beta band, men's clustering coefficient deltascore was significantly lower (M=-0.004) when compared to the women's score (M=-0.034; p=.007), indicating that beta band clustering significantly decreased in women but not in men (see table 2).

Table 2. Correlations between memory performance after injection and (changes in) network characteristics

	Lesion type		Lesion lateralization		Gender	
	U	**p-value**	**U**	**p-value**	**U**	**p-value**
Theta band						
C_w/C_{ws}	121	.94	89	.60	133	.96
L_w/L_{ws}	96	.30	98	.88	124	.71
S	91	.22	66	.12	127	.79
W_r	111	.64	77	.28	83.5	.06
Lower alpha band						
C_w/C_{ws}	83	.13	87	.53	128	.82
L_w/L_{ws}	87.5	.17	77.5	.29	126	.75
S	107	.54	91	.65	130	.87
W_r	115	.73	75	.23	110.5	.40
Upper alpha band						
C_w/C_{ws}	68.5	.04	91	.65	112	.42
L_w/L_{ws}	101.5	.41	99	.91	80	.05
S	100	.37	90.5	.61	92	.12
W_r	106	.51	91	.64	81	.05
Beta band						
C_w/C_{ws}	100	.38	93	.71	62	.007*
L_w/L_{ws}	116.5	.80	101	.98	80	.05
S	112.5	.68	92	.68	118	.56
W_r	88	.19	92.5	.69	134	.98

*Mann-Witney U-tests were used. P-values are before correcting for multiple testing, * indicate significance after applying the false discovery rate for controlling chance capitalization. C^w/C^{ws}=normalized clustering coefficient, L^w/L^{ws}=normalized path length, S=small-world index, W^r=normalized edge weight correlation.*

Exploring network characteristics and IAP memory score

Previous research has shown that network topology may be important for cognitive functioning [34, 155, 242]; therefore we explored the association between network topology after injection and IAP memory score. Kendall´s Tau was used to correlate network features with memory score of the healthy hemisphere (i.e. after injection in the lesioned hemisphere). Results showed a significant association between better memory score and higher small-world-index in the theta band after injection (Kendall's Tau=.299, p=.033), and a significant correlation was present between longer upper alpha path length after injection and better memory score (Kendall's Tau=.313, p=.026; see table 3 and figure 3). No correlations were present between memory performance and network topology before injection of amobarbital, nor were changes in topology associated with better or poorer cognitive functioning. These results indicate that more ordered networks in the theta band and longer upper alpha band path length after injection were related to better memory score.

Table 3. Correlations between memory performance after injection and (changes in) network characteristics

	Before injection	During injection	Deltascore
Theta band			
C_w/C_{ws}	-0.4 (.77)	0.25 (.07)	-0.20 (.15)
L_w/L_{ws}	-0.07 (.60)	0.01 (.93)	-0.08 (.55)
S	-0.05 (.74)	0.30 (.033)*	-0.27 (.06)
W_r	-.01 (.96)	-0.08 (.56)	0.05 (.74)
Lower alpha band			
C_w/C_{ws}	0.06 (.68)	0.10 (.48)	-0.06 (.65)
L_w/L_{ws}	0.11 (.43)	-0.04 (.76)	0 (1)
S	0.03 (.81)	0.13 (.34)	-0.02 (.88)
W_r	-0.13 (.37)	-0.14 (.32)	0.03 (.85)
Upper alpha band			
C_w/C_{ws}	0.18 (.19)	0.17 (.24)	0.06 (.65)
L_w/L_{ws}	0.14 (.31)	0.31 (.026)*	-0.02 (.87)
S	0.02 (.87)	-0.03 (.85)	0.07 (.63)
W_r	0.05 (.71)	-0.23 (.10)	0.15 (.28)
Beta band			
C_w/C_{ws}	-0.11 (.42)	0.18 (.19)	-0.20 (.15)
L_w/L_{ws}	-0.09 (.53)	0.11 (.43)	-0.21 (.13)
S	0.01 (.97)	0.07 (.63)	0.02 (.88)
W_r	0.05 (.71)	-0.03 (.82)	0.10 (.47)

*Note. Correlations between memory performance after injection and (changes in) network characteristics: Kendall's Tau (p-value). Before injection=network characteristics during rest, before injection of amobarbital, During injection=network characteristics during unilateral sedation, Deltascore=network characteristic value after injection subtracted from network characteristic before injection, Cw/Cws=normalized clustering coefficient, Lw/Lws=normalized path length, S=small-world index, Wr=normalized edge weight correlation. All p-values are uncorrected, * indicate significance without correction for multiple comparisons.*

DISCUSSION

Our results indicate that the topology of whole-brain functional networks become more random after sedation of one hemisphere by means of the intra-arterial amobarbital procedure, marked by a decrease in the normalized values of both local clustering and average path length. Changes in edge weight correlation in the theta and beta bands indicate that the network is closer to random and thus less optimized for information transport after injection. These changes are not related to lesion type, lesion lateralization, and age. Network properties are related to functioning to some extent:

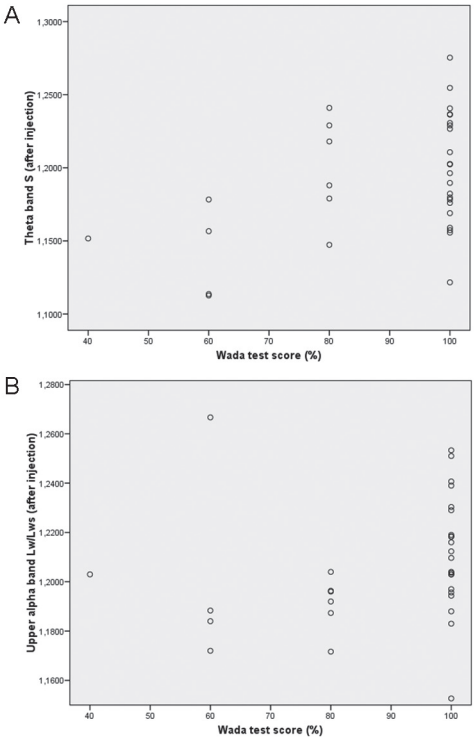

Figure 3. Scatterplots of correlations between network variables and memory performance during the IAP. (A) Correlation between theta band small-worldness (S) and memory score. (B) Correlation between upper alpha band path length and memory score.

both higher theta band small-world index and longer path length in the upper alpha band are associated with better memory performance of the presumably non-affected hemisphere.

Our study shows acute network effects in a human in vivo model for acute (reversible) brain lesioning, which seem related to memory functioning. These findings may lead to hypotheses about possible mechanisms of network changes in the brain after acute lesions occur. Research into the impact of such lesions on functional connectivity is rather sparse, and network features have rarely been investigated in this respect. Some work has been done on the influence of stroke on human functional connectivity: elaborate changes in connectivity throughout the brain have been shown in patients more than six months after their first ever stroke [157]. Decreased connectivity was even found between the topologically remote primary motor cortex and the cerebellum, while most short-distance connections gained coupling strength. Brain network effects of lesions in human subjects have only been researched in brain tumor patients. A mixed group of glioma patients showed both lower clustering coefficients and shorter average path length than healthy controls in the theta, beta, and gamma bands, pointing towards a more random network topology [9]. Contradictory findings have been reported in a more homogeneous group of low-grade glioma patients, which were compared to a control group matched on age, sex, and educational level [34]. These patients showed higher clustering than controls in the theta band, while the opposite was true in the

beta band. Average path length did not differ between patients and controls in this study. A computational study, using a macaque-based model of cortical functional connectivity, reports widespread changes in connectivity, especially when the most connected parts of the network ('hubs') were lesioned [109]. In the only human study simulating functional effects of lesions, a computational model based on human MRI data was used [4]. Functional connectivity mainly decreased in the lesioned hemisphere, but significant changes herein were also reported in the contralateral hemisphere and the brain as a whole. Unfortunately, Alstott and colleagues have not investigated changes in overall network topology after structural lesions.

Our current results partly corroborate previously mentioned studies, since sparse evidence suggests that brain networks become more random after the occurrence of lesions. But, how may these changes be explained? On the cellular level, several studies have indicated that structural plasticity occurs immediately after lesions [45, 80], but these effects are not in the same time-scale as the IAP. In induced stroke in monkeys, increased levels of sprouting-promoting environmental factors have been reported, inducing new connections in the area of the lesion [49]. Interestingly, this sprouting-boost may also occur at sites remote from the actual lesion, and might impact structural connectivity of the whole brain [45, 60]. A study modeling structural effects of stroke has shown that plastic responses occur in the actual area that is infarcted, in the penumbra (i.e. the region surrounding the infarction), and at remote locations as well [171]. Possibly, dynamic changes in connectivity and network topology are similar to structural plasticity: immediate random functional connectivity may be a 'stress-response' of the brain to local damage. Later, some sort of pruning of these (temporary) functional connections may occur, which may optimize network structure once again. An acute random connective boost would be congruent with our finding of network randomization directly after injection of the sedative.

In order to put our results into perspective, it would be of great interest to explore the longitudinal effects of lesions on brain networks. Several studies suggest that changes in connectivity and network topology may proceed during several phases [44, 107, 192]. These studies indicate that plasticity is not stationary, but evolves within itself. Moreover, functional rehabilitation is strongly shaped by activity [45], indicating that a great variability of changes may occur at an individual level. Furthermore, differences in plasticity may occur between lesion types. It is highly probable that network changes induced by slow-growing tumors are fundamentally different from the effects of an acute lesion such as stroke or the IAP. However, no attempt has been made up till now to compare different types of lesions, although these questions are addressed in ongoing studies of our group.

In our study, preserved small-worldness and longer path length after injection correlated with better cognitive performance during the IAP. Network changes also seem to have a functional correlate as well as clinical relevance in other studies. The removal of hubs in a scale-free Barabási-Albert model has been shown to relate to memory recall in the computational Hopfield memory model [189]. Research in non-human primates shows the importance of integration of several brain areas for normal functioning as well as functional rehabilitation after brain damage occurs [170, 171]. Post-lesional recovery in monkeys is characterized by marked changes in both intra- and inter-areal changes in connectivity and network structure [60]. Widespread connectivity changes in stroke seem related to functional status: neglect and its recovery has been shown to be related to functional connectivity in human stroke patients [171]. Furthermore, task-related connectivity analysis in stroke patients has shown that recovery of motor tasks is related to newly formed connectivity patterns [94, 115]. However, it is not clear what may be an optimal network topology for cognition. Better performance has previously been related to shorter path length in an fMRI study in very low frequency ranges

[242]. In an MEG study in brain tumor patients, we found an association between higher path length and poorer cognitive score in the lower alpha band [34]. The reported association between higher upper alpha path length and better memory performance in the current study are in line with the latter results.

A subtle but highly interesting finding of this study was the changing beta band clustering coefficient in women but not in men. Pre-existent differences in connectivity and network topology between men and women have not been reported as yet, but adaptation during mental challenge and reaction to disease may vary across genders according to previous reports. Local theta band complexity (which is related to decreased coupling or connectivity) measured by EEG is higher in men during a working memory task [207], while interhemispheric coherence (a measure of connectivity) is higher in women during photic stimulation and cognitive testing [17, 249]. An MEG study investigating changes in functional connectivity during an attentional task showed gender differences in the lower alpha band [92]. Further research into possible pre-existent differences between men and women regarding connectivity and network architecture should be performed in future studies. Moreover, longitudinal studies should focus on differences in network adaptation after lesions between men and women.

A limitation of this report includes the suboptimal setting of EEG recordings, since patients had their eyes open, and minimal movement artifacts could not be avoided. However, these factors are likely to influence only very low and very high frequency bands, and those were excluded from the current analyses. Also, volume conduction is always an issue in EEG studies. Volume conduction refers to the tendency of neighboring EEG electrodes to pick up activity of identical sources, resulting in strong correlations that do not reflect true functional connectivity. Although this problem may have impacted absolute values of our network analysis, the fact that this was a repeated measure design greatly diminishes the confounding influence of volume conduction on our results. A further shortcoming of this study is the fact that we did not investigate changes in network topology within the injected and non-injected hemispheres. Main reason for this was the number of electrodes of the EEG; the brain network consisted of only 17 nodes. This small number of nodes unfortunately prevented further study into network changes in the separate hemispheres. Furthermore, the current study investigates network topology of the brain. These analysis are based on raw time series in first place, after which functional connectivity was analyzed. It is important to note that all findings of the high-level network analysis are based on the previous two levels.

In conclusion, our results are new in the sense that they provide evidence for the global effects of sedation of one hemisphere of the brain, after which functional brain networks become more random and less optimally wired. This is especially interesting when comparing our results to previous studies in brain tumor patients, in whom similar findings have been reported. We also report a link between network properties and memory status, as have several previous studies. These results provide important evidence that brain network topology and cognitive functioning are interrelated. Further research should focus on brain network changes in lesions of varying origin (such as stroke), longitudinal network-related effects of lesions, and gender differences in these network parameters.

CHAPTER 10

Summary

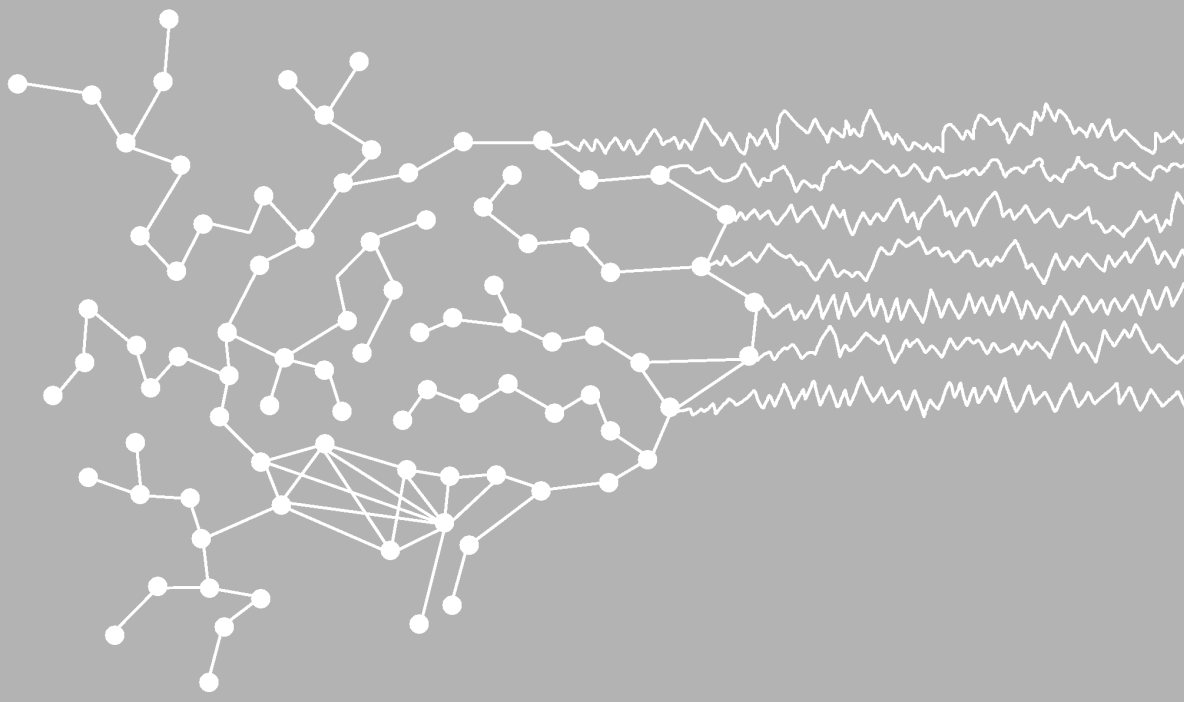

SUMMARY

In **chapter 1**, clinical aspects of gliomas, a type of primary brain tumors with high mortality, are reviewed. Patients with a glioma or other (non-neoplastic) focal lesion suffer from severe symptoms that are still poorly understood, such as epilepsy and cognitive impairment. Modern network theory provides a framework that may improve our understanding of brain functioning in patients with brain tumors and other focal lesions. As a central theme in this dissertation, modern network theory is used to study the global impact of focal brain lesions and their neurosurgical treatment. This thesis aims to apply these methods to neurophysiological recordings of patients with focal lesions in order to provide insight into the pathophysiology of complex symptoms in patients with brain lesions. The following research questions are discussed:

I) How do brain tumors or other, (non-neoplastic) lesions disturb functional brain networks?

II) How does network topology relate to epilepsy and how does it relate to cognitive deficits?

III) How are functional networks and, as a consequence, epilepsy and cognitive performance, affected by neurosurgery?

In **chapter 2**, as a starting point of this dissertation, a broad overview is given of network theory and its application in neuroscience and neurology. Neurophysiological recordings such as electroencephalography (EEG), magnetoencephalography (MEG) and electrocorticography (ECoG), can be used to measure neural activity. These recordings van be used to characterize functional connectivity, which denotes the statistical interdependencies between elements of the system, for instance the synchronization of two simultaneously recorded EEG signals between different brain regions. Subsequently, functional brain networks can be analyzed using measures from network theory. Both in general and in the brain, an optimal network topology combines highly interconnected, specialized regions with global integration (a 'small-world topology'). Functional connectivity in broad band (0.5-48 Hz) filtered neurophysiological recordings is decreased in patients with brain lesions, but different patterns are seen depending on the frequency band. It appears that the most significant disturbances are found in frequency bands below 10 Hz. In these lower frequencies, the small-world topology partly gets lost in patients with brain lesions, and alterations in functional connectivity are not restricted to the lesioned area. Importantly, these changes are related to cognitive deficits, and are affected by neurosurgical intervention. Moreover, functional connectivity increases during epileptic seizures, and interictal (i.e. in the period between two seizures) functional connectivity disturbances may be present in patients with lesional epilepsy. These changes seem to make the brain more vulnerable for the occurrence of epileptic seizures.

In section 2, a number of studies on local and global functional connectivity and functional networks in patients with brain lesions are described. **Chapter 3** investigates the correlation between epilepsy duration, measured as time since the first seizure, and local functional connectivity as well as small-world characteristics, in the lesioned area. Average functional connectivity, measured with the phase-lag index (PLI), local clustering (a measure of local segregation), and average shortest path length (a measure of global integration) were studied in ECoG registrations from the temporal lobe of temporal lobe epilepsy (TLE) patients. Lower

PLI, lower clustering coefficients, and lower small-world index in the broad frequency band (0.5-48 Hz) were correlated with longer epilepsy duration. This study showed that ongoing lesional epilepsy affects both the level of information exchange as well as the functional network organization in the affected temporal lobe of TLE patients. In **chapter 4**, global functional networks were reconstructed from preoperative resting-state magnetoencephalography (MEG) recordings in lesional epilepsy patients. Average functional connectivity strength and network topology were compared between patients with different histopathological lesions and healthy controls, and correlations with seizure frequency and cognitive deficits were explored. Low-grade glioma (LGG) patients showed decreased network synchronizability (i.e. stability of the synchronous state) and decreased global integration compared to healthy controls in the theta frequency range (4-8Hz). Patients with non-glial lesions (NGL) also showed decreased network synchronizability, as well as increased normalized average shortest path lengths, indicating a loss of global integration of information in the network. In contrast, networks of high-grade glioma (HGG) patients did not significantly differ from those of healthy controls. Altered global network characteristics correlated with seizure frequency in LGG patients, and with cognitive performance in both LGG and HGG patients. This chapter shows that the impact of lesions on functional networks differs between lesions with different histopathology, possibly due to variability in lesional growth pattern. Interestingly, decreased stability of the synchronous state in the theta band seems to make LGG patients more prone to the occurrence of seizures, whereas loss of global integration and stability of the synchronous state were related to cognitive decline. The correlation between network topology and seizure frequency is further explored in **chapter 5**. MEG recordings were made in glioma patients who were on levetiracetam monotherapy, directly after neurosurgery (T1), and six months later (T2). Higher theta band functional connectivity at T1 and T2 was related to a higher total number of seizures. Furthermore, a higher number of seizures was related to a less optimal, more random global network topology. No changes in global connectivity or network topology occurred over time. These results suggest that pathologically increased theta band connectivity is a hallmark of tumor-related epilepsy.

In section 3, the effects of interventions on functional connectivity and network organization are studied. In chapters 6 and 7, MEG recordings were projected on the standardized AAL atlas using beamforming, hereby providing an anatomical framework for this analysis. In **chapter 6,** functional connectivity changes within six months after surgery are studied in resting-state networks (RSN) of LGG patients, which are subnetworks with a known correlate to cognitive tasks. Lower alpha band connectivity in the default mode network (DMN) was increased after surgery, and this increase was related to improved verbal memory functioning. Similarly, right frontoparietal network (FPN) connectivity in the upper alpha band was increased after resection, which correlated with improved attention, working memory and executive functioning. These findings indicate that, at the source level, increased alpha band RSN functional connectivity in MEG recordings correlates with improved cognitive outcome after resective surgery. **Chapter 7** studies functional connectivity and functional network alterations related to epilepsy outcome after surgery. Functional neural network analysis is a promising technique for more accurate identification of the target areas for epilepsy surgery, but a better understanding of the correlations between functional network characteristics changes due to surgery and postoperative seizure status is required. These correlations were explored in a longitudinal magnetoencephalography (MEG) recordings of 20 lesional epilepsy patients. Resting-state MEG recordings were obtained at baseline (preoperatively; T0), and at 3-7 (T1) and 9-15 months after resection (T2). Functional networks were characterized with a new approach based upon the minimum spanning tree (MST), that might represent a critical backbone of information flow in weighted networks. We found a significant positive

correlation between functional connectivity in the lower alpha band and seizure frequency at T0, especially in regions where lesions were located. MST leaf fraction, a measure of integration of information in the network, was significantly increased between T2 and T0, only for the seizure-free patients. Finally, betweenness centrality, a measure of hub-status, decreased between T0 and T2 in seizure free patients in regions that were anatomically close to resection cavities. These results increase insight into functional network changes in successful epilepsy surgery and might eventually be utilised for optimization of neurosurgical approaches.

Chapter 8 describes a study of temporary sedation of one hemisphere with intra-arterial amobarbital, which was used to simulate a reversible brain lesion. The intra-arterial amobarbital procedure (IAP or Wada test) is used to determine language lateralization and contralateral memory functioning in patients eligible for temporal lobe resection because of pharmaco-resistant epilepsy. During selective sedation of one hemisphere, functioning of the contralateral hemisphere was assessed by means of neuropsychological tests. Whole-brain network topology changed significantly after amobarbital injection: local clustering decreased in all frequency bands, while average shortest path lengths decreased in the theta and lower alpha band, indicating a shift towards a more random network topology. Network characteristics after injection of amobarbital were correlated with memory score: higher theta band small-world index and increased upper alpha path length were related to better memory scores. The whole-brain network topology in patients eligible for epilepsy surgery becomes more random and less optimally organized after selective sedation of one hemisphere. Furthermore, memory functioning after injection was related to network topology, indicating that functional performance is related to topological network properties of the brain.

In section 4, a modeling study is described that was performed to integrate and interpret the empirical findings from the previous sections. More specifically, **chapter 9** aims to explain how focal lesions cause global alterations in functional brain networks, and the hypothesis is tested that interactions of damaged tissue with remaining brain areas globally affect functional connectivity. Local polymorphic delta activity (PDA), which typically characterizes EEG/MEG recordings of patients with cerebral lesions, was modeled and functional connectivity alterations were studied in an anatomically realistic model of human brain activity. Lesions were created by 1) altering parameters of individual neural masses in order to create PDA (i.e simulating acute focal brain damage); 2) combining this PDA with weakening of structural connections (i.e. simulating brain tumors), and 3) fully deleting structural connections (i.e. simulating a complete neurosurgical resection). Effects of these lesions on functional connectivity for remote regions were quantified using the synchronization likelihood while discarding direct connections with the lesioned areas. Not only structural disconnection but also PDA (in the context of intact structural connections) in itself caused functional connectivity decreases, and, interestingly, functional connectivity between regions that were not lesioned was also decreased. The specific pattern of connectivity alterations differed between lesion types. PDA in regions with a central role in the structural network had bigger impact than PDA in more isolated regions. These findings demonstrate that altered activity in damaged brain tissue, as measured with EEG/MEG, may cause global alterations in brain connectivity.

CHAPTER 11

General discussion

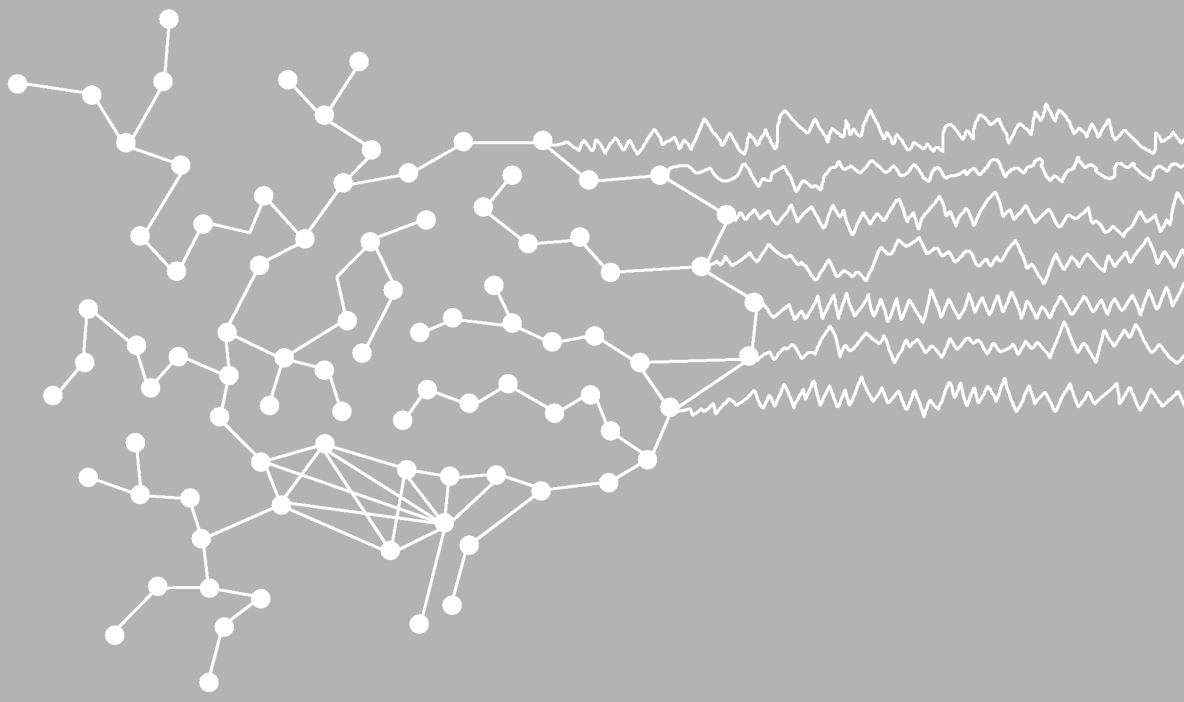

GENERAL DISCUSSION

The general aim of this dissertation was to describe the role of functional neural networks in the triad of brain lesions, symptoms, and surgical intervention. The results described in the previous chapters are discussed here in a broader perspective, with the research questions from the introduction as a starting point. In addition, some methodological considerations are presented, and I conclude with implications for further research.

How do brain tumors and other, non-neoplastic lesions, disturb functional brain networks?

How a lesion affects functional brain networks is partially determined by its histopathological finger print – and corresponding growth pattern – as is described in chapter 4. Patients with LGG, NGL, and HGG differ in their average connectivity strength and the topology of functional brain networks. LGG and NGL seem to cause widespread alterations of functional connectivity, especially in the theta band. Surprisingly, functional networks of HGG patients seem to be more similar to healthy control networks. A recent fMRI study that compared DMN activity during a memory task also showed differences between LGG patients and HGG patients; the spatial DMN pattern of HGG patients was similar to healthy controls. In LGG patients, however, DMN connectivity was decreased in the hemisphere where the tumor was located, while connectivity was increased in the hemisphere contralateral to the tumor [86]. Neural plasticity processes that cause reorganization of functional networks may be more outspoken in patients with slowly growing lesions than in patients with rapidly growing, highly invasive lesions. However, results in chapters 8 and 9 suggest that 'acute' lesions also cause alterations in functional connectivity between remote regions, as well as changes in network topology. A study in a larger cohort of patients, in which covariates could be taken into account, could in the future show altered functional networks in HGG as well. For example, lesion localization was also not corrected for in this study, while the model described in chapter 9 suggests that lesions in regions with a central role in the structural brain network have the largest impact on global brain functioning. This was also shown in an fMRI study by Gratton and colleagues, who showed that lesions in ''connector hubs'', which are crucial for communication between different subnetworks, have the most significant impact on global network organization [93]. Gratton and colleagues found that the medial and posterior cingulate cortex, the medial temporal lobe, and the inferior parietal cortex functioned as connector hubs, and lesions in these areas had most impact on global brain communication.

The results of chapter 4 suggest that especially LGG patients have altered, less optimal, theta band network topology: local clustering is increased, but the connectivity between modules is decreased, as well as the stability of the synchronous state. This is a clinically relevant deviation from network organization found in the healthy brain, as it is related to poorer cognitive performance and higher seizure frequency. When summarizing MEG studies performed prior to chapter 4, it was generally thought that lesions were associated with an increase of functional connectivity in lower frequency ranges, and loss of small-world characteristics. However, most of these studies were done on MEG recordings obtained after surgery, and surgery in itself may cause functional connectivity alterations in the theta and alpha bands ([71] and chapter 6). An overview of findings in studies performed prior to chapter 4 is shown in table 3 of chapter 4. Connectivity and network alterations in patients with non-

glial lesions were mostly studied in TLE. Functional connectivity, again of activity in lower frequency bands, is increased in TLE patients, while a decreased connectivity is observed using fMRI [25-27]. Functional networks become more ordered, as they are characterized by increased local clustering and longer path lengths (chapter 4 and [110]). Structural networks, characterized by cortical thickness correlations, are also more ordered in these patients (i.e. longer path lengths and higher local clustering) [24]. Structural networks based on white matter connectivity mapped with Diffusion Tensor Imaging (DTI), also show longer path lengths, but less local clustering, which was correlated with cognitive decline [234]. In summary, loss of a small-world topology has been observed in patients with lesional epilepsy with variable imaging techniques and neurophysiological recording modalities, and it is related to poorer cognitive performance, but the exact pattern of these alterations varies between studies. In addition, as was shown in chapter 4, network topology may vary between patients with different histopathological lesions, and networks in LGG and NGL patients are significantly different from HGG patients.

How do alterations in functional connectivity and network topology relate to epilepsy?

As described in chapter 3, lower local broad band functional connectivity in the temporal lobe is correlated with longer duration of TLE. A different pattern is seen in global functional connectivity and networks when measured with MEG/EEG instead of ECoG. Theta band functional connectivity is higher in the EEG of a general epilepsy population after a first seizure than in a control population [74]. It can even be used as a diagnostic marker of epilepsy when the visual interpretation of the EEG shows no disturbances. Theta and/or lower alpha band PLI is correlated with seizure frequency both prior to surgery, as shown in chapters 4 and 7, but also after surgery, as shown in chapter 5. This is thus a robust finding in different patient populations, with variable lesion pathology and before and after intervention. A potential confounder for this finding is the variability in the use of anti-epileptic drugs (AEDs). It could be expected that patients with a higher seizure frequency use higher doses of AEDs, and more often use combinations of various AEDs. However, the patients in chapter 5 were all using levetiracetam monotherapy and the correlation was still present. Therefore the increased theta band PLI seems to be a hallmark of epilepsy rather than a hallmark of AED effect.

Why would functional connectivity especially in the theta band be related to epilepsy? Microscopically, theta band oscillations may be regulated by GABAergic interneurons [122, 123]. Moreover, blockade of GABA receptors in induced epilepsy alters patterns of theta activity [144], and hubs consisting of GABAergic interneurons may determine network synchronization [32]. Also, neuronal changes associated with temporal lobe epilepsy can disrupt hippocampal theta function [145]. These studies point towards a possible link between temporal lobe epilepsy and the theta band. In human neurophysiological data, the association between the theta band and epilepsy has been studied increasingly over the past two decades. Pathological thalamo-cortical theta oscillations have been described in absence seizures [55], and increased theta band absolute spectral power is related to absence epilepsy [158] and generalized epilepsies [56]. Another study reports increased theta band power to be related to the severity of epilepsy [54]. Moreover, interhemispheric theta band coherence proved to be a selective feature of patients with generalized epilepsy [55].

In chapter 7, it was shown that the correlation between seizure frequency and average PLI was stronger in the lower alpha band than in the theta band, and analysis of the power spectrum showed that the cut-off between these frequency bands at 8 Hz may not be appropriate. It is therefore suggested to analyze epilepsy-related connectivity in a broad frequency band of

combined theta- and lower alpha bands (4-10 Hz). It is acknowledged that cerebral lesions cause a slowing of the dominant alpha rhythm that characterizes eyes-closed resting-state EEG and MEG recordings in healthy subjects, which is another reason to use this frequency range for analysis [64, 175, 221].

How do alterations in network topology relate to cognitive performance?

The findings described in chapter 4 suggest that in glioma patients, a modular brain organization, less local clustering, higher stability of the synchronized state and high between-module connectivity, all favor cognitive performance. A correlation between shorter path lengths and better memory performance or higher intelligence, is consistently found in DTI, MRI and MEG studies [76, 140, 242]. A previous study using post-operative MEG recordings in LGG patients showed that a shorter path length in the delta band was related to better performance in the attention and executive functioning domain, while less local clustering in the lower alpha band was related to better verbal memory test scores, in line with our results [34]. The cognitive domains studied in chapter 4 (attention, executive functioning and verbal memory) specifically require global integration of information. It could be suggested that modularity and between-module connectivity reflect the facilitation of functional communication. Interestingly, the correlations between these network parameters and cognition were found in the same frequency range, the theta band, as where the network differences between LGG patients and healthy controls were observed. The network alterations therefore seem to reflect the less optimal communication within the brain that leads to the impaired cognitive performance in patients with brain lesions.

Functional connectivity analysis of RSNs that are known to be involved in specific cognitive domains have not yet been compared between patients with brain tumors or lesional epilepsy and healthy controls. In chapter 6, however, connectivity in the DMN and right FPN was altered after resection in LGG patients, and the increase of connectivity strength correlated with cognitive performance. This approach may therefore also be of interest in glioma patients who have not yet been treated, as it could be hypothesized that a pathological decrease of connectivity in these RSNs is related to cognitive decline.

How are functional networks altered by neurosurgical intervention?

Chapter 6 showed increased RSN connectivity in LGG patients after resective brain surgery in the DMN and right FPN. One previous study on the effects of tumor resection described that functional connectivity patterns after resection change in a complex way, demonstrating a decrease in interhemispheric theta band connectivity [71]. Other work focused on the predictive value for surgical outcome of pre-operative connectivity in the tumor region. When the resected area is characterized by a high alpha band functional connectivity, this suggests eloquence for language or motor functioning [96, 148, 226]. In chapter 6, patients who showed the highest increase of alpha band RSN activity after surgery were also the ones with improved cognitive test scores. On the other hand, resection of nodes with a central role or high connectivity in the pre-operative network is possibly a predictor of seizure freedom after resection, depending on the frequency of the analyzed oscillations [173, 260]. In chapter 7, preoperative seizure frequency correlated with lower alpha band functional connectivity as measured by PLI, especially in regions with a high lesion load. In addition, MST betweenness centrality was significantly decreased in SF patients between T0 and T2 in regions close to resection cavities. Finally, an increase of leaf fraction (indicating a more integrated organization of core brain networks) was found in the lower alpha band after surgery in seizure free patients compared to patients with post-operative seizures. Surgical resection altered network topology in SF but not in POS patients; future work should explore whether

the impact of surgery could be predicted based on the baseline network characteristics of the target area for resection.

Methodological considerations

The study of functional connectivity and functional networks using neurophysiological recordings meets with several methodological challenges, and analysis techniques are evolving rapidly. In section 2 and chapter 8, functional connectivity and network analysis is performed at the level of EEG/MEG/ECoG sensors. This approach was used to characterize functional connectivity in signal space, providing insight in the functional interactions between EEG/MEG sensors. Several issues hinder the interpretation of these data. The signals of spatially separated sources are mixed in signal space analysis, which may lead to over/underestimation of functional connectivity, and the estimated connectivity lacks an anatomical substrate [104]. In addition, EEG recordings require the use of a reference, which may be a reference electrode or an average signal reference, and the choice of reference will affect the estimation of functional connectivity between sensors [95, 172]. Finally, multiple EEG/MEG sensors will pick up signals from a single source due to volume conduction and field spread [69]. This may lead to an erroneous estimation of functional connectivity with measures such as the SL [217], which was used in chapter 8. The use of the phase-lag index (PLI) as a measure for functional connectivity for EEG/MEG data makes it possible to discard spurious interactions between channels [214], although it has also been suggested that (small) volume conduction effects may even be present when using the PLI [176].

The use of a beamformer approach to project MEG signals to a standard space using an anatomical atlas makes it possible to study interactions between specific anatomical sources [104]. One approach that was also used in this thesis is the study of MEG functional connectivity in RSNs in source-space. Combined EEG/fMRI registrations in healthy controls have indicated that particularly synchronized activity in the alpha band has a spatial correlate with RSNs such as the DMN, which was also the frequency range where our results were found [116]. Previous MEG studies have validated these networks using Independent Component Analysis (ICA) applied to the Hilbert envelope of the MEG timeseries [39, 66, 105]. An important advantage of source space MEG functional connectivity analysis compared with application of fMRI techniques is that it measures neuronal activity directly with a high temporal resolution, which is done in a standardized anatomical space using the beamformer approach, while functional MRI studies estimate neural activity based on an indirect measure of metabolic changes.

The beamformer approach used in chapters 6 and 7 has some limitations, however. MEG beamformer solutions have a spatial resolution that is accurate up to 8 millimeters [8], which may be partially eliminated with continuous head position corrections, but this was not yet incorporated in the studies presented here [162]. As part of the analysis approach the patients' MRIs were normalized to a template brain (and then labeled voxels using a standard (AAL) atlas), while the patients had altered anatomy due to the tumor, which may have influenced results. Moreover, for the postoperative beamformer analysis, data were projected to voxels at locations where no actual cortical tissue was present anymore due to the resection. However, the latter issue was expected to have minimal effects, as the voxel with highest power was used as a representative source for each ROI, and voxels at locations without cortical tissue are not likely to show any activity apart from 'leakage' from surrounding sources (e.g. [8]). Finally, a reference of source space functional connectivity patterns in a large cohort of healthy controls is desirable, but inter-subject variability in these studies seems high [76]. To solve this problem, other studies in brain tumor patients on individual functional connectivity maps used the contralateral hemisphere as a reference [96, 226]. However, it has been shown, in this

thesis as well as in other studies, that functional connectivity patterns are globally disturbed in brain tumor and lesional epilepsy patients [9, 110].

A limitation of the functional connectivity measures used in this thesis, such as the PLI, is that they characterize the *strength* of coupling between sensors or ROIs, but contain no information about the *direction* of the interactions. The directed PLI (dPLI) was recently suggested as a tool to study not only the amount of functional interactions between brain regions, but also the direction of the information flow. As was recently shown by Varotto and colleagues in intracranial EEG recordings, characterizing the direction of information flow may be of interest during the spread of epileptic activity [245], and would be an interesting next step for the analysis of interactions between lesioned areas and the rest of the brain.

Apart from functional connectivity analysis, network analysis of human functional connectivity data involves its own challenges. Connectivity matrices are calculated using a correlation measure that characterizes interacting between channels or brain regions from neurophysiological or neuroimaging data. However, when weighted networks are reconstructed, some of the interactions in the matrix are likely to be spurious. In unweighted networks, an arbitrary of a threshold is used, above which a connection is thought to be present between two sources [243]. Important work by Van Wijk and others showed that the average level of connectivity and network size significantly affect the outcome of network analysis using either of those methods [243]. The use of the minimum spanning tree (MST), as demonstrated in chapter 7, provides a method to construct unique networks from neurophysiological data that is independent of average coupling strength, and has been used to characterize ECoG and EEG recordings of epilepsy patients [30, 136, 174]. Future work should elucidate how the MST relates to findings from previous work that was done using for example small-world characteristics, and show whether MST analysis is suitable for detecting disease-related network alterations in this particular patient population. For example, the diameter and leaf fraction of the MST may provide similar information as the path length in the small-world model. Characterization of spanning trees also allows for a broader description of network properties, such as centrality and the existence of hub nodes, which is not possible when using the small-world model [30, 219]. These network characteristics are also of interest in patients with brain lesions. Modeling studies can reveal whether measures of MST topology, such as tree hierarchy (a hierarchical tree organization is thought to be optimal for efficient communication while preventing information overload in hub regions), are able to capture all these properties in a holistic model.

Implications for further research

The application of functional neural network analysis in brain tumor and lesional epilepsy patients is at the point where observations from both empirical work and modeling studies might be implemented in clinical practice. More specifically, four applications of functional connectivity analysis in the neurological diagnostic process are promising.

First, the prediction of cognitive outcome after resection of brain lesions, and, subsequently, the planning of surgical procedures may benefit from presurgical functional connectivity analysis of MEG recordings in source-space. A recent publication by Tarapore and others shows that functional connectivity prior to surgery is related to surgical outcome with respect to neurological deficits [226]. High alpha band connectivity is a predictor of eloquent areas, and indicates that these regions cannot be resected without postsurgical deficits. Analysis of functional connectivity characteristics may also be used to mark areas that are eloquent for

more complex cognitive functioning, such as attention or memory. Identification of such areas would be of great clinical value, because the influence of resection on especially cognitive deficits is difficult to predict. However, this may require a more sophisticated approach; surgical resection of regions with low functional connectivity may be insufficient, and characterization of the role of the lesioned area in the global brain network will provide additional information. Moreover, as is suggested in chapter 7, resection of lesions can also alter functional networks in a way that is related to improved cognitive performance. In this thesis, several factors (such as lesional growth pattern and location of the lesion) have been identified that determine why some patients show larger connectivity increases than others after resection, or, in a broader perspective, what determines the impact of a lesion or resection on the global brain network. However, additional information is needed to fully understand the interaction between lesions, the functional brain network, and cognitive performance. As suggested in chapter 9, the role of the lesioned area in the structural network may be crucial in this respect. In addition, many infiltrative gliomas involve long projection fibers [114], which are candidate structures subserving resting-state networks that are known to be involved in complex cognitive functioning [240]. A recent study showed a correlation between vascular lesion load and loss of efficiency in white matter networks related to slowing of information processing in type 2 diabetes patients [186]. The role of white matter tracts that are affected by the tumor and surgical resection should therefore also be taken into account when explaining deficits in cognitive domains due to brain lesions.

Secondly, functional connectivity analysis may be used to diagnose epilepsy when traditional diagnostics are inconclusive, as was already suggested by Douw and colleagues [74]. Increased theta band connectivity is a predictor for the diagnosis epilepsy after a first event that is suspect for epilepsy, even when visual inspection of the EEG shows no disturbances [74]. In addition, network analysis may be used for the identification of the epileptogenic zone (EZ). This has been done in small patient populations using intracranial recordings [174, 245, 260], and a challenge would be to further translate this research to non-invasive neurophysiological registrations such as MEG and EEG.

A third direction of future research will be to further elucidate the pathophysiology of functional network alterations in patients with brain lesions. The effects of gliomas on structural network topology remain to be described. A loss of the coupling between functional and structural network characteristics was recently shown in idiopathic generalized epilepsy, and a similar analysis would also be of great interest in lesional epilepsy patients [262]. In addition, the molecular basis of network characteristics remain to be elucidated, and a recent attempt to elucidate these mechanisms suggested that altered network topology may link protein expression in the tumor region in glioma patients to their vulnerability for epilepsy (Douw et al., submitted).

Finally, the use of computational modeling to explain empirical findings may prove to be of great importance for our understanding of the impact of brain lesions. The modeling work described in this thesis has suggested that disturbed activity in lesioned brain areas affects global brain connectivity. Further development of this model, for example by implementing plasticity effects, should eventually make it possible to predict the impact of lesions and resections in individual patients. It would also be interesting to model the impact of lesions on information flow, as was recently done by Stam & van Straaten [218], as this may lead to individual predictions of cognitive deficits in patients with brain lesions. Finally, the model described in chapter 9 does not explain the vulnerability for the occurrence of seizures. A model that incorporates epileptic EEG phenomena would allow for simulation of interventions that could further increase the predictability, and, eventually, the probability of seizure-freedom after epilepsy surgery.

Conclusion

In this dissertation, disturbance of functional brain networks in patients with gliomas and in patients with lesional epilepsy is described. These functional networks were reconstructed from MEG, EEG and ECoG recordings. Network disturbances are related to the complex symptoms of epilepsy and cognitive deficits, and can be manipulated by neurosurgical intervention. A computational model, that was underpinned by findings demonstrated in this dissertation, was presented that shows how focally disturbed neural activity may lead to global alterations in brain communication. Further development of computational models could make it possible to simulate the effects of lesion-related plasticity, the impact of lesions on cognitive processing, and the vulnerability for epilepsy in patients with brain lesions. The ongoing improvement of analysis methods makes it possible to project non-invasive MEG recordings to anatomical sources and reconstruct networks that can be compared between imaging modalities and patients. Future work should further translate these findings to diagnostic markers that can be used to improve surgical outcome with respect to epilepsy and cognitive performance in patients with brain tumors and lesional epilepsy.

NEDERLANDSE SAMENVATTING

Lesies in het verbonden brein: een netwerk perspectief op hersentumoren en lokalisatiegebonden epilepsie

In **hoofdstuk 1** worden klinische aspecten van gliomen besproken, een type primaire hersentumoren met een hoge mortaliteit. Patiënten met een glioom of een andere (niet-neoplastische) focale laesie hebben symptomen die nog slecht worden begrepen, zoals epilepsie en cognitieve stoornissen. De toepassing van moderne netwerktheorie kan ons begrip van het functioneren van de hersenen vergroten en kan ons ook helpen te begrijpen wat er gebeurt bij patiënten met hersentumoren of met andere focale laesies.

Het centrale thema van deze dissertatie is het bestuderen van de globale invloed van focale hersenlaesies (en van de neurochirurgische behandeling van deze laesies) op het functioneren van de hersenen. En hierbij wordt van moderne netwerktheorie gebruik gemaakt. In dit proefschrift worden daartoe bij patiënten met focale hersenlaesies neurofysiologische registraties geanalyseerd met behulp van netwerktheorie, om op die manier inzicht te krijgen in de pathosfysiologie van complexe symptomen, zoals cognitieve stoornissen en het optreden van epileptische aanvallen in deze patiënten. De volgende onderzoeksvragen worden behandeld:

I) Hoe verstoren hersentumoren of andere, (niet-neoplastische) focale laesies functionele hersennetwerken?

II) Hoe is netwerktopologie gerelateerd aan epilepsie en aan cognitief functioneren?

III) Wat is het effect van neurochirurgische behandeling op functionele netwerken, en wat is de uitwerking van een operatie op epilepsie en cognitief functioneren?

In **hoofdstuk 2** wordt als inleiding van deze dissertatie een breed overzicht gegeven van netwerktheorie en de toepassingen van deze theorie in de neurowetenschappen en de neurologie. Neurofysiologische registraties zoals electroencefalografie (EEG), magnetoencefalografie (MEG) en electrocorticografie (ECoG) kunnen worden aangewend om hersenactiviteit te meten. Deze registraties kunnen vervolgens worden gebruikt om functionele connectiviteit te analyseren. Functionele connectiviteit beschrijft de samenhang tussen elementen in een systeem, bijvoorbeeld de samenhang van twee gelijktijdig opgenomen EEG signalen in verschillende hersengebieden: we spreken dan van synchronisatie De functionele hersennetwerken kunnen dan worden geanalyseerd met behulp van netwerktheorie.

Voor alle netwerken en ook voor de hersenen geldt dat een optimale netwerktopologie twee eigenschappen combineert, namelijk specialisatie in lokaal sterk verbonden gebieden, en globale integratie van informatie: er is dan sprake van een ‘’small-world topologie”. De functionele connectiviteit in breedband (0.5-48 Hz) gefilterde neurofysiologische registraties blijkt verlaagd te zijn bij patiënten met hersenlaesies, maar hierbij worden verschillende patronen waargenomen afhankelijk van de frequentieband waarin het signaal wordt gefilterd. De meest significante verstoringen lijken plaats te vinden in frequentiebanden onder de 10

Hz. In deze lagere frequentiebanden gaat de small-world topologie verloren bij patiënten met hersenlaesies, en de veranderingen in functionele connectiviteit blijken niet beperkt te blijven tot de gebieden waar de laesie is gelokaliseerd. Een belangrijke waarneming hierbij is dat deze veranderingen gerelateerd zijn aan cognitieve achteruitgang. Bovendien blijken de veranderingen te worden beïnvloed door neurochirurgische behandeling. Een andere waarneming is dat functionele connectiviteit toeneemt tijdens epileptische aanvallen, en dat interictale (dat wil zeggen in de periode tussen twee aanvallen) functionele connectiviteit mogelijk ook verstoord is bij patiënten met lokalisatiegebonden epilepsie. Dergelijke netwerkveranderingen lijken de hersenen dus kwetsbaar te maken voor het krijgen van epileptische aanvallen.

In het tweede deel van deze dissertatie wordt een aantal studies naar functionele connectiviteit en functionele netwerken in patiënten met lokalisatiegebonden epilepsie besproken.

Hoofdstuk 3 beschrijft onderzoek naar de correlatie tussen de duur van de epilepsie, gemeten als de tijd sinds de eerste epileptische aanval, enerzijds en locale functionele connectiviteit en netwerkeigenschappen in de regio van de laesie anderzijds. Met behulp van ECoG registraties werden in de temporaalkwab van patiënten met temporale epilepsie de volgende maten bestudeerd: (1) “gemiddelde functionele connectiviteit”, gemeten met de phase-lag index (PLI), (2) “locale clustering” (een maat voor lokale segregatie), en (3) “gemiddelde kortste padlengte” (een maat voor globale integratie). Een lagere PLI, een lagere clustering coëfficiënt, en een lagere small-world index in de breedband (0.5-48 Hz) waren gecorreleerd met een langere epilepsieduur.

Deze studie toont aan dat temporale epilepsie samen gaat met veranderingen in zowel de hoeveelheid van informatie-uitwisseling als de functionele netwerkorganisatie in de aangedane temporaalkwab.

In **hoofdstuk 4** zijn globale functionele netwerken gereconstrueerd in preoperatieve MEG registraties van patiënten met lokalisatiegebonden epilepsie. Gemiddelde functionele connectiviteit en netwerktopologie zijn vergeleken tussen patiënten met histopathologisch verschillende focale hersenafwijkingen en gezonde controles. De correlaties van deze verschillende histologische subtypen met epileptische aanvalsfrequentie en met cognitief functioneren zijn berekend. Hierbij werd een aantal verschillen tussen patiënten en gezonde controles werd waargenomen in de theta band (4-8Hz). “Synchronizability”, een maat voor de stabiliteit van synchronisatie van activiteit in het hersennetwerk, was bij patiënten met een laaggradig glioom (LGG) significant lager dan bij gezonde controles. Patiënten met niet-gliale laesies (NGL) toonden ook een significant verlaagde synchronizability, en daarnaast een verminderde globale netwerkintegratie vergeleken met gezonde controles, wat wijst op een verminderde integratie van informatie in het netwerk. De netwerken van patiënten met een hooggradig glioom (HGG) waren daarentegen niet significant verschillend van de netwerken van gezonde controles. Veranderde eigenschappen van het globale hersennetwerk correleerden met epileptische aanvalsfrequentie in LGG patiënten, en met cognitief functioneren in zowel LGG als HGG patiënten. Dit hoofdstuk laat zien dat de impact van focale hersenlaesies op functionele netwerken samenhangt met de histopathologie van die laesies. Dit is mogelijk het gevolg van verschillende groeipatronen. Interessant is daarbij dat de verminderde stabiliteit van de synchronisatie in de theta band bij LGG patiënten gepaard gaat met het vaker optreden van epileptische aanvallen, terwijl een verlies van globale integratie en verminderde stabiliteit van synchronisatie samen gaan met cognitieve stoornissen.

In **hoofdstuk 5** wordt de relatie tussen netwerktopologie en epileptische aanvalsfrequentie verder onderzocht in patiënten met een glioom die werden behandeld met het anti-epilepticum

levetiracetam. Direct na neurochirurgie (T1) en zes maanden later (T2) werden MEG registraties gemaakt. Een hogere functionele connectiviteit in de theta band was gecorreleerd met een hoger totaal aantal doorgemaakte epileptische aanvallen op zowel op tijdstip T1 als op tijdstip T2. Daarnaast was er een correlatie tussen een hoger aantal epileptische aanvallen en een minder optimale, (dat wil zeggen meer random georganiseerde) netwerktopologie. Er werden geen veranderingen gevonden in globale functionele connectiviteit of netwerktopologie tussen T1 en T2. Deze resultaten suggereren dat een pathologische toename van theta band connectiviteit een kenmerk is van tumorgerelateerde epilepsie.

In deel 3 van dit proefschrift worden de effecten van interventies op functionele connectiviteit en op netwerkorganisatie bestudeerd. In hoofdstuk 6 en 7 zijn MEG registraties geprojecteerd op de gestandaardiseerde AAL atlas door middel van beamforming, waardoor deze analyses konden plaatsvinden in een anatomisch kader. Beamforming is een techniek waarbij de activiteit die gemeten wordt in de MEG sensoren wordt geprojecteerd op de anatomische bronnen waar deze activiteit plaatsvindt.

In **hoofdstuk 6** zijn veranderingen in functionele connectiviteit bestudeerd in de eerste zes maanden na neurochirurgie. Hiertoe werden de resting-state netwerken (RSN) van LGG patiënten geanalyseerd. Dit zijn subnetwerken die een bekende relatie hebben met cognitieve taken. Zo bleek dat de connectiviteit in de lage alfa band (8-10 Hz) in het default mode netwerk (DMN) was toegenomen na operatie, wat gepaard ging met een verbeterd verbaal geheugen. Een soortgelijke verandering werd waargenomen in het rechter frontoparietale netwerk (FPN), waar connectiviteit was toegenomen in de hoge alfa band (10-13 Hz), en wat gecorreleerd bleek te zijn aan een verbetering in aandacht, werkgeheugen en executief functioneren. Deze bevindingen tonen aan dat toegenomen alfaband RSN connectiviteit in MEG registraties gecorreleerd is met verbeterd postoperatief cognitief functioneren.

Hoofdstuk 7 beschrijft veranderingen in functionele connectiviteit en netwerken die gerelateerd zijn aan epilepsie na operatie bij patiënten die tumorchirurgie of epilepsiechirurgie hebben ondergaan. Functionele netwerken werden gekarakteriseerd met behulp van een nieuwe methode gebaseerd op de zogenaamde “minimum spanning tree” (MST), die mogelijk de belangrijkste verbindingen in het netwerk bevat. De MST is het sterkst verbonden subnetwerk dat alle punten in het netwerk met elkaar verbindt zonder dat loops worden gevormd. Een voordeel van de MST boven andere maten voor netwerkanalyse is dat deze onafhankelijk is van de gemiddelde functionele connectiviteit in het netwerk. Functionele connectiviteit en MST netwerkmaten werden gerelateerd aan epileptische aanvalsfrequentie in een cross-sectionele analyse. Daarnaast werden PLI en MST veranderingen na operatie vergeleken tussen patiënten die postoperatief aanvalsvrij waren, en patiënten met postoperatieve aanvallen. PLI in de lage alfa band was significant gecorreleerd met een hogere aanvalsfrequentie op baseline, in het bijzonder in de hersengebieden waar de laesies zich bevonden. MST leaf fraction in de lage alfa band bleek bij aanvalsvrije patiënten ongeveer een jaar na operatie te zijn toegenomen ten opzichte van de preoperatieve meting, wat wijst op een meer geïntegreerde netwerkorganisatie van de MST, terwijl de leaf fraction in patiënten met postoperatieve aanvallen onveranderd bleef. Tot slot was de betweenness centrality, een maat voor de centrale rol of hub-status die een gebied speelt in het hersennetwerk, significant verlaagd bij aanvalsvrije patiënten in gebieden rondom de resectieholte. Deze studie laat zien dat er significante verschillen zijn tussen patiënten die postoperatief wel en patiënten die postoperatief niet aanvalsvrij zijn. De MST is mogelijk een bruikbare maat om veranderingen in de functionele hersennetwerken van deze patiënten te meten.

In **Hoofdstuk 8** wordt een studie beschreven waarin tijdelijke uitschakeling van een

hemisfeer door middel van intra-arteriëel toegediend amobarbital werd gebruikt om een omkeerbare hersenlaesie te simuleren. De intra-arteriële amobarbital procedure (IAP of Wada test) wordt gebruikt om de lateralisatie van taal en contralateraal geheugen te bepalen bij medicatieresistente temporale epilepsiepatiënten die kandidaat zijn voor resectie van de temporaalkwab. Tijdens de selectieve uitschakeling van een hemisfeer wordt het functioneren van de contralaterale hemisfeer gemeten met behulp van neuropsychologische tests. De netwerktopologie van de hersenen als geheel veranderde significant na amobarbital injectie: locale clustering nam af in alle frequentiebanden, en de padlengte werd korter in de theta en lage alfa band, wat wijst op een verschuiving naar een meer random georganiseerde netwerktopologie. Netwerkeigenschappen na amobarbital injectie correleerden met geheugenscore: een hogere theta band small-world index en een toegenomen hoge alfa band padlengte gingen gepaard met betere geheugenscores. Het globale hersennetwerk bij deze kandidaten voor epilepsiechirurgie wordt na selectieve uitschakeling van een hemisfeer meer random en minder optimaal georganiseerd. Daarnaast was het functioneren van het geheugen na de injectie gerelateerd aan netwerktopologie, wat erop wijst dat cognitief functioneren gerelateerd is aan netwerkeigenschappen van de hersenen.

In deel 4 wordt een modelstudie beschreven die is verricht om de empirische bevindingen uit de eerdere delen van dit proefschrift te integreren en interpreteren. **Hoofdstuk 9** heeft tot doel om te verklaren hoe focale laesies globale veranderingen in functionele hersennetwerken veroorzaken. De hypothese dat interacties tussen beschadigd hersenweefsel en resterende hersengebieden een globaal effect hebben op functionele connectiviteit wordt hier getest. Locale polymorfe delta activiteit (PDA), een typerende eigenschap in EEG/MEG registraties van patiënten met cerebrale laesies, werd gemodelleerd en veranderingen in functionele connectiviteit werden bestudeerd in een anatomisch realistisch model van menselijke hersenactiviteit. Laesies werden gesimuleerd door 1) veranderingen van parameters van individuele neural masses om PDA te creëren (simulatie van acute focale hersenschade); 2) deze PDA te combineren met verzwakking van structurele verbindingen (simulatie van hersentumoren), en 3) volledige verwijdering van structurele verbindingen (simulatie van een volledige neurochirurgische resectie). De effecten van deze laesies op functionele connectiviteit in op afstand gelegen hersengebieden werd gekwantificeerd met de synchronization likelihood (SL). Niet alleen structurele ontkoppeling maar ook PDA (in de context van intacte structurele verbindingen) veroorzaakte op zichzelf een afname van functionele connectiviteit. Een interessante observatie hierbij was dat functionele connectiviteit ook afnam tussen buiten de laesie gelegen gebieden. Het specifieke patroon van veranderingen in connectiviteit was verschillend voor de 3 verschillende typen laesies die hierboven staan beschreven. Bovendien bleek dat PDA in regio's met een centrale rol in het structurele netwerk meer impact had dan PDA in meer geïsoleerd gelegen regio's. Deze resultaten tonen aan dat veranderde activiteit in beschadigd hersenweefsel, zoals die gemeten kan worden met EEG/MEG, globale veranderingen in connectiviteit in de hersenen als geheel kan veroorzaken.

Concluderend worden in dit proefschrift functionele hersennetwerken beschreven van patiënten met een glioom en patiënten met lokalisatiegebonden epilepsie. Deze functionele hersennetwerken werden gereconstrueerd uit MEG, EEG en ECoG registraties. Netwerkverstoringen bij deze patiënten zijn gerelateerd aan complexe symptomen zoals epilepsie en cognitieve schade, en kunnen worden beïnvloed door neurochirurgische behandeling. Een computermodel, dat was gebaseerd op empirische bevindingen zoals die in deze dissertatie zijn beschreven, toont aan hoe focale verstoring van neurale activiteit kan leiden tot globale veranderingen in communicatie in de hersenen. De voortschrijdende verbetering van analysemethoden maakt het mogelijk om non-invasieve MEG registraties

te projecteren op anatomische bronnen en zodoende netwerken te reconstrueren. Deze netwerken kunnen vervolgens worden gebruikt om verschillende beeldvormende modaliteiten en verschillende patiënten onderling te vergelijken. Toekomstige studies moeten deze bevindingen verder vertalen naar diagnostische markers die kunnen worden ingezet om de uitkomst van operaties – gemeten aan epilepsie en cognitief functioneren – bij patiënten met hersentumoren en patiënten met lokalisatiegebonden epilepsie te verbeteren.

REFERENCES

1. Aaronson, N.K., et al., *Compromised health-related quality of life in patients with low-grade glioma.* J Clin Oncol, 2011. **29**(33): p. 4430-5.
2. Achard, S., et al., *A resilient, low-frequency, small-world human brain functional network with highly connected association cortical hubs.* J Neurosci, 2006. **26**(1): p. 63-72.
3. Aertsen, A.M., et al., *Dynamics of neuronal firing correlation: modulation of "effective connectivity".* J.Neurophysiol., 1989. **61**(5): p. 900-917.
4. Alstott, J., et al., *Modeling the impact of lesions in the human brain.* PLoS Comput Biol, 2009. **5**(6): p. e1000408.
5. Arenas, A., et al., *Synchronization in complex networks.* Physics Reports, 2008. **469**(3): p. 93-153.
6. Ashburner, J. and K.J. Friston, *Unified segmentation.* Neuroimage, 2005. **26**(3): p. 839-51.
7. Barahona, M. and L.M. Pecora, *Synchronization in small-world systems.* Phys.Rev. Lett., 2002. **89**(5): p. 054101.
8. Barnes, G.R., et al., *Realistic spatial sampling for MEG beamformer images.* Hum Brain Mapp, 2004. **23**(2): p. 120-7.
9. Bartolomei, F., et al., *Disturbed functional connectivity in brain tumour patients: evaluation by graph analysis of synchronization matrices.* Clin.Neurophysiol., 2006. **117**(9): p. 2039-2049.
10. Bartolomei, F., et al., *How do brain tumors alter functional connectivity? A magnetoencephalography study.* Ann.Neurol., 2006. **59**(1): p. 128-138.
11. Bartolomei, F., P. Chauvel, and F. Wendling, *Epileptogenicity of brain structures in human temporal lobe epilepsy: a quantified study from intracerebral EEG.* Brain, 2008. **131**(Pt 7): p. 1818-1830.
12. Bartolomei, F., F. Wendling, and P. Chauvel, *[The concept of an epileptogenic network in human partial epilepsies.].* Neurochirurgie, 2008. **54**(3): p. 174-184.
13. Bartolomei, F., et al., *Pre-ictal synchronicity in limbic networks of mesial temporal lobe epilepsy.* Epilepsy Res, 2004. **61**(1-3): p. 89-104.
14. Bassett, D.S. and E. Bullmore, *Small-world brain networks.* Neuroscientist, 2006. **12**(6): p. 512-23.
15. Bassett, D.S., et al., *Dynamic reconfiguration of human brain networks during learning.* Proc Natl Acad Sci U S A, 2011. **108**(18): p. 7641-6.
16. Beaumont, A. and I.R. Whittle, *The pathogenesis of tumour associated epilepsy.* Acta Neurochir (Wien), 2000. **142**(1): p. 1-15.
17. Beaumont, J. and M. Rugg, *The specificity of intrahemispheric EEG alpha coherence asymmetry related to psychological task.* Biological Psychology, 1979. **9**(4): p. 237-248.
18. Behin, A., et al., *Primary brain tumours in adults.* Lancet, 2003. **361**(9354): p. 323-31.
19. Ben-Ari, Y., V. Crepel, and A. Represa, *Seizures beget seizures in temporal lobe epilepsies: the boomerang effects of newly formed aberrant kainatergic synapses.* Epilepsy Curr., 2008. **8**(3): p. 68-72.
20. Berg, A.T., *Understanding the delay before epilepsy surgery: who develops intractable focal epilepsy and when?* CNS.Spectr., 2004. **9**(2): p. 136-144.
21. Berg, A.T., *The natural history of mesial temporal lobe epilepsy.* Curr.Opin.Neurol., 2008. **21**(2): p. 173-178.

22. Berg, A.T., et al., *How long does it take for partial epilepsy to become intractable?* Neurology, 2003. **60**(2): p. 186-190.
23. Bernasconi, N., J. Natsume, and A. Bernasconi, *Progression in temporal lobe epilepsy: differential atrophy in mesial temporal structures.* Neurology, 2005. **65**(2): p. 223-228.
24. Bernhardt, B.C., et al., *Graph-Theoretical Analysis Reveals Disrupted Small-World Organization of Cortical Thickness Correlation Networks in Temporal Lobe Epilepsy.* Cereb Cortex, 2011.
25. Bettus, G., et al., *Decreased basal fMRI functional connectivity in epileptogenic networks and contralateral compensatory mechanisms.* Hum.Brain Mapp., 2008.
26. Bettus, G., et al., *Interictal functional connectivity of human epileptic networks assessed by intracerebral EEG and BOLD signal fluctuations.* PLoS One, 2011. **6**(5): p. e20071.
27. Bettus, G., et al., *Enhanced EEG functional connectivity in mesial temporal lobe epilepsy.* Epilepsy Res, 2008. **81**(1): p. 58-68.
28. Blume, W.T., *The progression of epilepsy.* Epilepsia, 2006. **47 Suppl 1**: p. 71-78.
29. Boccaletti, S., et al., *Complex Networks: Structure and dynamics.* Physics reports, 2006(424): p. 175-308.
30. Boersma, M., et al., *Growing trees in child brains: Graph theoretical analysis of EEG derived minimum spanning tree in 5 and 7 year old children reflects brain maturation.* Brain Connect, 2012.
31. Boersma, M., et al., *Network analysis of resting state EEG in the developing young brain: structure comes with maturation.* Hum Brain Mapp, 2011. **32**(3): p. 413-25.
32. Bonifazi, P., et al., *GABAergic hub neurons orchestrate synchrony in developing hippocampal networks.* Science, 2009. **326**(5958): p. 1419-24.
33. Bosma, I., et al., *Synchronized brain activity and neurocognitive function in patients with low-grade glioma: a magnetoencephalography study.* Neuro Oncol, 2008. **10**(5): p. 734-44.
34. Bosma, I., et al., *Disturbed functional brain networks and neurocognitive function in low-grade glioma patients: a graph theoretical analysis of resting-state MEG.* Nonlinear Biomed Phys, 2009. **3**(1): p. 9.
35. Bosma, I., et al., *The influence of low-grade glioma on resting state oscillatory brain activity: a magnetoencephalography study.* J.Neurooncol., 2008. **88**(1): p. 77-85.
36. Bragin, A., C.L. Wilson, and J. Engel, Jr., *Chronic epileptogenesis requires development of a network of pathologically interconnected neuron clusters: a hypothesis.* Epilepsia, 2000. **41 Suppl 6**: p. S144-S152.
37. Bressler, S.L., *Understanding cognition through large-scale cortical networks.* Current Directions in Psychological Science, 2002. **11**(2): p. 58-61.
38. Brogna, C., S. Gil Robles, and H. Duffau, *Brain tumors and epilepsy.* Expert Rev Neurother, 2008. **8**(6): p. 941-55.
39. Brookes, M.J., et al., *Investigating the electrophysiological basis of resting state networks using magnetoencephalography.* Proc Natl Acad Sci U S A, 2011. **108**(40): p. 16783-8.
40. Broyd, S.J., et al., *Default-mode brain dysfunction in mental disorders: a systematic review.* Neurosci Biobehav Rev, 2009. **33**(3): p. 279-96.
41. Bullmore, E. and O. Sporns, *Complex brain networks: graph theoretical analysis of structural and functional systems.* Nat Rev Neurosci, 2009. **10**(3): p. 186-98.
42. Bullmore, E. and O. Sporns, *The economy of brain network organization.* Nat Rev Neurosci, 2012. **13**(5): p. 336-49.
43. Butz, M., et al., *Perilesional pathological oscillatory activity in the magnetoencephalogram of patients with cortical brain lesions.* Neurosci Lett, 2004. **355**(1-2): p. 93-6.

44. Butz, M., A. van Ooyen, and F. Worgotter, *A model for cortical rewiring following deafferentation and focal stroke.* Front Comput Neurosci, 2009. **3**: p. 10.
45. Butz, M., F. Wörgötter, and A. van Ooyen, *Activity-dependent structural plasticity.* Brain research reviews, 2009. **60**(2): p. 287.
46. Buxton, R.B., E.C. Wong, and L.R. Frank, *Dynamics of blood flow and oxygenation changes during brain activation: the balloon model.* Magn Reson Med, 1998. **39**(6): p. 855-64.
47. Cabral, J., et al., *Modeling the outcome of structural disconnection on resting-state functional connectivity.* Neuroimage, 2012. **62**(3): p. 1342-53.
48. Campbell, S.L., S.C. Buckingham, and H. Sontheimer, *Human glioma cells induce hyperexcitability in cortical networks.* Epilepsia, 2012. **53**(8): p. 1360-70.
49. Carmichael, S.T., et al., *Growth-associated gene expression after stroke: evidence for a growth-promoting region in peri-infarct cortex.* Exp Neurol, 2005. **193**(2): p. 291-311.
50. Chang, E.F., et al., *Seizure characteristics and control following resection in 332 patients with low-grade gliomas.* J Neurosurg, 2008. **108**(2): p. 227-35.
51. Chavez, M., et al., *Synchronization is enhanced in weighted complex networks.* Phys Rev Lett, 2005. **94**(21): p. 218701.
52. Chavez, M., et al., *Functional modularity of background activities in normal and epileptic brain networks.* http://arxiv.org/abs/0811.3131v3, 2009.
53. Chen, Z.J., et al., *Revealing modular architecture of human brain structural networks by using cortical thickness from MRI.* Cereb Cortex, 2008. **18**(10): p. 2374-81.
54. Clemens, B., *Abnormal quantitative EEG scores identify patients with complicated idiopathic generalised epilepsy.* Seizure, 2004. **13**(6): p. 366-74.
55. Clemens, B., *Pathological theta oscillations in idiopathic generalised epilepsy.* Clin Neurophysiol, 2004. **115**(6): p. 1436-41.
56. Clemens, B., G. Szigeti, and Z. Barta, *EEG frequency profiles of idiopathic generalised epilepsy syndromes.* Epilepsy Res, 2000. **42**(2-3): p. 105-15.
57. Cole, M.W. and W. Schneider, *The cognitive control network: Integrated cortical regions with dissociable functions.* Neuroimage, 2007. **37**(1): p. 343-60.
58. Corbetta, M., G. Patel, and G.L. Shulman, *The reorienting system of the human brain: from environment to theory of mind.* Neuron, 2008. **58**(3): p. 306-24.
59. Damoiseaux, J.S., et al., *Consistent resting-state networks across healthy subjects.* Proc Natl Acad Sci U S A, 2006. **103**(37): p. 13848-53.
60. Dancause, N., et al., *Extensive cortical rewiring after brain injury.* The Journal of neuroscience, 2005. **25**(44): p. 10167-10179.
61. de Groot, M., et al., *Epilepsy in patients with a brain tumour: focal epilepsy requires focused treatment.* Brain, 2012. **135**(4): p. 1002-1016.
62. de Haan, W., et al., *Activity dependent degeneration explains hub vulnerability in Alzheimer's disease.* PLoS Comput Biol, 2012. **8**(8): p. e1002582.
63. de Haan, W., et al., *Disrupted modular brain dynamics reflect cognitive dysfunction in Alzheimer's disease.* Neuroimage, 2012. **59**(4): p. 3085-93.
64. de Jongh, A., et al., *The influence of brain tumor treatment on pathological delta activity in MEG.* Neuroimage, 2003. **20**(4): p. 2291-301.
65. de Jongh, A., et al., *The localization of spontaneous brain activity: first results in patients with cerebral tumors.* Clin Neurophysiol, 2001. **112**(2): p. 378-85.
66. de Pasquale, F., et al., *A cortical core for dynamic integration of functional networks in the resting human brain.* Neuron, 2012. **74**(4): p. 753-64.
67. de Vico Fallani, F., et al., *Evaluation of the brain network organization from EEG signals: a preliminary evidence in stroke patient.* Anat Rec (Hoboken), 2009. **292**(12): p. 2023-31.

68. Desmurget, M., F. Bonnetblanc, and H. Duffau, *Contrasting acute and slow-growing lesions: a new door to brain plasticity.* Brain, 2007. **130**(Pt 4): p. 898-914.
69. Domínguez, L.G., et al., *Enhanced measured synchronization of unsynchronized sources: inspecting the physiological significance of synchronization analysis of whole brain electrophysiological recordings.* Int. J. Phys. Sci, 2007. **2**(11): p. 305-317.
70. Dosenbach, N.U., et al., *Distinct brain networks for adaptive and stable task control in humans.* Proc Natl Acad Sci U S A, 2007. **104**(26): p. 11073-8.
71. Douw, L., et al., *Treatment-related changes in functional connectivity in brain tumor patients: A magnetoencephalography study.* Exp.Neurol., 2008. **212**(2): p. 285-90.
72. Douw, L., et al., *Functional connectivity in the brain before and during intra-arterial amobarbital injection (Wada test).* Neuroimage, 2009. **46**(3): p. 584-8.
73. Douw, L., et al., *Local MEG networks: The missing link between protein expression and epilepsy in glioma patients?* Neuroimage, 2013.
74. Douw, L., et al., *'Functional connectivity' is a sensitive predictor of epilepsy diagnosis after the first seizure.* PLoS One, 2010. **5**(5): p. e10839.
75. Douw, L., et al., *Cognitive and radiological effects of radiotherapy in patients with low-grade glioma: long-term follow-up.* Lancet Neurol, 2009. **8**(9): p. 810-8.
76. Douw, L., et al., *Cognition is related to resting-state small-world network topology: an magnetoencephalographic study.* Neuroscience, 2011. **175**: p. 169-77.
77. Douw, L., et al., *The lesioned brain: still a small world?* Frontiers in Human Neuroscience, 2010. **4**: p. 12.
78. Douw, L., et al., *Epilepsy is related to theta band brain connectivity and network topology in brain tumor patients.* BMC Neuroscience, 2010. **11**(11:103).
79. Dubovik, S., et al., *The behavioral significance of coherent resting-state oscillations after stroke.* Neuroimage, 2012. **61**(1): p. 249-57.
80. Duffau, H., *Brain plasticity: from pathophysiological mechanisms to therapeutic applications.* J Clin Neurosci, 2006. **13**(9): p. 885-97.
81. Duffau, H., et al., *Medically intractable epilepsy from insular low-grade gliomas: improvement after an extended lesionectomy.* Acta Neurochir (Wien), 2002. **144**(6): p. 563-72; discussion 572-3.
82. Dyhrfjeld-Johnsen, J., et al., *Topological determinants of epileptogenesis in large-scale structural and functional models of the dentate gyrus derived from experimental data.* J Neurophysiol, 2007. **97**(2): p. 1566-87.
83. Eguiluz, V.M., et al., *Scale-free brain functional networks.* Phys Rev Lett, 2005. **94**(1): p. 018102.
84. Elger, C.E., C. Helmstaedter, and M. Kurthen, *Chronic epilepsy and cognition.* Lancet Neurol, 2004. **3**(11): p. 663-72.
85. Engel, J.J., et al., *Outcome with respect to epileptic seizures*, in *Surgical treatment of the epilepsies, 2nd edition*1993, Raven Press: Ney York. p. 609-621.
86. Esposito, R., et al., *Modifications of default-mode network connectivity in patients with cerebral glioma.* PLoS One, 2012. **7**(7): p. e40231.
87. Ferrarini, L., et al., *Hierarchical functional modularity in the resting-state human brain.* Hum Brain Mapp, 2009. **30**(7): p. 2220-31.
88. Fornito, A., et al., *Competitive and cooperative dynamics of large-scale brain functional networks supporting recollection.* Proc Natl Acad Sci U S A, 2012. **109**(31): p. 12788-93.
89. French, J.A., et al., *Characteristics of medial temporal lobe epilepsy: I. Results of history and physical examination.* Ann.Neurol., 1993. **34**(6): p. 774-780.
90. Gong, G., et al., *Mapping anatomical connectivity patterns of human cerebral cortex using in vivo diffusion tensor imaging tractography.* Cereb Cortex, 2009. **19**(3): p. 524-36.

91. Gong, G., et al., *Age- and gender-related differences in the cortical anatomical network.* J Neurosci, 2009. **29**(50): p. 15684-93.
92. Gootjes, L., et al., *Attention modulates hemispheric differences in functional connectivity: evidence from MEG recordings.* Neuroimage, 2006. **30**(1): p. 245-53.
93. Gratton, C., et al., *Focal brain lesions to critical locations cause widespread disruption of the modular organization of the brain.* J Cogn Neurosci, 2012. **24**(6): p. 1275-85.
94. Grefkes, C., et al., *Cortical connectivity after subcortical stroke assessed with functional magnetic resonance imaging.* Ann Neurol, 2007. **63**(2): p. 236-246.
95. Guevara, R., et al., *Phase synchronization measurements using electroencephalographic recordings.* Neuroinformatics, 2005. **3**(4): p. 301-313.
96. Guggisberg, A.G., et al., *Mapping functional connectivity in patients with brain lesions.* Ann.Neurol., 2008. **63**(2): p. 193-203.
97. Guimera, R., et al., *The worldwide air transportation network: Anomalous centrality, community structure, and cities' global roles.* Proc Natl Acad Sci U S A, 2005. **102**(22): p. 7794-9.
98. Hagmann, P., et al., *Mapping the structural core of human cerebral cortex.* PLoS Biol, 2008. **6**(7): p. e159.
99. He, Y., Z.J. Chen, and A.C. Evans, *Small-world anatomical networks in the human brain revealed by cortical thickness from MRI.* Cereb Cortex, 2007. **17**(10): p. 2407-19.
100. Heimans, J.J. and J.C. Reijneveld, *Factors affecting the cerebral network in brain tumor patients.* J Neurooncol, 2012. **108**(2): p. 231-7.
101. Hildebrand, J., et al., *Epileptic seizures during follow-up of patients treated for primary brain tumors.* Neurology, 2005. **65**(2): p. 212-215.
102. Hilgetag, C.C., et al., *Anatomical connectivity defines the organization of clusters of cortical areas in the macaque monkey and the cat.* Philos Trans R Soc Lond B Biol Sci, 2000. **355**(1393): p. 91-110.
103. Hillebrand, A. and G.R. Barnes, *A quantitative assessment of the sensitivity of whole-head MEG to activity in the adult human cortex.* Neuroimage, 2002. **16**(3 Pt 1): p. 638-50.
104. Hillebrand, A., et al., *Frequency-dependent functional connectivity within resting-state networks: an atlas-based MEG beamformer solution.* Neuroimage, 2012. **59**(4): p. 3909-21.
105. Hipp, J.F., et al., *Large-scale cortical correlation structure of spontaneous oscillatory activity.* Nat Neurosci, 2012. **15**(6): p. 884-90.
106. Hofmeijer, J. and M.J. van Putten, *Ischemic cerebral damage: an appraisal of synaptic failure.* Stroke, 2012. **43**(2): p. 607-15.
107. Holme, P., et al., *Attack vulnerability of complex networks.* Physical Review E, 2002. **65**(5): p. 056109.
108. Honey, C.J., et al., *Network structure of cerebral cortex shapes functional connectivity on multiple time scales.* Proc Natl Acad Sci U S A, 2007. **104**(24): p. 10240-5.
109. Honey, C.J. and O. Sporns, *Dynamical consequences of lesions in cortical networks.* Hum Brain Mapp, 2008. **29**(7): p. 802-9.
110. Horstmann, M.T., et al., *State dependent properties of epileptic brain networks: Comparative graph-theoretical analyses of simultaneously recorded EEG and MEG.* Clin Neurophysiol, 2010. **121**(2): p. 172-185.
111. Houx, P.J. and J. Jolles, *Vulnerability factors for age-related cognitive decline*, in *The vulnerable brain and environmental risks*, R.L. Isaacson and K.F. Jensen, Editors. 1994, Plenum Press: New York. p. 25– 41.

112. Humphries, M.D. and K. Gurney, *Network 'small-world-ness': a quantitative method for determining canonical network equivalence.* PLoS One, 2008. **3**(4): p. e0002051.
113. Ioannides, A.A., *Dynamic functional connectivity.* Curr Opin Neurobiol, 2007. **17**(2): p. 161-70.
114. Ius, T., et al., *Evidence for potentials and limitations of brain plasticity using an atlas of functional resectability of WHO grade II gliomas: towards a "minimal common brain".* Neuroimage, 2011. **56**(3): p. 992-1000.
115. James, G.A., et al., *Changes in resting state effective connectivity in the motor network following rehabilitation of upper extremity poststroke paresis.* Topics in Stroke Rehabilitation, 2009. **16**(4): p. 270-281.
116. Jann, K., et al., *BOLD correlates of EEG alpha phase-locking and the fMRI default mode network.* Neuroimage, 2009. **45**(3): p. 903-16.
117. Jolles, J., et al., *[The Maastricht aging study (MAAS). The longitudinal perspective of cognitive aging].* Tijdschr Gerontol Geriatr, 1998. **29**(3): p. 120-9.
118. Kahana, M.J., *The cognitive correlates of human brain oscillations.* J Neurosci, 2006. **26**(6): p. 1669-72.
119. Kaiser, M., et al., *Simulation of robustness against lesions of cortical networks.* Eur J Neurosci, 2007. **25**(10): p. 3185-92.
120. Karnofsky, D.A., et al., *The use of the nitrogen mustards in the palliative treatment of carcinoma. .* Cancer, 1948. **1**(634-656).
121. Keidel, J.L., S.R. Welbourne, and M.A. Lambon Ralph, *Solving the paradox of the equipotential and modular brain: a neurocomputational model of stroke vs. slow-growing glioma.* Neuropsychologia, 2010. **48**(6): p. 1716-24.
122. Klausberger, T., et al., *Brain-state- and cell-type-specific firing of hippocampal interneurons in vivo.* Nature, 2003. **421**(6925): p. 844-8.
123. Klausberger, T. and P. Somogyi, *Neuronal diversity and temporal dynamics: the unity of hippocampal circuit operations.* Science, 2008. **321**(5885): p. 53-7.
124. Klein, M., H. Dufau, and P.C. De Witt Hamer, *Cognition and resective surgery for diffuse infiltrative glioma: an overview.* J. Neurooncol., 2012. **108**(2): p. 309-318.
125. Klein, M., et al., *Epilepsy in low-grade gliomas: the impact on cognitive function and quality of life.* Ann Neurol, 2003. **54**(4): p. 514-20.
126. Klein, M., et al., *Effect of radiotherapy and other treatment-related factors on mid-term to long-term cognitive sequelae in low-grade gliomas: a comparative study.* Lancet, 2002. **360**(9343): p. 1361-8.
127. Klimesch, W., *EEG alpha and theta oscillations reflect cognitive and memory performance: a review and analysis.* Brain Res Brain Res Rev, 1999. **29**(2-3): p. 169-95.
128. Kohler, B.A., et al., *Annual report to the nation on the status of cancer, 1975-2007, featuring tumors of the brain and other nervous system.* J Natl Cancer Inst, 2011. **103**(9): p. 714-36.
129. Kotter, R. and F.T. Sommer, *Global relationship between anatomical connectivity and activity propagation in the cerebral cortex.* Philos Trans R Soc Lond B Biol Sci, 2000. **355**(1393): p. 127-34.
130. Kramer, M.A. and S.S. Cash, *Epilepsy as a disorder of cortical network organization.* Neuroscientist, 2012. **18**(4): p. 360-72.
131. Kramer, M.A., E.D. Kolaczyk, and H.E. Kirsch, *Emergent network topology at seizure onset in humans.* Epilepsy Res., 2008. **79**(2-3): p. 173-186.
132. Krouwer, H.G., J.L. Pallagi, and N.M. Graves, *Management of seizures in brain tumor patients at the end of life.* J Palliat Med, 2000. **3**(4): p. 465-75.

133. Kruskal, J.B., *On the shortest spanning subtree of a graph and the traveling salesman problem.* Proceedings of the American Mathematical society, 1956. **7**(1): p. 48-50.
134. Laufs, H., *Endogenous brain oscillations and related networks detected by surface EEG-combined fMRI.* Hum Brain Mapp, 2008. **29**(7): p. 762-9.
135. Le Van Quyen, M., et al., *Preictal state identification by synchronization changes in long-term intracranial EEG recordings.* Clin.Neurophysiol., 2005. **116**(3): p. 559-568.
136. Lee, U., S. Kim, and K.Y. Jung, *Classification of epilepsy types through global network analysis of scalp electroencephalograms.* Phys Rev E Stat Nonlin Soft Matter Phys, 2006. **73**(4 Pt 1): p. 041920.
137. Legler, J.M., et al., *Cancer surveillance series [corrected]: brain and other central nervous system cancers: recent trends in incidence and mortality.* J Natl Cancer Inst, 1999. **91**(16): p. 1382-90.
138. Lehnertz, K., et al., *Synchronization phenomena in human epileptic brain networks.* J Neurosci Methods, 2009. **183**(1): p. 42-8.
139. Lezak, M.D., *Neuropsychological Assessment* 3rd ed1995, New York: Oxford University Press.
140. Li, Y., et al., *Brain anatomical network and intelligence.* PLoS Comput Biol, 2009. **5**(5): p. e1000395.
141. Liao, W., et al., *Altered functional connectivity and small-world in mesial temporal lobe epilepsy.* PLoS One, 2010. **5**(1): p. e8525.
142. Lopes da Silva, F., et al., *Epilepsies as dynamical diseases of brain systems: basic models of the transition between normal and epileptic activity.* Epilepsia, 2003. **44 Suppl 12**: p. 72-83.
143. Lopes da Silva, F.H., et al., *Model of brain rhythmic activity. The alpha-rhythm of the thalamus.* Kybernetik, 1974. **15**(1): p. 27-37.
144. Mackenzie, L., et al., *Picrotoxin-induced generalised convulsive seizure in rat: changes in regional distribution and frequency of the power of electroencephalogram rhythms.* Clin Neurophysiol, 2002. **113**(4): p. 586-96.
145. Marcelin, B., et al., *h channel-dependent deficit of theta oscillation resonance and phase shift in temporal lobe epilepsy.* Neurobiol Dis, 2009. **33**(3): p. 436-47.
146. Marchiori, M. and V. Latora, *Harmony in the small world.* Physica A, 2000(285): p. 539-546.
147. Markand, O.N., et al., *Health-related quality of life outcome in medically refractory epilepsy treated with anterior temporal lobectomy.* Epilepsia, 2000. **41**(6): p. 749-59.
148. Martino, J., et al., *Resting functional connectivity in patients with brain tumors in eloquent areas.* Ann Neurol, 2011. **69**(3): p. 521-32.
149. Maslov, S. and K. Sneppen, *Specificity and stability in topology of protein networks.* Science, 2002. **296**(5569): p. 910-3.
150. Mathern, G.W., et al., *Hippocampal neuron damage in human epilepsy: Meyer's hypothesis revisited.* Prog.Brain Res., 2002. **135**: p. 237-251.
151. Medvedovsky, M., et al., *Fine tuning the correlation limit of spatio-temporal signal space separation for magnetoencephalography.* J Neurosci Methods, 2009. **177**(1): p. 203-11.
152. Meunier, D., et al., *Age-related changes in modular organization of human brain functional networks.* Neuroimage, 2009. **44**(3): p. 715-23.
153. Meunier, D., et al., *Hierarchical modularity in human brain functional networks.* Front Neuroinformatics, 2009. **3**: p. 37.
154. Micheloyannis, S., et al., *Small-world networks and disturbed functional connectivity in schizophrenia.* Schizophr.Res., 2006. **87**(1-3): p. 60-66.

155. Micheloyannis, S., et al., *Using graph theoretical analysis of multi channel EEG to evaluate the neural efficiency hypothesis.* Neurosci.Lett., 2006. **402**(3): p. 273-277.
156. Micheloyannis, S., et al., *Neural networks involved in mathematical thinking: evidence from linear and non-linear analysis of electroencephalographic activity.* Neurosci.Lett., 2005. **373**(3): p. 212-217.
157. Mintzopoulos, D., et al., *Connectivity alterations assessed by combining fMRI and MR-compatible hand robots in chronic stroke.* Neuroimage, 2009. **47**: p. T90-T97.
158. Mirsky, A.F. and C.F. Grady, *Toward the development of alternative treatments in absence epilepsy*, in *Elements of petit mal epilepsy*, M.S. Myslobodsky and A.F. Mirsky, Editors. 1988, Peter Lang: New York, U.S.A. p. 285-310.
159. Mizuki, Y., et al., *Periodic appearance of theta rhythm in the frontal midline area during performance of a mental task.* Electroencephalogr Clin Neurophysiol, 1980. **49**(3-4): p. 345-51.
160. Montez, T., et al., *Synchronization likelihood with explicit time-frequency priors.* Neuroimage, 2006. **33**(4): p. 1117-25.
161. Morgan, R.J. and I. Soltesz, *Nonrandom connectivity of the epileptic dentate gyrus predicts a major role for neuronal hubs in seizures.* Proc.Natl.Acad.Sci.U.S.A, 2008. **105**(16): p. 6179-6184.
162. Nenonen, J., et al., *Validation of head movement correction and spatiotemporal signal space separation in magnetoencephalography.* Clin Neurophysiol, 2012. **123**(11): p. 2180-91.
163. Netoff, T.I., et al., *Epilepsy in small-world networks.* J.Neurosci., 2004. **24**(37): p. 8075-8083.
164. Newman, *The Structure and Function of Complex Networks.* SIAM Rev., 2003. **45**(2): p. 167-256.
165. Newman, M.E., *Mixing patterns in networks.* Phys Rev E Stat Nonlin Soft Matter Phys, 2003. **67**(2 Pt 2): p. 026126.
166. Nichols, T.E. and A.P. Holmes, *Nonparametric permutation tests for functional neuroimaging: a primer with examples.* Hum Brain Mapp, 2002. **15**(1): p. 1-25.
167. Nir, Y., et al., *Coupling between neuronal firing rate, gamma LFP, and BOLD fMRI is related to interneuronal correlations.* Curr Biol, 2007. **17**(15): p. 1275-85.
168. Nolte, G., et al., *Identifying true brain interaction from EEG data using the imaginary part of coherency.* Clin Neurophysiol, 2004. **115**(10): p. 2292-307.
169. Nomura, E.M., et al., *Double dissociation of two cognitive control networks in patients with focal brain lesions.* Proc Natl Acad Sci U S A, 2010. **107**(26): p. 12017-22.
170. Nudo, R., et al., *Use-dependent alterations of movement representations in primary motor cortex of adult squirrel monkeys.* Journal of Neuroscience, 1996. **16**(2): p. 785-807.
171. Nudo, R.J., *Postinfarct cortical plasticity and behavioral recovery.* Stroke, 2007. **38**(2): p. 840-845.
172. Nunez, P.L., et al., *EEG coherency: I: statistics, reference electrode, volume conduction, Laplacians, cortical imaging, and interpretation at multiple scales.* Electroencephalogr Clin Neurophysiol, 1997. **103**(5): p. 499-515.
173. Ortega, G.J., et al., *Synchronization clusters of interictal activity in the lateral temporal cortex of epileptic patients: intraoperative electrocorticographic analysis.* Epilepsia, 2008. **49**(2): p. 269-280.
174. Ortega, G.J., R.G. Sola, and J. Pastor, *Complex network analysis of human ECoG data.* Neurosci.Lett., 2008. **447**(2-3): p. 129-133.
175. Oshino, S., et al., *Magnetoencephalographic analysis of cortical oscillatory activity in patients with brain tumors: Synthetic aperture magnetometry (SAM) functional imaging of delta band activity.* Neuroimage, 2007. **34**(3): p. 957-64.

176. Peraza, L.R., et al., *Volume conduction effects in brain network inference from electroencephalographic recordings using phase lag index.* J Neurosci Methods, 2012.
177. Percha, B., et al., *Transition from local to global phase synchrony in small world neural network and its possible implications for epilepsy.* Phys.Rev.E.Stat.Nonlin. Soft.Matter Phys., 2005. **72**(3 Pt 1): p. 031909.
178. Picot, M.C., et al., *The prevalence of epilepsy and pharmacoresistant epilepsy in adults: a population-based study in a Western European country.* Epilepsia, 2008. **49**(7): p. 1230-8.
179. Pitkanen, A. and T.P. Sutula, *Is epilepsy a progressive disorder? Prospects for new therapeutic approaches in temporal-lobe epilepsy.* Lancet Neurol., 2002. **1**(3): p. 173-181.
180. Ponten, S.C., F. Bartolomei, and C.J. Stam, *Small-world networks and epilepsy: graph theoretical analysis of intracerebrally recorded mesial temporal lobe seizures.* Clin.Neurophysiol., 2007. **118**(4): p. 918-927.
181. Ponten, S.C., et al., *The relationship between structural and functional connectivity: Graph theoretical analysis of an EEG neural mass model.* Neuroimage, 2009.
182. Ponten, S.C., et al., *Indications for network regularization during absence seizures: Weighted and unweighted graph theoretical analyses.* Exp Neurol, 2009.
183. Posthuma, D., et al., *Genetic components of functional connectivity in the brain: the heritability of synchronization likelihood.* Hum Brain Mapp, 2005. **26**(3): p. 191-8.
184. Ramasco, J.J. and B. Goncalves, *Transport on weighted networks: When the correlations are independent of the degree.* Phys Rev E Stat Nonlin Soft Matter Phys, 2007. **76**(6 Pt 2): p. 066106.
185. Rampil, I.J., *A primer for EEG signal processing in anesthesia.* Anesthesiology, 1998. **89**(4): p. 980-1002.
186. Reijmer, Y.D., et al., *Disruption of the cerebral white matter network is related to slowing of information processing speed in patients with type 2 diabetes.* Diabetes, 2013.
187. Reijneveld, J.C., et al., *The application of graph theoretical analysis to complex networks in the brain.* Clin.Neurophysiol., 2007. **118**(11): p. 2317-2331.
188. Robinson, S.E. and J. Vrba, *Functional neuroimaging by synthetic aperture magnetometry (SAM)*, in *Recent advances in biomagnetism*, T. Yoshimoto, et al., Editors. 1999, Tohoku University Press: Sendai, Japan. p. 302-5.
189. Rodrigues, E., M. Barbosa, and L.D.F. Costa, *On the importance of hubs in Hopfield complex neuronal networks under attack.* arXiv preprint cond-mat/0507677, 2005.
190. Rosazza, C. and L. Minati, *Resting-state brain networks: literature review and clinical applications.* Neurol Sci, 2011. **32**(5): p. 773-85.
191. Rosenow, F. and H. Luders, *Presurgical evaluation of epilepsy.* Brain, 2001. **124**(Pt 9): p. 1683-700.
192. Rubinov, M., et al., *Simulation of neuronal death and network recovery in a computational model of distributed cortical activity.* American Journal of Geriatric Psych, 2009. **17**(3): p. 210-217.
193. Rubinov, M. and O. Sporns, *Complex network measures of brain connectivity: Uses and interpretations.* Neuroimage, 2009.
194. Ryvlin, P., *Beyond pharmacotherapy: surgical management.* Epilepsia, 2003. **44 Suppl 5**: p. 23-28.
195. Salvador, R., et al., *Neurophysiological architecture of functional magnetic resonance images of human brain.* Cereb Cortex, 2005. **15**(9): p. 1332-42.

196. Salvador, R., et al., *Undirected graphs of frequency-dependent functional connectivity in whole brain networks.* Philos Trans R Soc Lond B Biol Sci, 2005. **360**(1457): p. 937-46.
197. Sant, M., et al., *Survival of European patients with central nervous system tumors.* Int J Cancer, 2012. **131**(1): p. 173-85.
198. Schindler, K., et al., *Assessing seizure dynamics by analysing the correlation structure of multichannel intracranial EEG.* Brain, 2007. **130**(Pt 1): p. 65-77.
199. Schindler, K.A., et al., *Evolving functional network properties and synchronizability during human epileptic seizures.* Chaos, 2008. **18**(3): p. 033119.
200. Sharp, D.J., et al., *Default mode network functional and structural connectivity after traumatic brain injury.* Brain, 2011. **134**(Pt 8): p. 2233-47.
201. Singer, W., *Neuronal synchrony: a versatile code for the definition of relations?* Neuron, 1999. **24**(1): p. 49-65, 111-25.
202. Smit, D.J., et al., *Endophenotypes in a dynamically connected brain.* Behav Genet, 2009. **40**(2): p. 167-77.
203. Smit, D.J., et al., *Heritability of "small-world" networks in the brain: a graph theoretical analysis of resting-state EEG functional connectivity.* Hum Brain Mapp, 2008. **29**(12): p. 1368-78.
204. Sporns, O. and C.J. Honey, *Small worlds inside big brains.* Proc Natl Acad Sci U S A, 2006. **103**(51): p. 19219-20.
205. Sporns, O., G. Tononi, and G.M. Edelman, *Theoretical neuroanatomy: relating anatomical and functional connectivity in graphs and cortical connection matrices.* Cereb Cortex, 2000. **10**(2): p. 127-41.
206. Srinivas, K.V., et al., *Small-world network topology of hippocampal neuronal network is lost, in an in vitro glutamate injury model of epilepsy.* Eur.J.Neurosci., 2007. **25**(11): p. 3276-3286.
207. Stam, C., *Brain dynamics in theta and alpha frequency bands and working memory performance in humans.* Neurosci Lett, 2000. **286**(2): p. 115.
208. Stam, C.J., *Functional connectivity patterns of human magnetoencephalographic recordings: a 'small-world' network?* Neurosci.Lett., 2004. **355**(1-2): p. 25-28.
209. Stam, C.J., *Characterization of anatomical and functional connectivity in the brain: a complex networks perspective.* Int J Psychophysiol, 2010. **77**(3): p. 186-94.
210. Stam, C.J., et al., *Graph theoretical analysis of magnetoencephalographic functional connectivity in Alzheimer's disease.* Brain, 2009. **132**(Pt 1): p. 213-24.
211. Stam, C.J., et al., *Emergence of Modular Structure in a Large-Scale Brain Network with Interactions between Dynamics and Connectivity.* Front Comput Neurosci, 2010. **4**.
212. Stam, C.J., et al., *Magnetoencephalographic evaluation of resting-state functional connectivity in Alzheimer's disease.* Neuroimage, 2006. **32**(3): p. 1335-44.
213. Stam, C.J., et al., *Small-world networks and functional connectivity in Alzheimer's disease.* Cereb.Cortex, 2007. **17**(1): p. 92-99.
214. Stam, C.J., G. Nolte, and A. Daffertshofer, *Phase lag index: assessment of functional connectivity from multi channel EEG and MEG with diminished bias from common sources.* Hum.Brain Mapp., 2007. **28**(11): p. 1178-1193.
215. Stam, C.J. and J.C. Reijneveld, *Graph theoretical analysis of complex networks in the brain.* Nonlinear.Biomed.Phys., 2007. **1**(1): p. 3.
216. Stam, C.J., A.M. van Cappellen van Walsum, and S. Micheloyannis, *Variability of EEG synchronization during a working memory task in healthy subjects.* Int J Psychophysiol, 2002. **46**(1): p. 53-66.
217. Stam, C.J. and B.W. van Dijk, *Synchronization likelihood: an unbiased measure of generalized synchronization in multivariate data sets.* Phys. D, 2002. **163**(3): p. 236-251.

218. Stam, C.J. and E.C. van Straaten, *Go with the flow: use of a directed phase lag index (dPLI) to characterize patterns of phase relations in a large-scale model of brain dynamics.* Neuroimage, 2012. **62**(3): p. 1415-28.
219. Stam, C.J. and E.C. van Straaten, *The organization of physiological brain networks.* Clin Neurophysiol, 2012. **123**(6): p. 1067-87.
220. Stephan, K.E., et al., *The Brain Connectivity Workshops: Moving the frontiers of computational systems neuroscience.* Neuroimage., 2008.
221. Steriade, M., et al., *Report of IFCN Committee on Basic Mechanisms. Basic mechanisms of cerebral rhythmic activities.* Electroencephalogr Clin Neurophysiol, 1990. **76**(6): p. 481-508.
222. Stupp, R., et al., *Radiotherapy plus concomitant and adjuvant temozolomide for glioblastoma.* N Engl J Med, 2005. **352**(10): p. 987-96.
223. Supekar, K., et al., *Network analysis of intrinsic functional brain connectivity in Alzheimer's disease.* PLoS Comput Biol, 2008. **4**(6): p. e1000100.
224. Supekar, K., M. Musen, and V. Menon, *Development of large-scale functional brain networks in children.* PLoS Biol, 2009. **7**(7): p. e1000157.
225. Taphoorn, M.J. and M. Klein, *Cognitive deficits in adult patients with brain tumours.* Lancet Neurol., 2004. **3**(3): p. 159-168.
226. Tarapore, P.E., et al., *Magnetoencephalographic Imaging of Resting-State Functional Connectivity Predicts Postsurgical Neurological Outcome in Brain Gliomas.* Neurosurgery, 2012(DOI: 10.1227/NEU.0b013e31826d2b78).
227. Taulu, S. and R. Hari, *Removal of magnetoencephalographic artifacts with temporal signal-space separation: demonstration with single-trial auditory-evoked responses.* Hum Brain Mapp, 2009. **30**(5): p. 1524-34.
228. Taulu, S. and J. Simola, *Spatiotemporal signal space separation method for rejecting nearby interference in MEG measurements.* Phys Med Biol, 2006. **51**(7): p. 1759-68.
229. Tellez-Zenteno, J.F., et al., *Long-term outcomes in epilepsy surgery: antiepileptic drugs, mortality, cognitive and psychosocial aspects.* Brain, 2007. **130**(Pt 2): p. 334-45.
230. Tellez-Zenteno, J.F., R. Dhar, and S. Wiebe, *Long-term seizure outcomes following epilepsy surgery: a systematic review and meta-analysis.* Brain, 2005. **128**(Pt 5): p. 1188-98.
231. Tononi, G. and G.M. Edelman, *Consciousness and the integration of information in the brain.* Adv Neurol, 1998. **77**: p. 245-79; discussion 279-80.
232. Tzourio-Mazoyer, N., et al., *Automated anatomical labeling of activations in SPM using a macroscopic anatomical parcellation of the MNI MRI single-subject brain.* Neuroimage, 2002. **15**(1): p. 273-89.
233. Uhlhaas, P.J. and W. Singer, *Neural synchrony in brain disorders: relevance for cognitive dysfunctions and pathophysiology.* Neuron, 2006. **52**(1): p. 155-68.
234. Vaessen, M.J., et al., *White matter network abnormalities are associated with cognitive decline in chronic epilepsy.* Cereb Cortex, 2012. **22**(9): p. 2139-47.
235. van Breemen, M.S., E.B. Wilms, and C.J. Vecht, *Epilepsy in patients with brain tumours: epidemiology, mechanisms, and management.* Lancet Neurol, 2007. **6**(5): p. 421-30.
236. van Dellen, E., et al., *Connectivity in MEG resting-state networks increases after resective surgery for low-grade glioma and correlates with improved cognitive performance.* NeuroImage: Clinical, 2013. **2**(1): p. 1-7.
237. van Dellen, E., et al., *Long-term effects of temporal lobe epilepsy on local neural networks: a graph theoretical analysis of corticography recordings.* PLoS One, 2009. **4**(11): p. e8081.

238. van Dellen, E., et al., *MEG Network Differences between Low- and High-Grade Glioma Related to Epilepsy and Cognition.* PLoS One, 2012. **7**(11): p. e50122.
239. van den Bent, M.J., et al., *Adjuvant Procarbazine, Lomustine, and Vincristine Chemotherapy in Newly Diagnosed Anaplastic Oligodendroglioma: Long-Term Follow-Up of EORTC Brain Tumor Group Study 26951.* J Clin Oncol, 2012.
240. van den Heuvel, M.P., et al., *High-cost, high-capacity backbone for global brain communication.* Proc Natl Acad Sci U S A, 2012. **109**(28): p. 11372-7.
241. van den Heuvel, M.P., et al., *Small-world and scale-free organization of voxel-based resting-state functional connectivity in the human brain.* Neuroimage, 2008. **43**(3): p. 528-39.
242. van den Heuvel, M.P., et al., *Efficiency of functional brain networks and intellectual performance.* J Neurosci, 2009. **29**(23): p. 7619-24.
243. van Wijk, B.C., C.J. Stam, and A. Daffertshofer, *Comparing brain networks of different size and connectivity density using graph theory.* PLoS One, 2010. **5**(10): p. e13701.
244. Varela, F., et al., *The brainweb: phase synchronization and large-scale integration.* Nat.Rev.Neurosci., 2001. **2**(4): p. 229-239.
245. Varotto, G., et al., *Epileptogenic networks of type II focal cortical dysplasia: a stereo-EEG study.* Neuroimage, 2012. **61**(3): p. 591-8.
246. Veauthier, J., H. Haettig, and H.J. Meencke, *Impact of levetiracetam add-on therapy on different EEG occipital frequencies in epileptic patients.* Seizure, 2009. **18**(6): p. 392-5.
247. Vlooswijk, M.C., et al., *Loss of network efficiency associated with cognitive decline in chronic epilepsy.* Neurology, 2011.
248. Vrba, J., et al., *151-Channel whole-cortex MEG system for seated or supine positions.*, in *Recent advances in biomagnetism.* , T. Yoshimoto, et al., Editors. 1999, Tohoku University Press: Sendai, Japan. p. 93-6.
249. Wada, J. and T. Rasmussen, *Intracarotid injection of sodium amytal for the lateralization of cerebral speech dominance.* J Neurosurg, 1960. **106**(6): p. 1117-33.
250. Wade, D.T. and C. Collin, *The Barthel ADL Index: a standard measure of physical disability?* Int Disabil Stud, 1988. **10**(2): p. 64-7.
251. Wang, H., J.M. Hernandez, and P. Van Mieghem, *Betweenness centrality in a weighted network.* Phys Rev E Stat Nonlin Soft Matter Phys, 2008. **77**(4 Pt 2): p. 046105.
252. Wang, J., et al., *Parcellation-dependent small-world brain functional networks: a resting-state fMRI study.* Hum Brain Mapp, 2009. **30**(5): p. 1511-23.
253. Watts, D.J. and S.H. Strogatz, *Collective dynamics of 'small-world' networks.* Nature, 1998. **393**(6684): p. 440-442.
254. Weiskopf, N., et al., *Unified segmentation based correction of R1 brain maps for RF transmit field inhomogeneities (UNICORT).* Neuroimage, 2011. **54**(3): p. 2116-24.
255. Wen, P.Y., et al., *Medical management of patients with brain tumors.* J Neurooncol, 2006. **80**(3): p. 313-32.
256. Wendling, F., et al., *Interictal to ictal transition in human temporal lobe epilepsy: insights from a computational model of intracerebral EEG.* J.Clin.Neurophysiol., 2005. **22**(5): p. 343-356.
257. Westlake, K.P., et al., *Resting state alpha-band functional connectivity and recovery after stroke.* Exp Neurol, 2012. **237**(1): p. 160-9.
258. Whalen, C., et al., *Validation of a method for coregistering scalp recording locations with 3D structural MR images.* Hum Brain Mapp, 2008. **29**(11): p. 1288-301.
259. Wiebe, S., et al., *A randomized, controlled trial of surgery for temporal-lobe epilepsy.* N.Engl.J.Med., 2001. **345**(5): p. 311-318.

260. Wilke, C., G. Worrell, and B. He, *Graph analysis of epileptogenic networks in human partial epilepsy.* Epilepsia, 2010. **52**(1): p. 84-93.
261. Zetterberg, L.H., L. Kristiansson, and K. Mossberg, *Performance of a model for a local neuron population.* Biol Cybern, 1978. **31**(1): p. 15-26.
262. Zhang, Z., et al., *Altered functional-structural coupling of large-scale brain networks in idiopathic generalized epilepsy.* Brain, 2011. **134**(Pt 10): p. 2912-28.
263. Zhou, C., A.E. Motter, and J. Kurths, *Universality in the synchronization of weighted random networks.* Phys Rev Lett, 2006. **96**(3): p. 034101.

DANKWOORD

Ik ben een aantal mensen veel dank verschuldigd voor hun hulp bij het tot stand komen van dit proefschrift. In de eerste plaats aan alle patiënten en vrijwilligers die met veel betrokkenheid en inzet aan deze onderzoeksprojecten hebben deelgenomen. Daarnaast aan het Nationaal Epilepsie Fonds de ONWAR voor de financiering van mijn onderzoek.

Graag bedank ik mijn promotoren en co-promotoren. Jullie hebben een grote gok genomen door mij de ruimte te geven dit onderzoek te combineren met mijn coschappen, en ik ben erg dankbaar voor dat vertrouwen. Beste Kees, jij hebt mij als promotor niet alleen begeleid bij mijn onderzoek, maar een geheel nieuwe kijk gegeven op wetenschap en de werking van de hersenen. Jouw vermogen om met veel enthousiasme allerlei disciplines op een begrijpelijke manier bij elkaar te brengen, van non-lineaire dynamica tot filosofie en van netwerktheorie tot literatuur, is een enorme bron van inspiratie. De besprekingen op de KNF zijn vanaf het moment dat ik ze enigszins kon volgen voor mij uitgegroeid tot hoogtepunten van de week. Ik hoop dat ik in de toekomst nog veel met je kan samenwerken.

Beste Jan, je hebt ervoor gewaakt dat ik niet op een dwaalspoor ben beland in de theorie, en mij erop gewezen als mijn manuscripten te veel op dialogen uit slechte science fiction begonnen te lijken. Hoe vol jouw agenda ook is, als ik je hulp nodig had leek je alle tijd van de wereld te hebben. Ik heb erg veel geleerd van jouw leiderschap en overzicht en kennis van de neuro-oncologie.

Beste Jaap, vijf jaar geleden kwam ik langs op zoek naar een scriptieonderwerp zonder een goed idee wat ik wilde, en jij hebt mij precies op de juiste plek gezet. Ik heb erg veel geleerd van jouw dagelijkse begeleiding, kritische blik, en vermogen om mensen en ideeën bij elkaar te brengen. Daarnaast heb je me erg geholpen met mijn carrière buiten mijn onderzoeksprojecten.

Beste Linda, toen ik stage bij je kwam lopen wist je niet helemaal met wie je opgezadeld werd, maar er gelukkig was er een gemene deler in onze interesse voor dit onderzoek en natuurlijk in Gummbah. Het was briljant om urenlang te discussiëren, eerst op 1F en later via de Boston-Amsterdam hotline. Dank voor alles wat ik van je heb geleerd, en voor de overdaad aan slechte grappen. Ik hoop dat het Institute for Dark Thoughts snel van de grond komt!

Ik dank de leden van de leescommissie voor hun tijd en moeite om dit proefschrift te lezen en beoordelen. Dr. Hillebrand, beste Arjan, zonder jouw begeleiding zou ik nog steeds in het duister tasten over alle fysica die de basis vormt voor dit onderzoek. Dank voor alle geduld, uitleg en borrels, ik hoop dat we ook in de toekomst kunnen blijven samenwerken. Dr. De Witt Hamer, beste Philip, dank voor vele inspirerende discussies, jouw klinische benadering van dit soms abstracte onderzoek, en de fijne samenwerking. Prof.dr. Roelfsema, beste Pieter, dank voor de leerzame samenwerking bij de single neuron studie, die vast nog veel interessante resultaten gaat brengen. Prof.dr. Scheltens, beste Philip, ik kijk er erg naar uit om samen te werken in het onderzoek naar dementie en delirium. Prof.dr. Geurts, beste Jeroen, dank voor een aantal inspirerende gesprekken en jouw brede, filosofische blik op wetenschappelijk onderzoek. Dr. van den Heuvel, beste Martijn, jouw studies zijn een grote inspiratie geweest. Prof.dr. Hueges Duffau, thank you for your willingness to participate in my doctoral committee, and for the opportunity to contribute to your excellent book on Brain Mapping.

De collega's van de afdeling neuro-oncologie: dank aan Tjeerd (voor jouw oog voor bijzondere patiënten, en zeker ook voor de goede sfeer), Ingeborg (ook op de afdeling), Martin Klein (voor de mooie vergaderingen en vele anekdotes), Wilmy, Martin Taphoorn, Claudia, Alieke en Lies voor de fijne samenwerking, de mooie congressen en goede etentjes.

Mijn collega's van 1F en omstreken: Frok, Shine, Sizoe, Florien, Gwenda, Hinke, David, Johan, Sanne, Linda D en Eline, dank voor de opvoeding van een kamerkleuter, de Music challenges, Lamborghini's, kattenfilmpjes, drink smakelijks, eekhoorns met refluxklachten, Charly en vele anderen.

Erg inspirerend waren ook de mooie discussies, borrels en congressen met mijn collega-netwerkers, Willem, Maria, Menno, Rikkert, Kim, Prejaas, Hanneke en Marjolein. Ook ben ik veel dank verschuldigd aan de collega's van de klinische neurofysiologie, Ilse, Hanneke en Bob voor de scherpe beschouwingen, en Ndedi (ook voor de beschouwingen op het fenomeen de maandagborrel), PeterJan, Irene, en Karin voor hun hulp bij alle metingen. Ik dank de collega's van de epilepsie werkgroep: Steven Claus, Dimitri Velis, Stylian Kalitzyn en Willem Alpherts. Hans, je hebt mij erg veel geleerd over de epilepsiechirurgie,en heb met ontzettend veel plezier samengewerkt. The colleagues from the NIN and from Toulouse: Matt, Judith and Leila, thank you for the always fascinating trips to Heemstede.

Lotte Jonkman, heel erg bedankt voor je expertise en flexibiliteit bij het opmaken van dit boekje.

Sandra Mooren, dank voor het wekken van mijn interesse voor de wetenschap.

Waar is een mens zonder vrienden? Precies. In het bijzonder dank ik: Adam en vele anderen, Casper, Renko en Maarten en de trouwste groupie Anna, voor alle takjes en Elandjes. De Jongens, Léon en Wouter, en alle gastspelers, voor alle snoeppuntjes, bonusspelen en caramboles. Duijf, voor al uw steunbakkies, avondprogramma's en verhuizingen. Roderick voor de momenten dat hij de Raaf wordt. Freek voor de conditietraining op de squashbaan, en Roeland voor het meetrainen. Joep en René voor de broodnodige brandstof. Chris voor de ochtenden op de stoep van de Mozartlaan. Thomas voor het kennen en benoemen van alle (al dan niet bestaande) referenties in het werk van David Lynch. Diederik, Angela en Snorky Pop voor alle weekendjes warm welkom. Linker voor alle verrassingsbezoekjes uit Engeland. En Sportchamps Heren 1, Kieffer, Wouter 2, Black, Flip, Rikkie, Green en Motivator Vos voor het niet aflatende vertrouwen dat ik nog eens een wedstrijd voor jullie ga winnen.

In het bijzonder dank ik mijn familie en mijn schoonfamilie, Jan, Yvette, Susan en Mark. Vati, ik heb enorm veel steun aan jouw vertrouwen en wijsheid. Marjolein, dank voor jouw zorgzaamheid, en eeuwige zoektocht naar de beste ingrediënten. Judith, het zussenkind, dank voor alle *This may be spam*, en voor de wekelijks mooier wordende verhalen.

Lotte, je bent fantastisch. En er is niemand die met zo veel plezier 'hubs' kan zeggen. Ik hoop dat we samen zulke avonturen blijven beleven als de afgelopen vier jaar, en dat je met zoveel passie voor mij blijft zorgen (en vice versa natuurlijk).

LIST OF PUBLICATIONS

E. van Dellen, L. Douw, A. Hillebrand, P.C. de Witt Hamer, J.C. Baayen, J.J. Heimans, J.C. Reijneveld, C.J. Stam. “Minimum spanning tree” alterations predict seizure-freedom in lesional epilepsy: a longitudinal MEG study. Submitted.

E. van Dellen, A. Hillebrand, L. Douw, J.J. Heimans, J.C. Reijneveld, C.J. Stam. Locally disturbed neural activity in cortical lesions has global impact on functional connectivity. Submitted.

L. Douw, M. de Groot, **E. van Dellen**, E. Aronica, J.J. Heimans, M. Klein, C.J. Stam, J.C. Reijneveld, A. Hillebrand. Local MEG networks: The missing link between protein expression and epilepsy in glioma patients? NeuroImage (2013), 75, p. 203–211.

E. van Dellen, P.C. de Witt Hamer, L. Douw, m. Klein, J.J. Heimans, C.J. Stam, J.C. Reijneveld, A. Hillebrand. Increased connectivity in MEG resting-state networks after tumor resection is related to improved cognitive performance. NeuroImage: Clinical (2013), **2**(1): p. 1-7.

E. van Dellen, L. Douw, A. Hillebrand, J.J. Heimans, M. Klein, D.N. Velis, I.H.M. Ris Hilgersom, M.M. Schoonheim, J.C. Baayen, P.C. de Witt Hamer, C.J. Stam, J.C. Reijneveld, MEG network differences between low- and high grade glioma related to epilepsy and cognition. PLoS ONE (2012), **7**(11):e50122.

E. van Dellen, L. Douw, I. Bosma, J.J. Heimans, C.J. Stam, J.C. Reijneveld. Neural network analysis and its application in neurosurgical planning. In: H. Duffau (Ed.) (2011). Brain Mapping: From Neural Basis of Cognition to Surgical Applications, p. 373-388, Springer Verlag, Wien.

E. van Dellen*, L. Douw*, J.C. Baayen, M. Klein, D.N. Velis, W. Alpherts, J.J. Heimans, J.C. Reijneveld, C.J. Stam. The lesioned brain: still a small-world? Front. Hum. Neurosci. (2010), 4: p. 12. * Equal contribution

L. Douw, **E. van Dellen**, M. de Groot, J.J. Heimans, C.J. Stam, J.C. Reijneveld. Epilepsy is related to theta band brain connectivity and network topology in brain tumor patients. BMC Neuroscience (2010), 11:103.

L. Douw, M. de Groot, **E. van Dellen**, J.J. Heimans, H.E. Ronner, C.J. Stam, J.C. Reijneveld. ‘Functional connectivity’ is a sensitive predictor of epilepsy diagnosis after the first seizure. PLoS ONE (2010), **5**(5), e10839.

E. van Dellen, L. Douw, J.C. Baayen, J.J. Heimans, S.C. Ponten, W.P. Vandertop, D.N. Velis, C.J. Stam, J.C. Reijneveld. Long-term effects of temporal lobe epilepsy on local neural networks: a graph theoretical analysis of corticography recordings. PLoS ONE (2009), **4**(11), e8081.

CURRICULUM VITAE

Edwin van Dellen was born on May 31st 1985 in Leiderdorp. He went to the Christelijk Gymnasium in Utrecht in 1997, where he became interested in medicine and neuroscience. In 2003, he started his study medicine at the University of Amsterdam and Academic Medical Center Amsterdam.

During his studies, he became interested in medical ethics and medical education, and participated in the student council of the Royal Dutch Medical Society (KNMG) of which he was chairman in 2008, and was the student representative in the KNMG federation board.

In 2008, he performed his scientific internship at the department of neurology at the VU University Medical Center, and wrote his MSc-thesis graph analysis of electrocorticography recordings in lesional epilepsy patients under supervision of Prof.dr C.J. Stam, Prof.dr J.J. Heimans, Dr J.C. Reijneveld, and Dr L. Douw. In 2009, he started as PhD candidate at the same department. In 2010-2012, he performed his clerkships (co-schappen) at the Academic Medical Center Amsterdam and affiliated hospitals, after which he obtained his Doctor of Medicine degree. He performed clinical internships at the department of neuroradiology of Heidelberg University Hospital under supervision of Prof.dr M. Bendszus, and at the department of neurology of the VU University Medical Center.

In April 2013, he started working as a post-doctoral researcher at the Alzheimer Center and department of Clinical Neurophysiology of the VU University Medical Center, and the Intensive Care Unit of the University Medical Center Utrecht, where he studies functional brain networks in patients with dementia and delirium.